

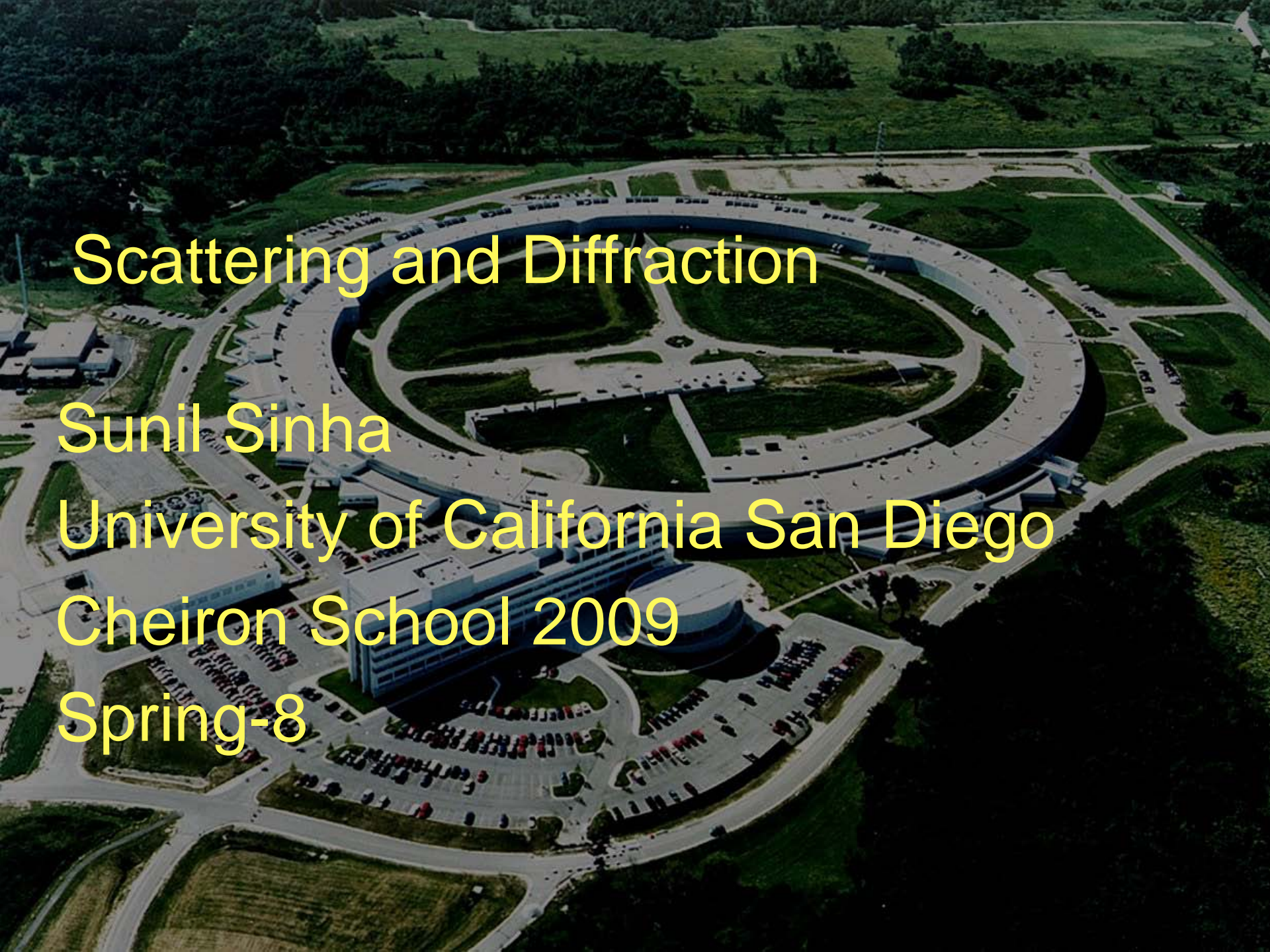
# Scattering and Diffraction

Sunil Sinha

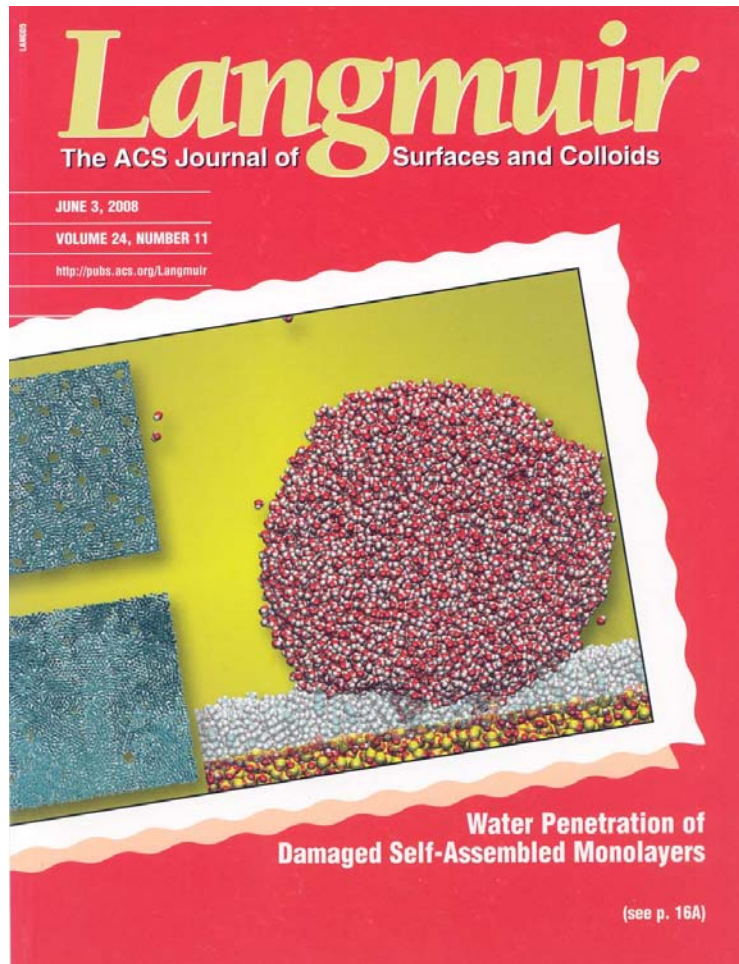
University of California San Diego

Cheiron School 2009

Spring-8



# People want pretty pictures (in Space and Time!)

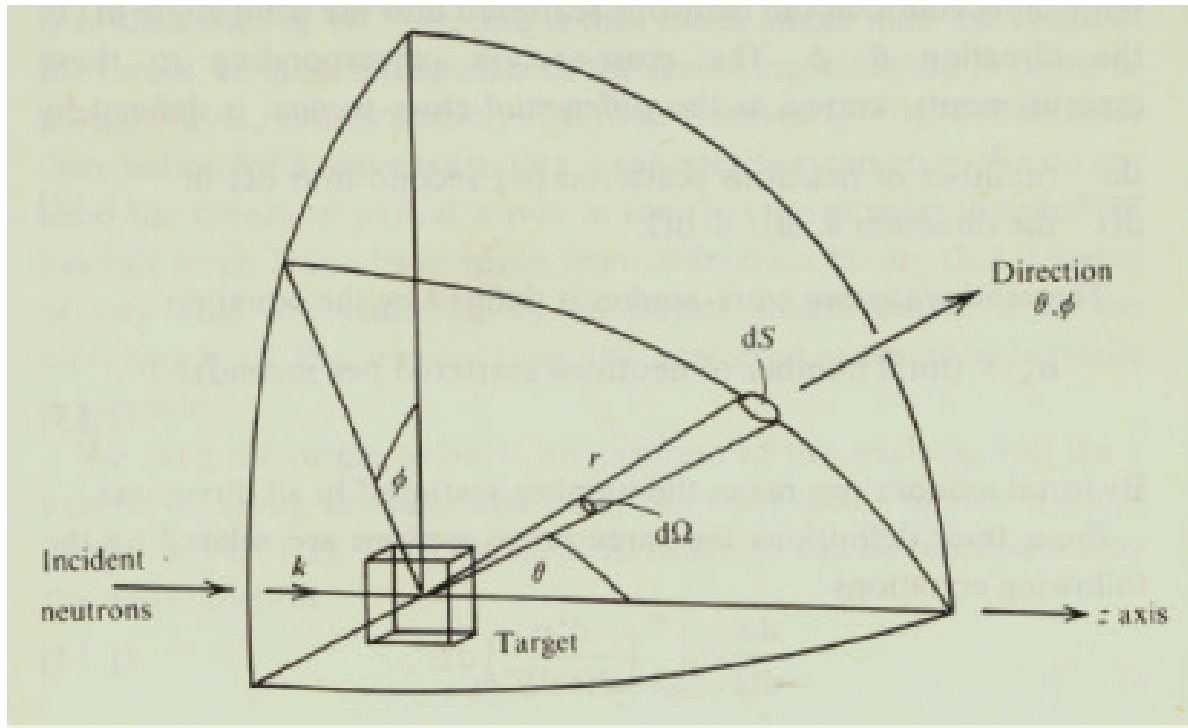


# X-Ray Scattering

- Indirect
- Global Statistical Information
- Non-destructive
- Buried Interfaces
- Magnetic and Structural
- Dynamics
- Can use with high pressures, magnetic fields,etc.

# S.R. based research can help us to understand:

- How the constituent molecules self-assemble to form nanoparticles.
- How these self-organize into assemblies
- How structure and dynamics lead to function
- How emergent or collective properties arise



$\Phi$  = number of incident neutrons per  $\text{cm}^2$  per second

$\sigma$  = total number of neutrons scattered per second /  $\Phi$

$$\frac{d\sigma}{d\Omega} = \frac{\text{number of neutrons scattered per second into } d\Omega}{\Phi d\Omega}$$

$$\frac{d^2\sigma}{d\Omega dE} = \frac{\text{number of neutrons scattered per second into } d\Omega \text{ & } dE}{\Phi d\Omega dE}$$

# Intrinsic Cross Section: X-Rays

$$\vec{E}_{\text{in}} = \vec{E}_0 e^{i(\vec{k} \cdot \vec{r} - \omega t)}$$

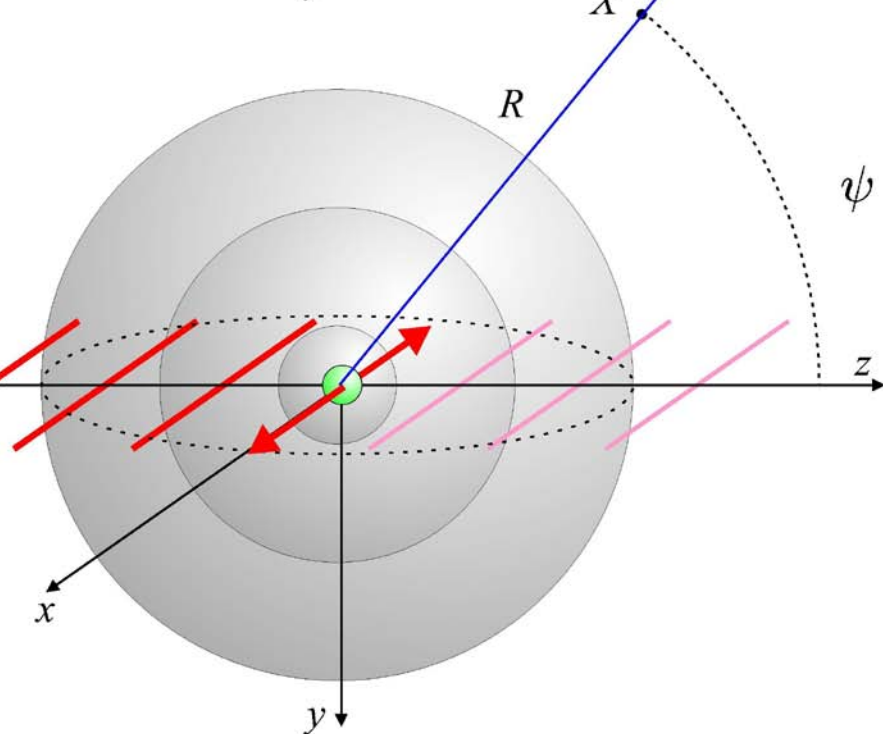
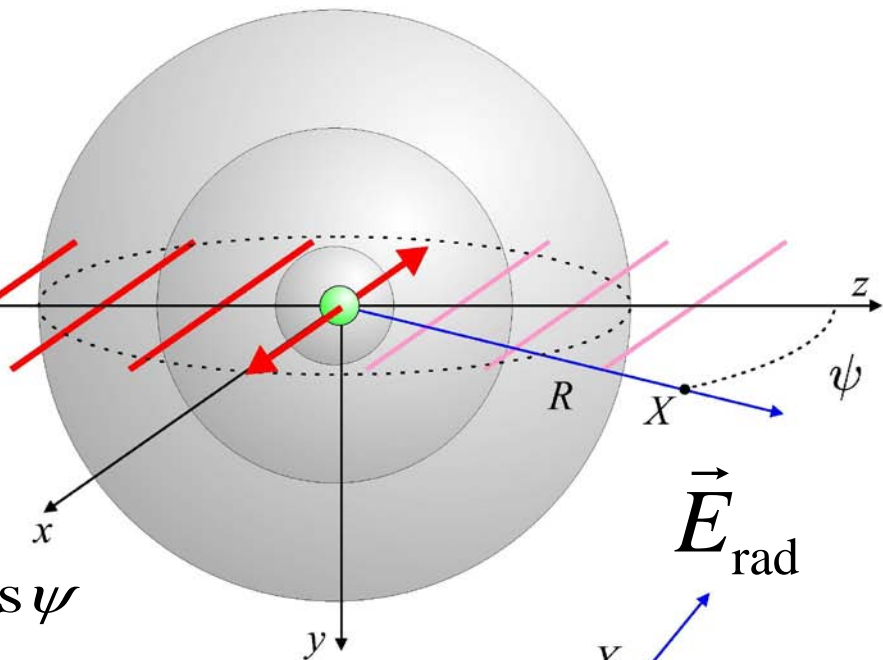
$$E_{\text{rad}}(R, t) = \frac{e}{4\pi\epsilon_0 c^2 R} \ddot{x}(t - R/c)$$

$$\ddot{x}(t - R/c) = -\frac{e}{m} \alpha(\omega) E_{\text{in}} e^{i\omega R/c} \cos \psi$$

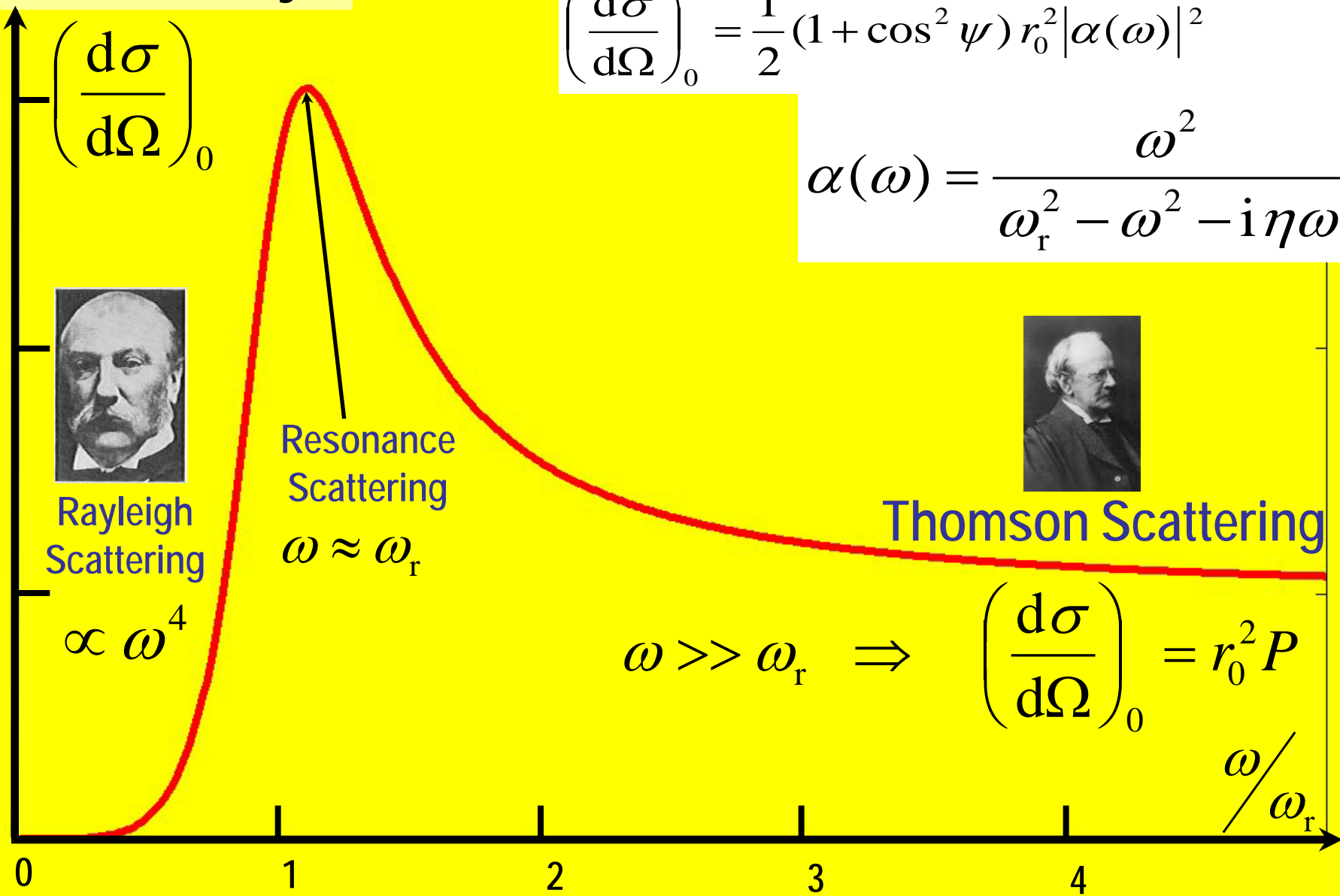
$$\frac{E_{\text{rad}}(R, t)}{E_{\text{in}}} = -r_0 \alpha(\omega) \frac{e^{ikR}}{R} \cos \psi$$

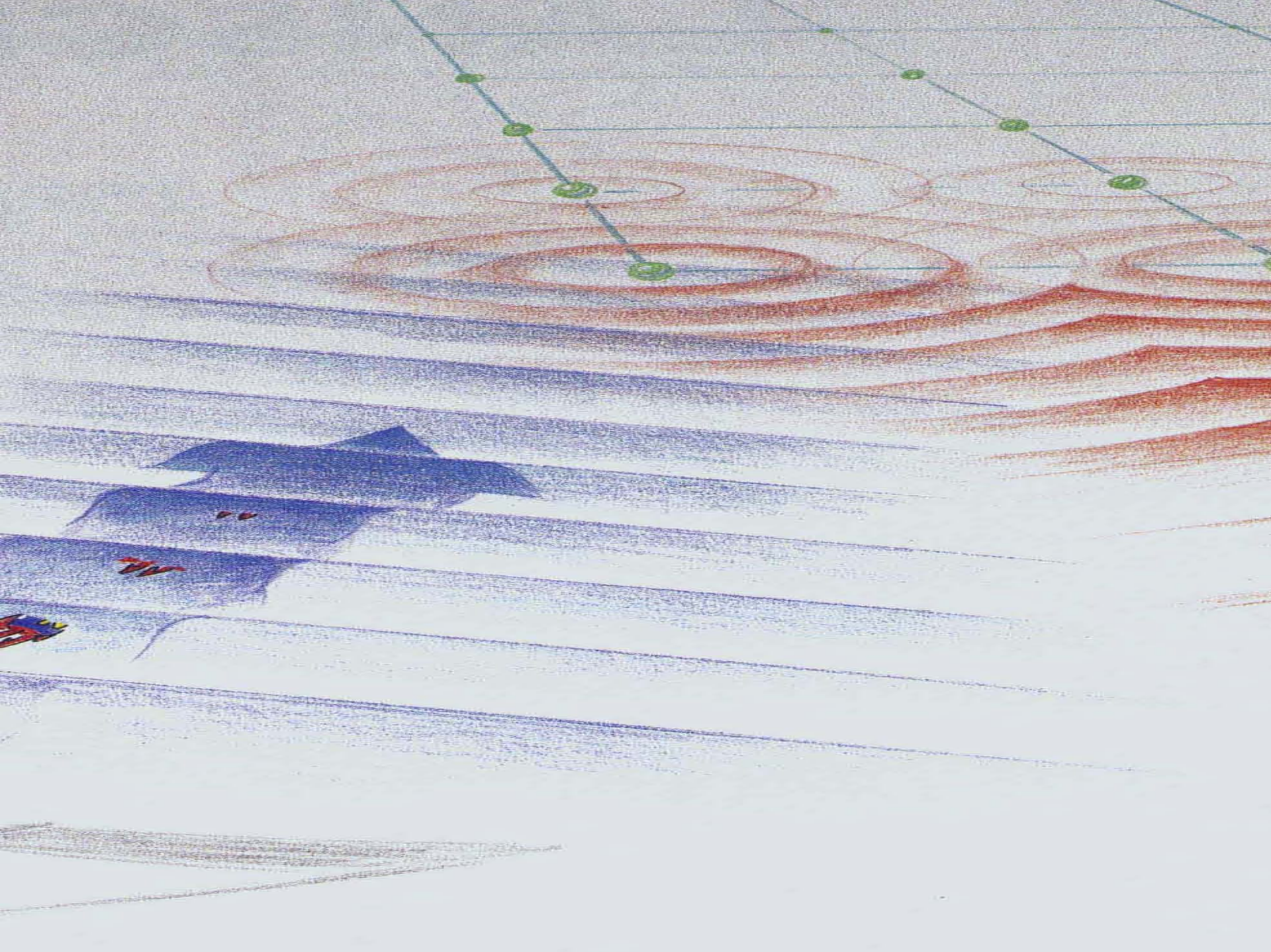
Thomson Scattering Length  
of the Electron  
(classical electron radius):

$$r_0 = \frac{e^2}{4\pi\epsilon_0 mc^2} = 2.82 \times 10^{-15} \text{ m}$$

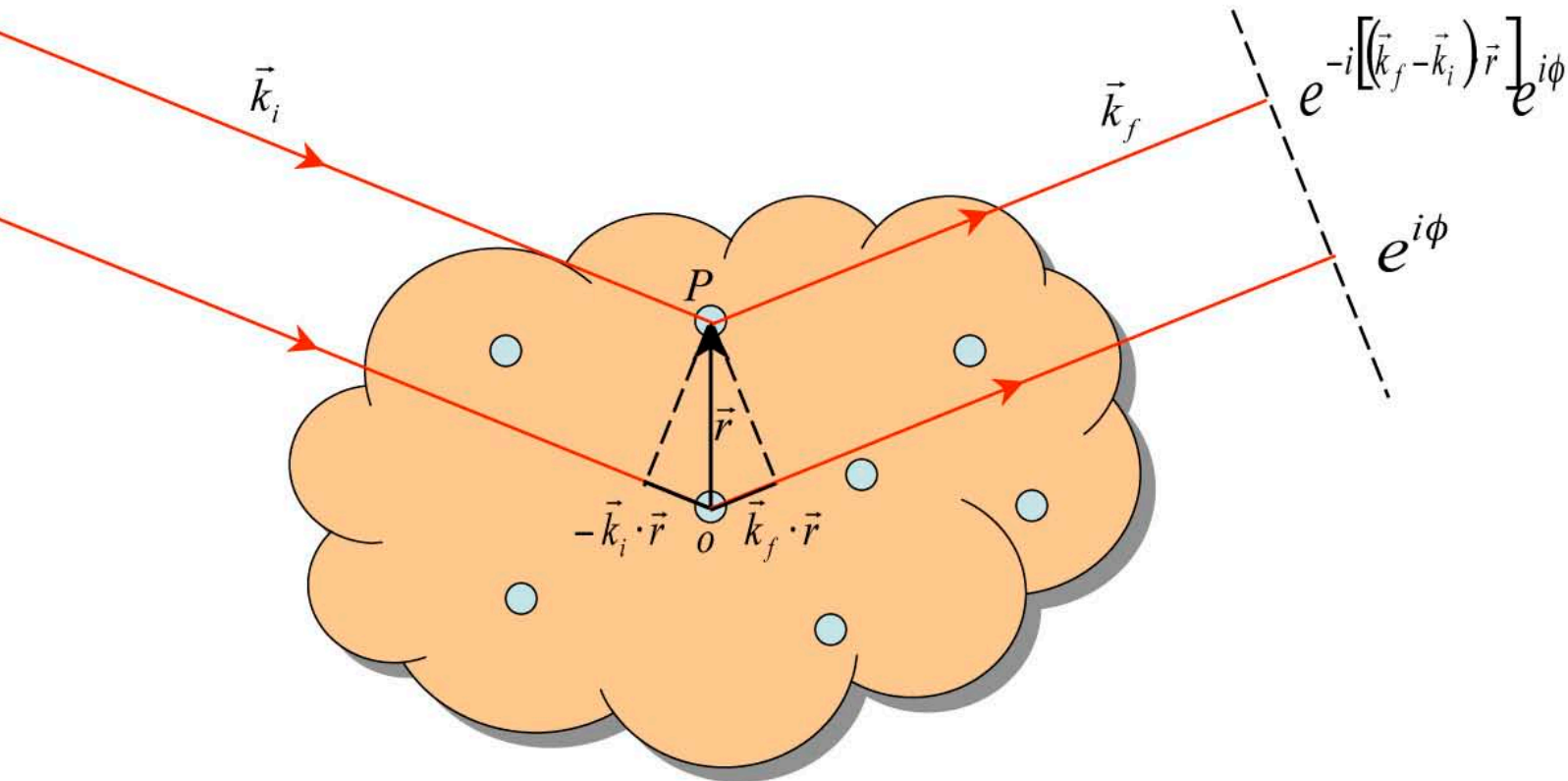


# Intrinsic Cross Section: X-Rays





Adding up phases at the detector of the wavelets scattered from all the scattering centers in the sample:



## X-rays

$$\frac{d\sigma}{d\Omega} = r_0^2 \sum_{ij} e^{-iq \cdot (\vec{r}_i - \vec{r}_j)} \times \left( \frac{1 + \cos^2(2\theta)}{2} \right)$$

$\vec{r}_i \rightarrow$  electron coordinates

Wave vector transfer is defined as

$$\mathbf{q} = \mathbf{k}_f - \mathbf{k}_i$$

## X-rays

$$\frac{d\sigma}{d\Omega} = r_0^2 \frac{[1 + \cos^2(2\theta)]}{2} S(\mathbf{q})$$

$$S(\mathbf{q}) = \langle \sum_{ij} \exp[-i\mathbf{q} \cdot (\mathbf{r}_i - \mathbf{r}_j)] \rangle$$

$\{\mathbf{r}_i\}$  == electron positions.

Now,  $\sum_i \exp[-i\mathbf{q} \cdot \mathbf{R}_i] = \rho_{el}(\mathbf{q})$  Fourier Transform of electron density

### Proof:

$$\rho_{el}(\mathbf{r}) = \sum_i \delta(\mathbf{r} - \mathbf{R}_i)$$

$$\begin{aligned}\rho_{el}(\mathbf{q}) &= \int \rho_{el}(\mathbf{r}) \exp[-i\mathbf{q} \cdot \mathbf{r}] d\mathbf{r} = \int \sum_i \delta(\mathbf{r} - \mathbf{R}_i) \exp[-i\mathbf{q} \cdot \mathbf{r}] d\mathbf{r} \\ &= \sum_i \exp[-i\mathbf{q} \cdot \mathbf{R}_i]\end{aligned}$$

So, for x-rays,  $S(\mathbf{q}) = \langle \rho_{el}(\mathbf{q}) \rho_{el}^*(\mathbf{q}) \rangle$

If electrons are bound to atoms centered on  $\vec{R}_i$

$$\rho_{el}(\vec{r}) = \sum_i f_{el}(\vec{r} - \vec{R}_i)$$

$$\rho_{el}(\vec{q}) = \int d\vec{r} e^{-i\vec{q} \cdot \vec{r}} \sum_i f(\vec{r} - \vec{R}_i)$$

$$= \sum_i \left[ \int d\vec{r} e^{-i\vec{q} \cdot (\vec{r} - \vec{R}_i)} f(\vec{r} - \vec{R}_i) \right] e^{-i\vec{q} \cdot \vec{R}_i}$$

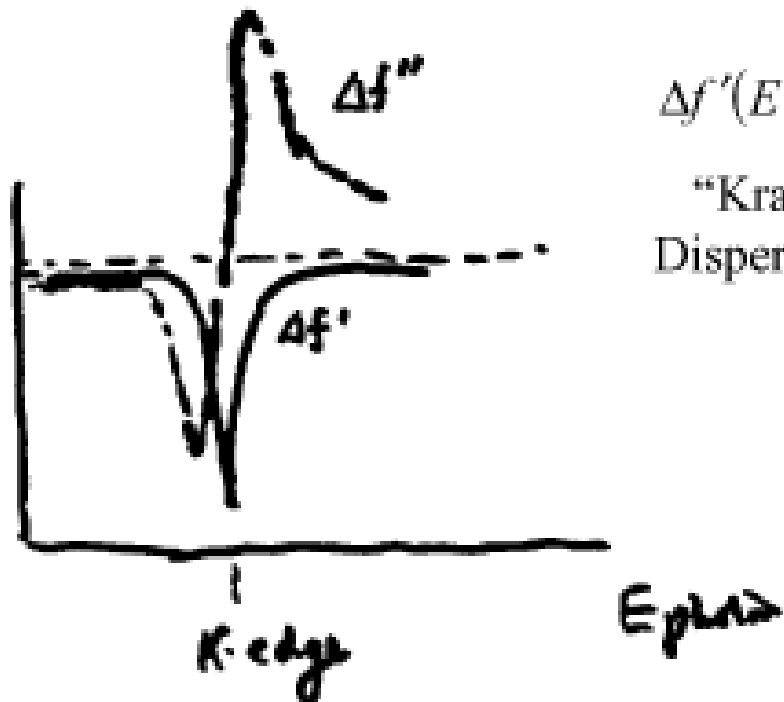
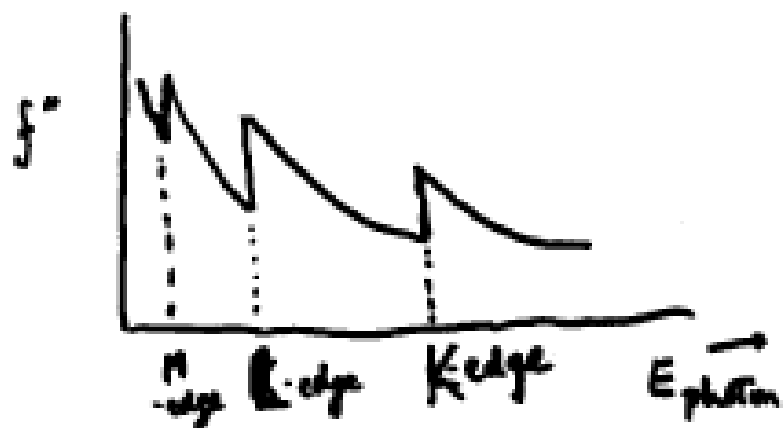
$$= Zf(\vec{q}) \sum_i e^{-i\vec{q} \cdot \vec{R}_i} = Zf(\vec{q}) \rho_N(\vec{q})$$

$\swarrow$   
atomic form factor

## X-rays

$$f = f_0 + \underbrace{\Delta f' + i\Delta f''}_{\text{"anomalous" big at edges}} + Zf(q)$$

"Scattering factor"



$$\Delta f'(E) = 2\pi \int \frac{\Delta f''(E')}{E - E'} dE'$$

"Kramers-Kronig  
Dispersion Relations"

$$S(q) = \langle |\rho_N(\vec{q})|^2 \rangle \quad [\times |f(q)|^2] \text{ for x-rays}$$

$$\rho_N(\vec{q}) = \int d\vec{r} e^{-i\vec{q} \cdot \vec{r}} \rho_N(\vec{r})$$

$$\Rightarrow S(q) = \iint d\vec{r} d\vec{r}' e^{-i\vec{q} \cdot (\vec{r} - \vec{r}')} \langle \rho_N(\vec{r}) \rho_N(\vec{r}') \rangle$$

If  $\langle \rho_N(\vec{r}) \rho_N(\vec{r}') \rangle = \text{Fn. of } (\vec{r} - \vec{r}')$  only,

$$S(q) = V \int d\vec{r}' e^{-i\vec{q} \cdot \vec{R}} \langle \rho_N(\vec{r}) \rho_N(\vec{r} - \vec{R}) \rangle$$

$$= \int d\vec{R} e^{-i\vec{q} \cdot \vec{R}} g(\vec{R})$$

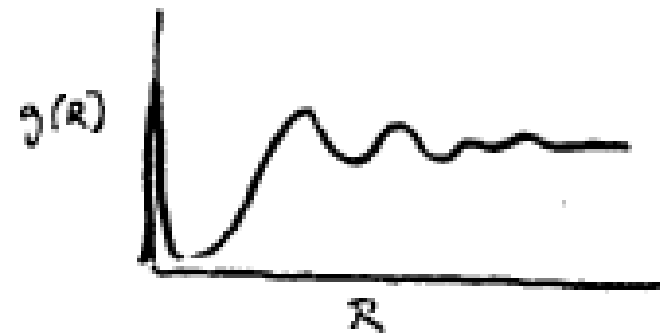
$g(\vec{R})$  = Pair-distribution function

$$= V \langle \rho_N(\vec{r}) \rho_N(\vec{r} - \vec{R}) \rangle$$

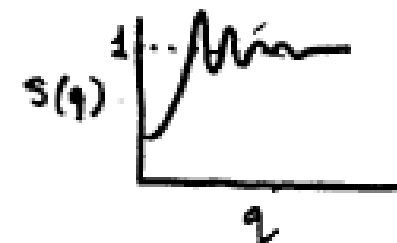
$\Rightarrow$  Probability that given a particle at  $\vec{r}$ , there is distance  $\vec{R}$  from it (per unit volume)

$$g(\vec{R}) = \delta(\vec{R}) + g_d(\vec{R}) \quad S(q) - 1 = \int d\vec{R} e^{-i\vec{q} \cdot \vec{R}} g_d(\vec{R})$$

$$g_d(\vec{R})_{R \rightarrow \infty} \rightarrow V \langle \rho \rangle^2$$



### Liquids and Glasses



$g(\vec{R})$  and hence  $S(q)$  are isotropic.

$g_d(R)$  = Reverse F.T. of  $[S(q) - 1]$

$$= 4\pi \int_0^\infty dq q^2 \frac{\sin(qR)}{(qR)} [S(q) - 1]$$

# $S(Q)$ and $g(r)$ for Simple Liquids

- Note that  $S(Q)$  and  $g(r)/\rho$  both tend to unity at large values of their arguments
- The peaks in  $g(r)$  represent atoms in “coordination shells”
- $g(r)$  is expected to be zero for  $r <$  particle diameter – ripples are truncation errors from Fourier transform of  $S(Q)$

Fig. 5.1 The structure factor  $S(\kappa)$  for  $^{36}\text{Ar}$  at 85 K. The curve through the experimental points is obtained from a molecular dynamics calculation of Verlet based on a Lennard-Jones potential. (After Yarnell *et al.*, 1973.)

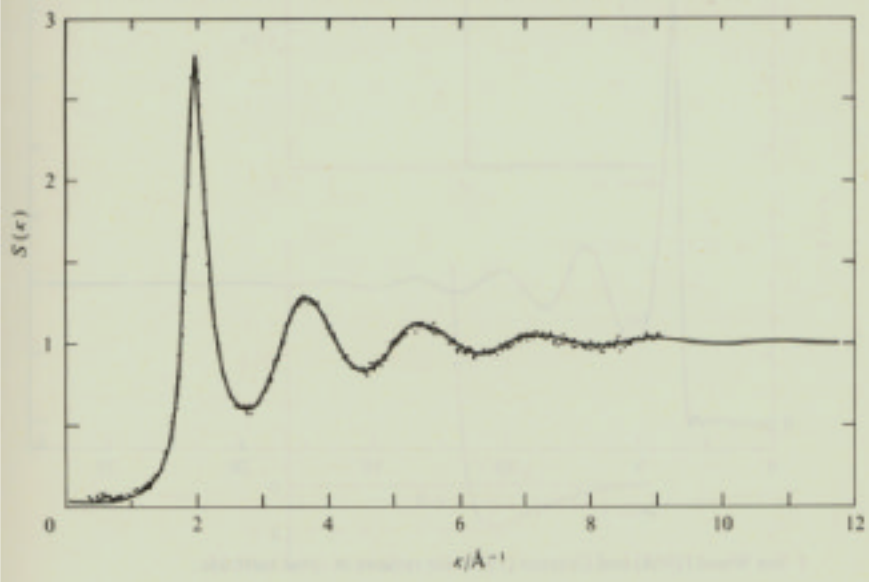
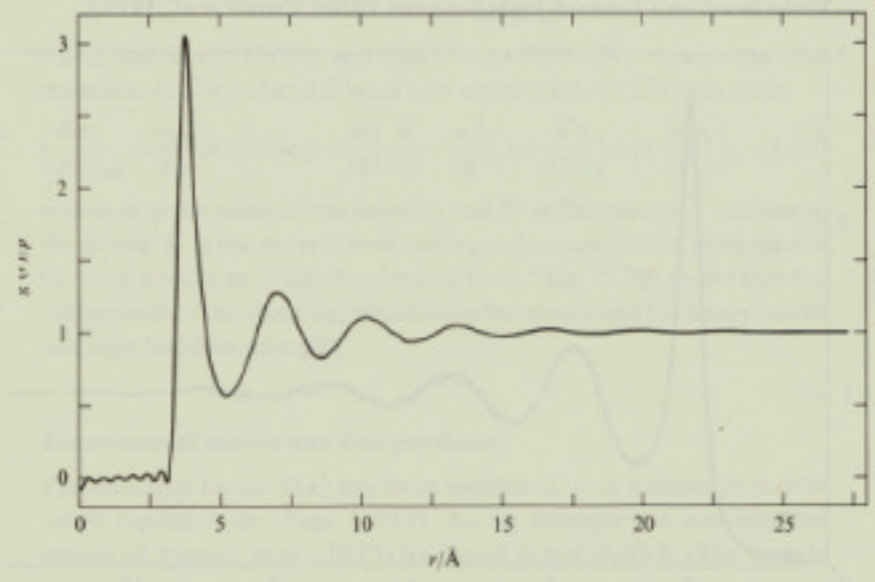


Fig. 5.2 The pair-distribution function  $g(r)$  obtained from the experimental results in Fig. 5.1. The mean number density is  $\rho = 2.13 \times 10^{28} \text{ atoms m}^{-3}$ . (After Yarnell *et al.*, 1973.)



## X-rays

$$I(q) = \sum_{K,K'} (r_0)^2 Z_K Z_{K'} f_K(q) f_{K'}^*(q) S_{KK'}(q)$$

$$\times \left[ 1 + \frac{\cos^2(2\theta)}{2} \right]$$

( $K, K'$  = Different atomic types)

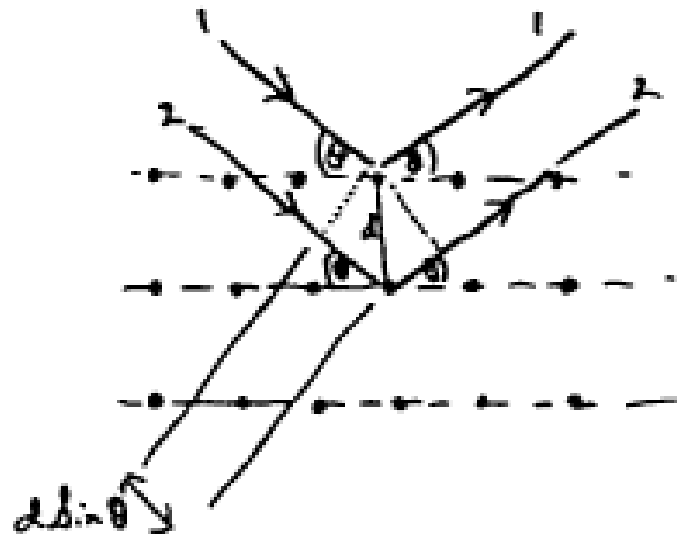
$$S_{KK'}(q) = \left\langle \sum_{i(K)j(K')} e^{-i\vec{q} \cdot [R_i(K) - R_j(K')]} \right\rangle$$

⇒ partial structure factor

These can be unscrambled by simultaneous measurements  
of  $\frac{d\sigma}{d\Omega}$  for neutrons, different  
isotopes + x-rays.

In general, in a scattering experiment

$$|\vec{q}| = 2k \sin \theta = \frac{4\pi}{\lambda} \sin \theta$$



A simple way to see Bragg's Law:

Path length difference between rays reflected from successive planes (1 and 2) =  $2d \sin \theta$

∴ Constructive interference when

$$n\lambda = 2d \sin \theta$$

Define 3 other vectors:

$$\bar{b}_1 = 2\pi(\bar{a}_2 \times \bar{a}_3)/v_0$$

$$\bar{b}_2 = 2\pi(\bar{a}_3 \times \bar{a}_1)/v_0$$

$$v_0 = \bar{a}_1 \cdot (\bar{a}_2 \times \bar{a}_3)$$

= unit cell vol.

$$\bar{b}_3 = 2\pi(\bar{a}_1 \times \bar{a}_2)/v_0$$

These have the property that  $\bar{a}_i \cdot \bar{b}_j = 2\pi\delta_{ij}$

So if we choose any vector  $\bar{G}$  on the lattice defined by  $\bar{b}_1, \bar{b}_2, \bar{b}_3$ :

$$\bar{G} = n_1\bar{b}_1 + m_2\bar{b}_2 + m_3\bar{b}_3$$

then for any  $\bar{G}, \bar{R}_\ell$ ,

$\bar{G} \cdot \bar{R}_\ell = 2\pi \times \text{integer} \rightarrow$  Implies  $\bar{G}$  is normal to sets of planes of atoms spaced  $2\pi/G$  apart.



## Reciprocal Lattice

Lattice Vectors  $\bar{R}_\ell = m_1\bar{a}_1 + m_2\bar{a}_2 + m_3\bar{a}_3$

$\bar{a}_1, \bar{a}_2, \bar{a}_3 \rightarrow$  primitive translation vectors of unit cell.

S.K. Sinha

OR

$$e^{i\bar{G} \cdot \bar{R}_\ell} = 1$$

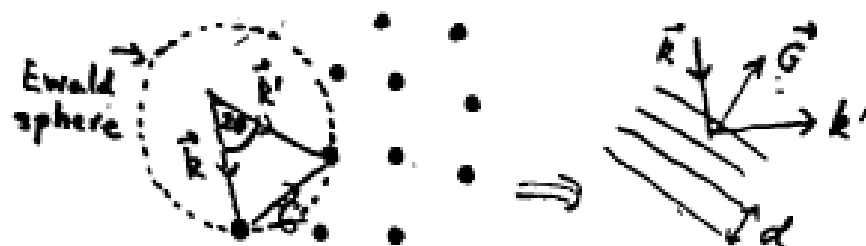
$$\sum_{\mathbf{l}} e^{-i\mathbf{q} \cdot \mathbf{R}_{\mathbf{l}}} = \frac{(2\pi)^3}{V_0} \sum_G \delta(\mathbf{q} - \mathbf{G})$$

(Introduce  $e^{-2W}$  = "Form factor" for thermal smearing of atoms =  $e^{-\langle(\vec{q} \cdot \vec{u})^2\rangle}$   $\Rightarrow$  Debye-Waller factor)

Similarly,

$$\left( \frac{d\sigma}{d\Omega} \right)_{x-rays} = Z^2 r_0^2 \left( \frac{1 + \cos^2(2\theta)}{2} \right) f^2(\vec{q}) e^{-2W}$$

$$N \cdot \frac{(2\pi)^3}{v_0} \sum_{\vec{G}} \delta(\vec{q} - \vec{G})$$



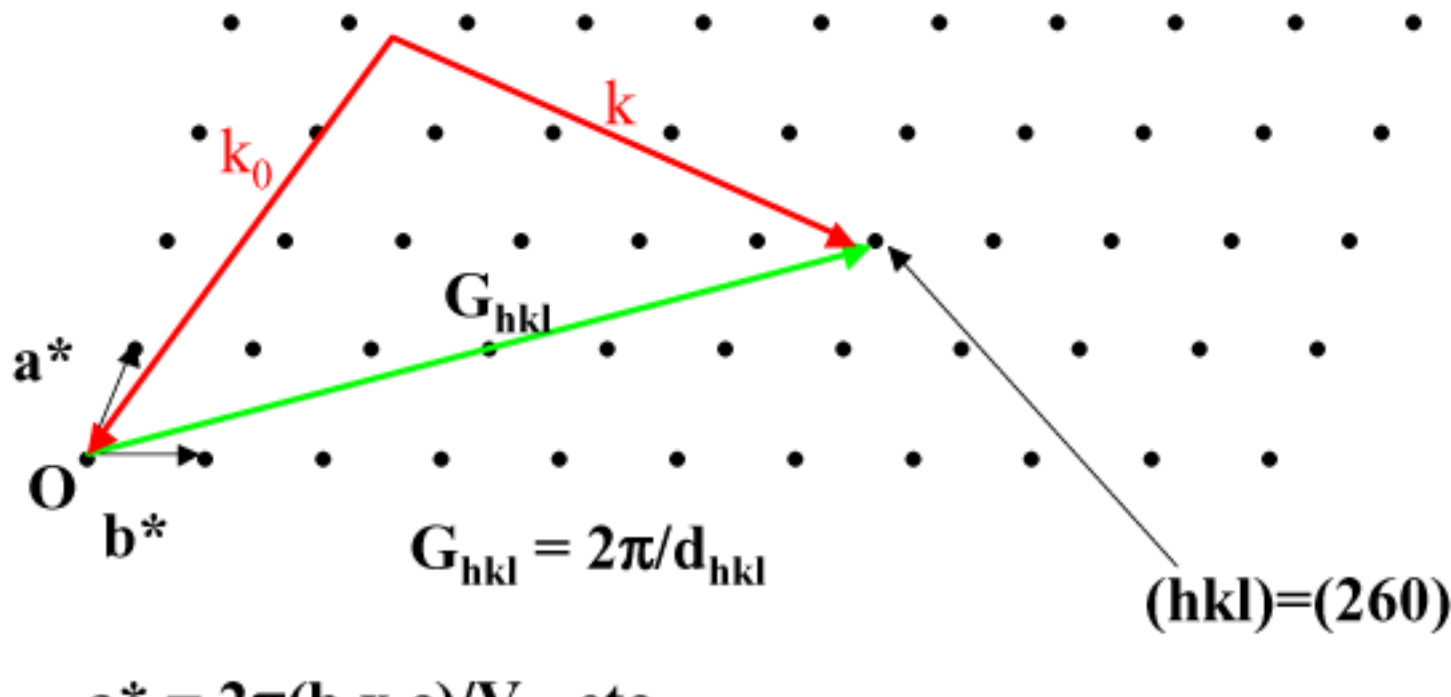
Bragg Reflections:

$$\vec{k}' - \vec{k} = \vec{G}$$

$$2k \sin \theta = G = \frac{2\pi}{d}$$

$$\rightarrow \boxed{\lambda = 2d \sin \theta} \quad \text{Bragg's Law}$$

## Reciprocal Space – An Array of Points ( $hkl$ ) that is Precisely Related to the Crystal Lattice



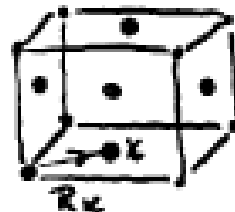
A single crystal has to be aligned precisely to record Bragg scattering

# Crystals with Complex Unit Cells (more than one type of atom/cell)

## Generalization

$$\left( \frac{d\sigma}{d\Omega} \right) = \left\langle \sum_{\substack{\ell\ell' \\ KK'}} b_K b_{K'} e^{-i\vec{q} \cdot (\vec{R}_\ell + \vec{R}_{K'} - \vec{R}_{\ell'} - \vec{R}_{K'})} \right\rangle$$

where  $b_K$  is coherent scattering length  $\langle b \rangle$  for  $K$ -type atom in unit cell at position  $\vec{R}_K$ .



$$= \left| \sum_K f_K e^{-i\vec{q} \cdot \vec{R}_K} e^{-2W_K} \right|^2 \sum_{\ell\ell'} e^{-i\vec{q} \cdot (\vec{R}_\ell - \vec{R}_{\ell'})}$$

F (structure factor)

$$\left( \frac{d\sigma}{d\Omega} \right)_{neutron} = \frac{N \cdot (2\pi)^3}{v_0} \sum_G |F_G|^2 \delta(\vec{q} - \vec{G})$$

$$\left( \frac{d\sigma}{d\Omega} \right)_{x-ray} = \frac{N \cdot (2\pi)^3}{v_0} \sum_G |F_G|^2 \delta(\vec{q} - \vec{G}) \left( \frac{1 + \cos^2(2\theta)}{2} \right)$$

where

$$F_G = \sum_K Z_K f_K(\vec{G}) r_0 e^{-2W_K} e^{-i\vec{G} \cdot \vec{R}_K}$$

- x-ray structure factor

Measurement of Structure Factors  $\rightarrow$  Structure

BUT what is measured is  $|F_G|^2$  NOT  $F_G$ !

$\rightarrow$  "Phase Problem"  $\rightarrow$  Special Methods

Note that  $|F_G|^2$  can be written  $\sum_{KK'} \mu_K \mu_{K'} e^{-i\vec{G} \cdot (\vec{R}_K - \vec{R}_{K'})}$

so that its F.T. yields information about pairs of atoms

separated by  $\vec{R}_K - \vec{R}_{K'} \Rightarrow$  Patterson Function.

We would be better off if diffraction measured phase of scattering rather than amplitude!  
Unfortunately, nature did not oblige us.

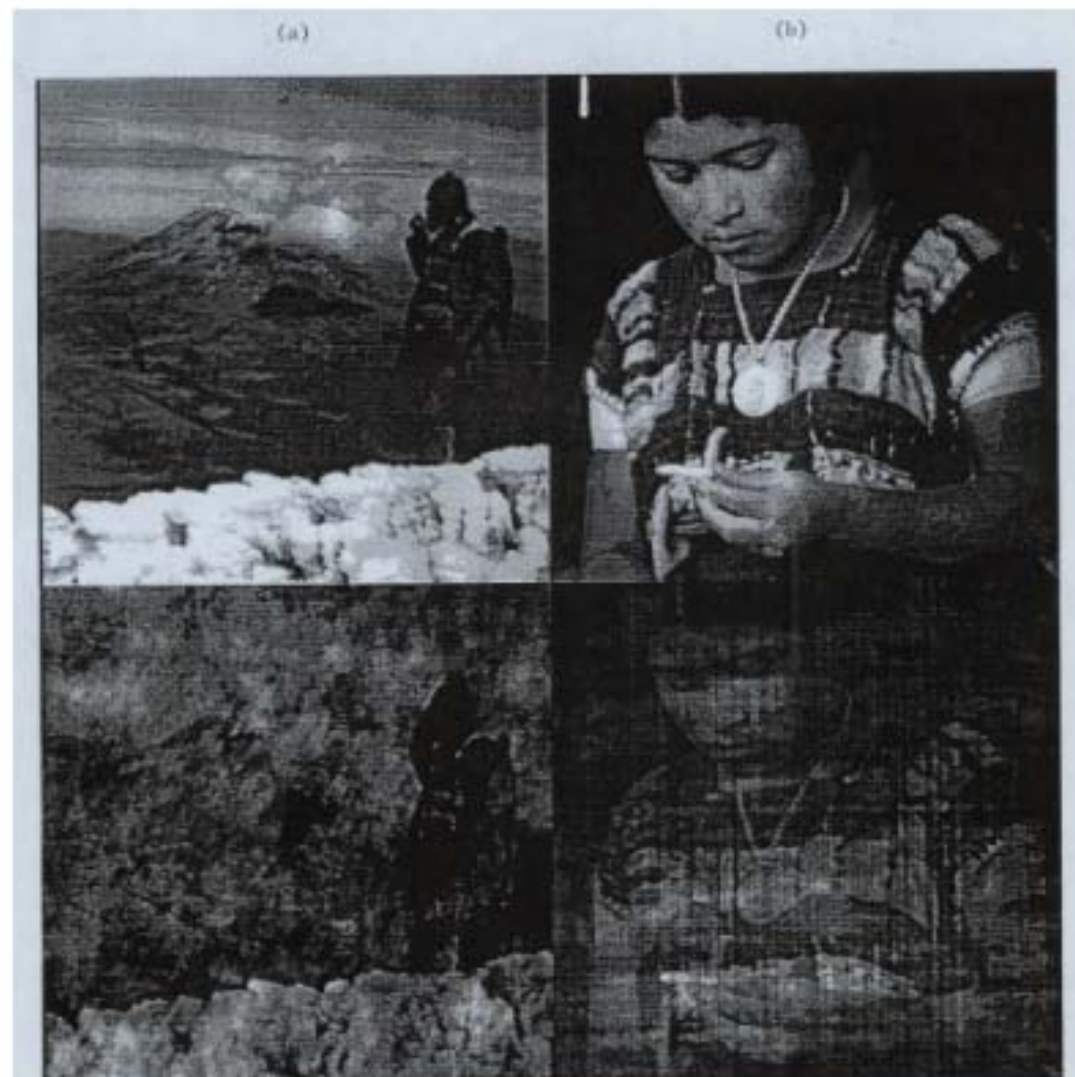


Figure 1.2

A graphic illustration of the phase problem: (a) and (b) are the original images. (c) is the (Fourier) reconstruction which has the Fourier phases of (a) and Fourier amplitudes of (b); (d) is the reconstruction with the phases of (b) and the amplitudes of (a).

## 2-D Crystals (Adsorbed Monolayers, Films)

If  $\bar{R}_\ell$  are all restricted to say the  $(x,y)$  plane,  $z$ -component of  $\bar{q}$  will not affect

$\Rightarrow$  diffraction is on rods in reciprocal space through the  $\bar{G}_{\parallel}$  and parallel to  $z$ -axis

$$S(\bar{q}) = \sum_{\ell\ell'} e^{i\bar{q} \cdot (\bar{R}_\ell - \bar{R}_{\ell'})}$$

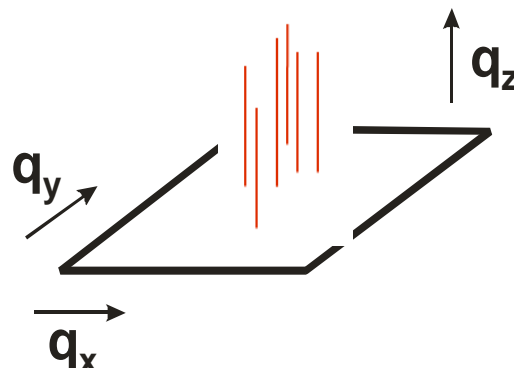
which is thus independent of  $q_z$ .

$$S(q) \propto \sum_{G_{\parallel}} \delta(\bar{q}_{\parallel} - \bar{G}_{\parallel})$$

where

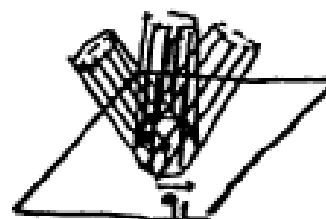
$\bar{G}_{\parallel}$  is 2-D reciprocal lattice vector in plane

$\bar{q}_{\parallel}$  is  $(x,y)$  plane component of  $\bar{q}$



Only  $q_z$ -dependence of I along rod is due to  $f(\bar{q})e^{-2W}$  (functions of  $q_z$  but slowly varying)

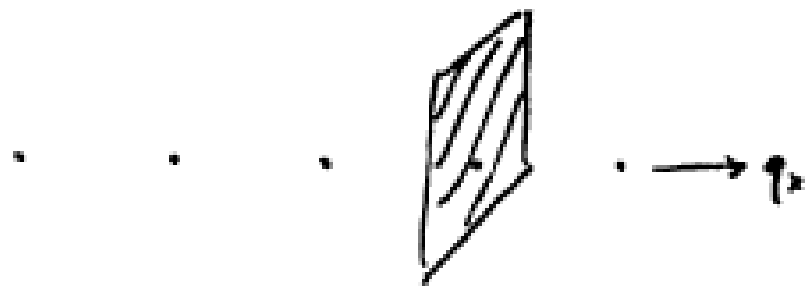
### Powders of 2-D Crystals



asymmetric (saw-tooth) powder peak shape

(Warren)

## 1-D Crystals



$S(\bar{q})$  independent of  $q_z$  and  $q_y$ . Planes of scattering in reciprocal space.

# Small Angle Scattering (SANS) (SAXS)

Length scale probed in a scattering experiment at

wave-vector transfer  $\bar{q}$  is  $\sim \left( \frac{2\pi}{q} \right)$  (e.g., Bragg scattering  $d_{hkl} \sim \frac{2\pi}{G_{hkl}}$ )

Thus small  $\bar{q}$  scattering probes large length scales, not atomic or molecular structure.

At small  $q$ , one can consider “smeared out” nuclear or electron density varying relatively slowly in space.

$$I(\bar{q}) \propto \iiint d\bar{r} d\bar{r}' e^{-i\bar{q} \cdot (\bar{r} - \bar{r}')} \langle \rho_s(\bar{r}) \rho_s(\bar{r}') \rangle$$

where

$\rho_s(\bar{r})$  = scattering length (average) density for  
neutrons  
= electron density for electrons.

Since uniform  $\rho_s(\vec{r})$  would give only forward scattering, we use the deviations (contrast) from the average density

$$I(q) \propto \iint d\vec{r} d\vec{r}' e^{-i\vec{q} \cdot (\vec{r} - \vec{r}')} \langle \delta\rho_s(\vec{r}) \delta\rho_s(\vec{r}') \rangle$$

### Single Particles (Dilute Limit)

Let  $\rho_0$  be average *sld* (e.g., embedding media or solvent)

$\rho_1$  be average *sld* of particle (assume uniform)

$$I(\vec{q}) \propto (\rho_1 - \rho_0)^2 \left| \int_V d\vec{r} e^{-i\vec{q} \cdot \vec{r}} \right|^2 = (\rho_1 - \rho_0)^2 |f(\vec{q})|$$

where  $V$  is over volume of particle,  $f(\vec{q})$  is determined by shape of particle, e.g., for sphere of radius  $R$ ,

$$f(q) = (V_0) \frac{\sin(qR) - qR \cos(qR)}{(qR)^3} \quad V_0 = \text{Particle Volume}$$

origin of  $\vec{r}$  is taken as centroid of particle.

Expanding exponential,

$$\int_V d\vec{r} e^{-i\vec{q} \cdot \vec{r}} = V_0 - i\vec{q} \cdot \int_V \vec{r} d\vec{r} - \frac{1}{2} \int_V d\vec{r} (\vec{q} \cdot \vec{r})^2 + \dots$$

$$\simeq V_0 \left[ 1 - \frac{1}{2} \frac{\int_V d\vec{r} (\vec{q} \cdot \vec{r})^2}{\int_V d\vec{r}} + \dots \right]$$

$$= V_0 \left[ 1 - \frac{q^2}{6} \frac{\int_V d\vec{r} r^2}{\int_V d\vec{r}} + \dots \right]$$

$r_G^2 \quad r_G = \text{radius of gyration}$

$$\text{so } I(\vec{q}) \propto (\rho_1 - \rho_0)^2 V_0^2 = \left[ 1 - \frac{1}{3} q^2 r_G^2 + \dots \right] \quad \text{approx.}$$

$$I(\vec{q}) \simeq A (\rho_1 - \rho_0)^2 V_0^2 e^{-\frac{1}{3} q^2 r_G^2}$$

↓  
Guinier Approxn.

## Determining Particle Size From Dilute Suspensions

- Particle size is usually deduced from dilute suspensions in which inter-particle correlations are absent
- In practice, instrumental resolution (finite beam coherence) will smear out minima in the form factor
- This effect can be accounted for if the spheres are mono-disperse
- For poly-disperse particles, maximum entropy techniques have been used successfully to obtain the distribution of particles sizes

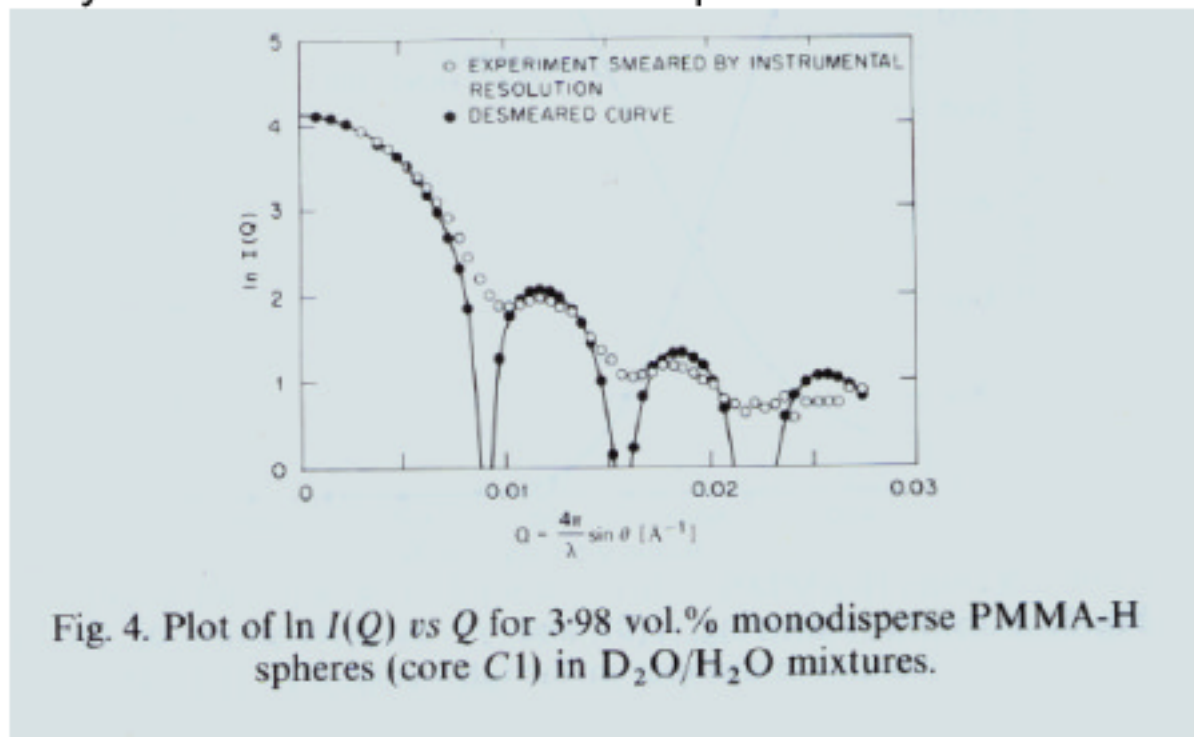
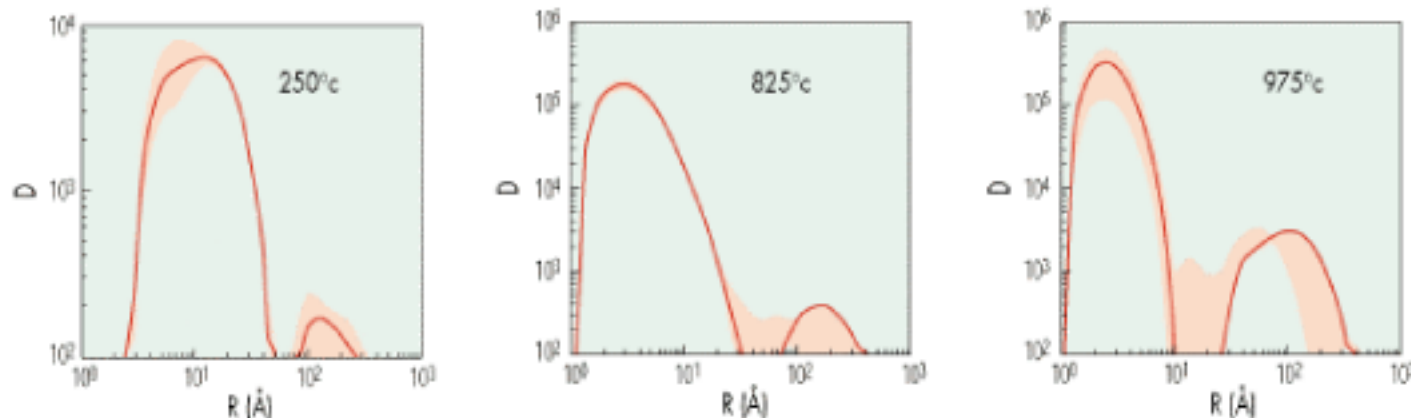
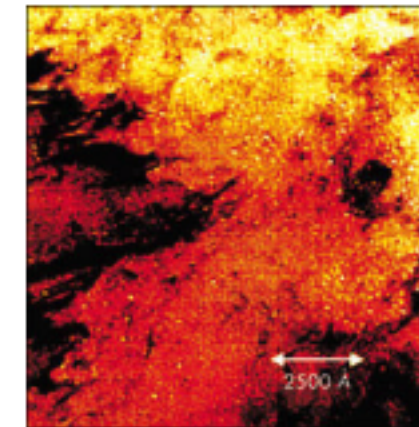


Fig. 4. Plot of  $\ln I(Q)$  vs  $Q$  for 3.98 vol.% monodisperse PMMA-H spheres (core C1) in  $\text{D}_2\text{O}/\text{H}_2\text{O}$  mixtures.

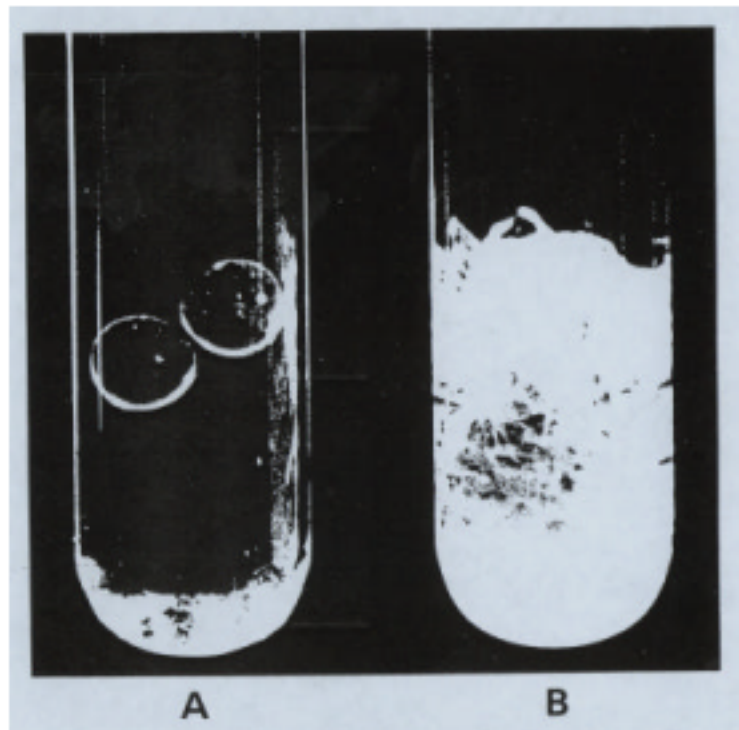
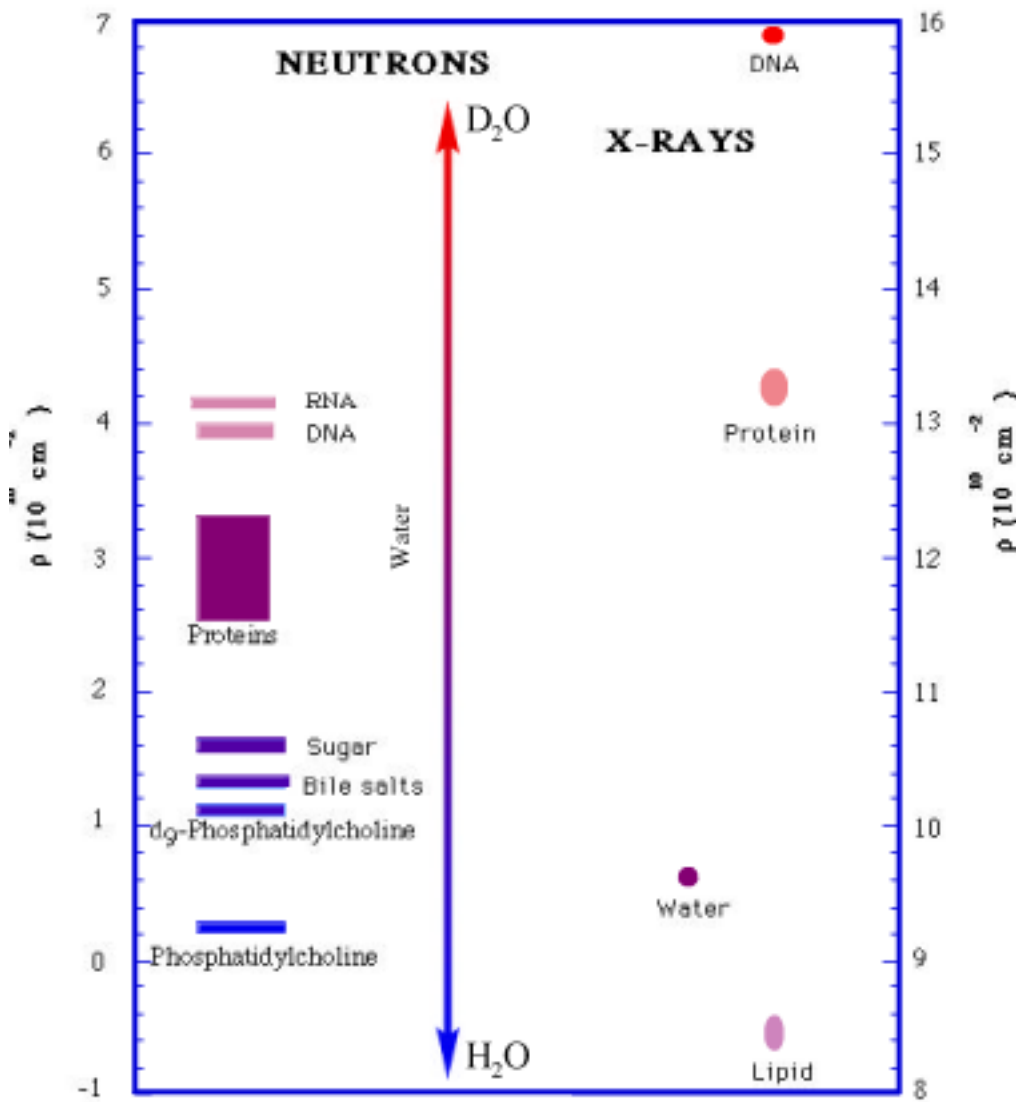
# Size Distributions Have Been Measured for Helium Bubbles in Steel

- The growth of He bubbles under neutron irradiation is a key factor limiting the lifetime of steel for fusion reactor walls
  - Simulate by bombarding steel with alpha particles
- TEM is difficult to use because bubble are small
- SANS shows that larger bubbles grow as the steel is annealed, as a result of coalescence of small bubbles and incorporation of individual He atoms



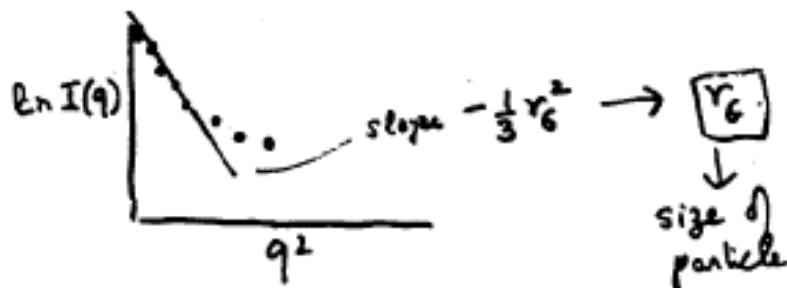
SANS gives bubble volume (arbitrary units on the plots) as a function of bubble size at different temperatures. Red shading is 80% confidence interval.

# Contrast & Contrast Matching



Both tubes contain borosilicate beads + pyrex fibers + solvent. (A) solvent refractive index matched to pyrex;. (B) solvent index different from both beads and fibers – scattering from fibers dominates

\* Chart courtesy of Rex Hjelm



$$S_0(\bar{q}) = \sum_{\ell\ell'} e^{i\bar{q} \cdot (\bar{R}_\ell - \bar{R}_{\ell'})} = \text{S.F. of centers of particles}$$

→ Liquid- or glass-like

**Fractals** These are systems which are scale-invariant (usually in a statistically averaged sense) i.e.,  $R \rightarrow \kappa R$ , the object resembles itself ("self-similarity")

**Property:** If  $n(R)$  is number of particles inside a sphere of radius  $R$

$$n(R) \sim R^D$$

$D$  = Fractal (Hausdorff) Dimension

It follows that

$$4\pi R^2 dR g(R) = CR^{D-1} dR \quad C = \text{constant}$$

$$\therefore g(R) = \frac{C}{4\pi} R^{D-3} = \frac{C}{4\pi} \frac{1}{R^{3-D}}$$

$$\therefore S_0(\bar{q}) = \int d\bar{R} e^{-i\bar{q} \cdot \bar{R}} g(R) = \text{Const} \times \frac{1}{q^D}$$

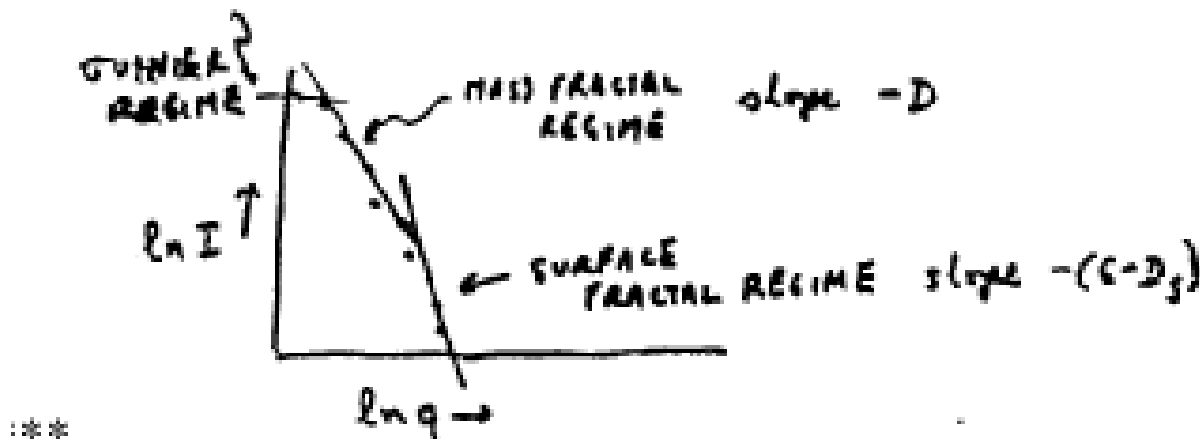
### Small-Angle Scattering Is Used to Study:

- { Sizes } of particles in dilute solution (Polymers, Shapes Micelles, Colloids, Proteins, Precipitates, ...)
- Correlation between particles in concentrated solutions (Aggregates, Fractals, Colloidal Crystals and Liquids)
- 2-component or multicomponent systems (Binary fluid mixtures, Porous Media, Spinodal Decomposition)

For colloidal, micellar liquids:

$$S(\bar{q}) = \sum_{\ell\ell'} f_\ell(\bar{q}) f_{\ell'}^*(\bar{q}) e^{i\bar{q} \cdot (\bar{R}_\ell - \bar{R}_{\ell'})}$$

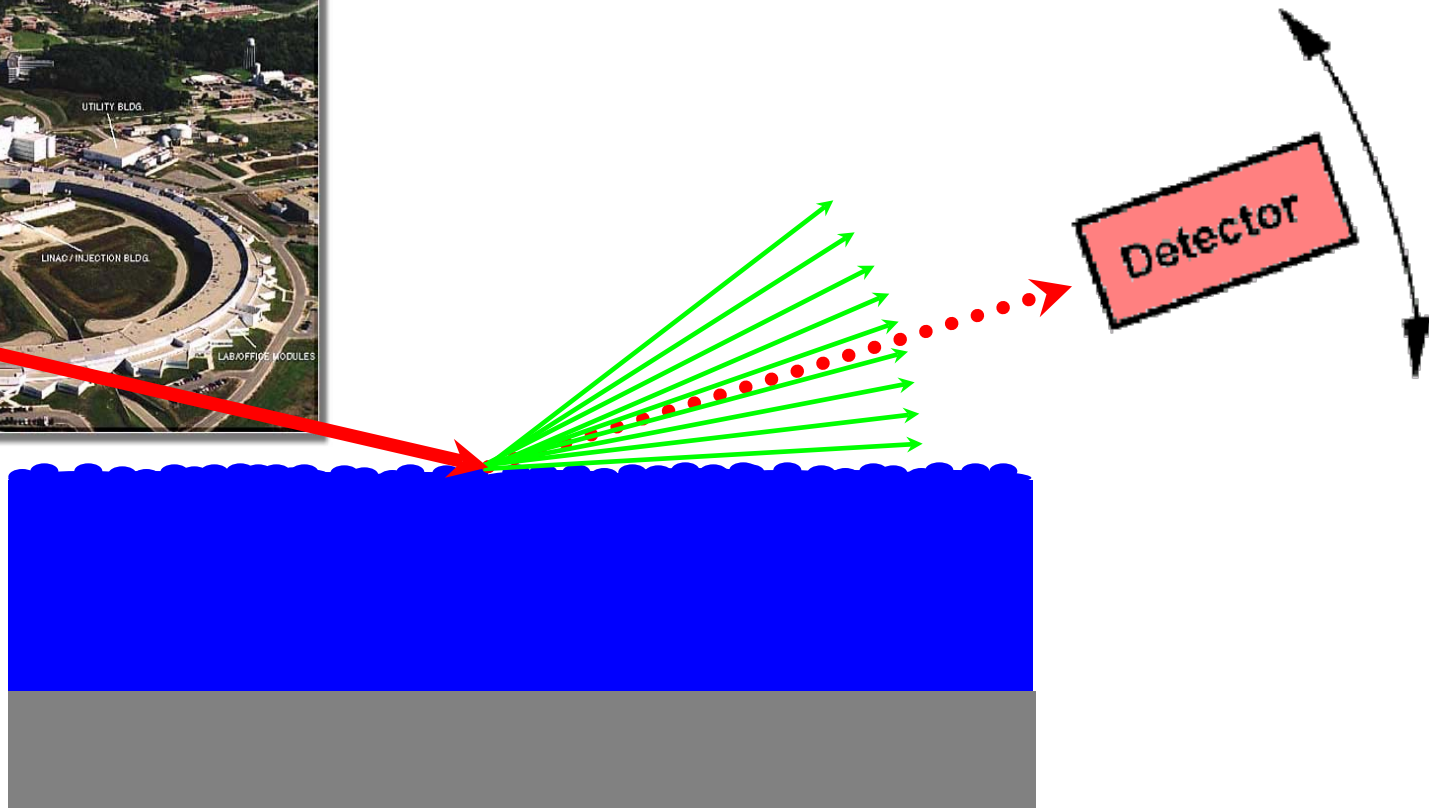
$$\xrightarrow{\text{Form Factor}} = [f_\ell(\bar{q})]^2 S_0(\bar{q}) \xleftarrow{\text{Structure Factor}}$$



examples: Aggregates of micelles, colloids, granular materials, rocks\*

$$\text{Surface fractals } S(q) \sim \frac{1}{q^{S-D_S}}$$

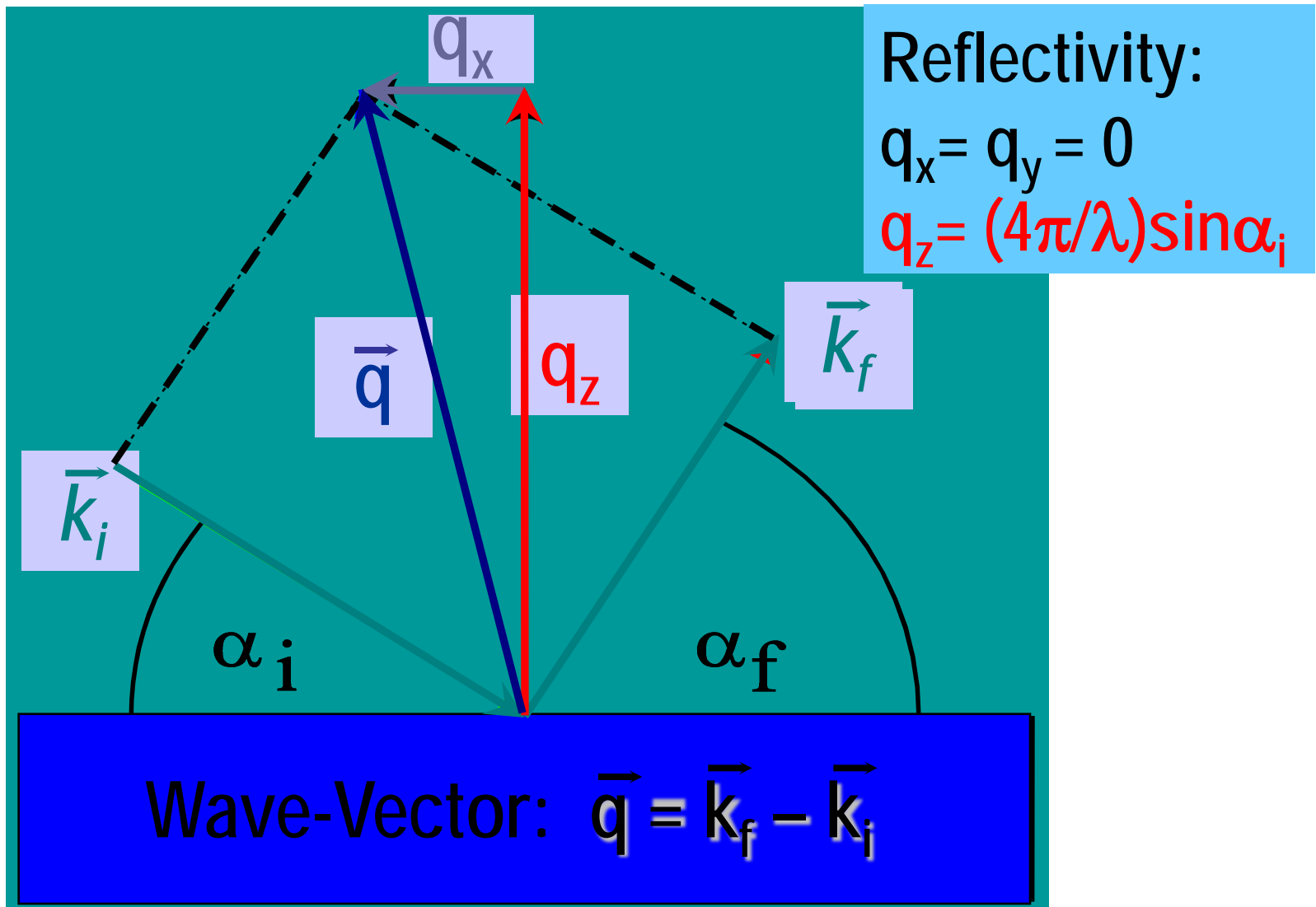
# X-Ray Scattering from Surfaces and Interfaces



# Applications of Surface/Interface Scattering

- study the morphology of surface and interface roughness
- wetting films
- film growth exponents
- capillary waves on liquid surfaces (polymers, microemulsions, liquid metals, etc.)
- islands on block copolymer films
- pitting corrosion
- magnetic roughness
- study the morphology of magnetic domains in magnetic films.
- Nanodot arrays
- Tribology, Adhesion, Electrodeposition

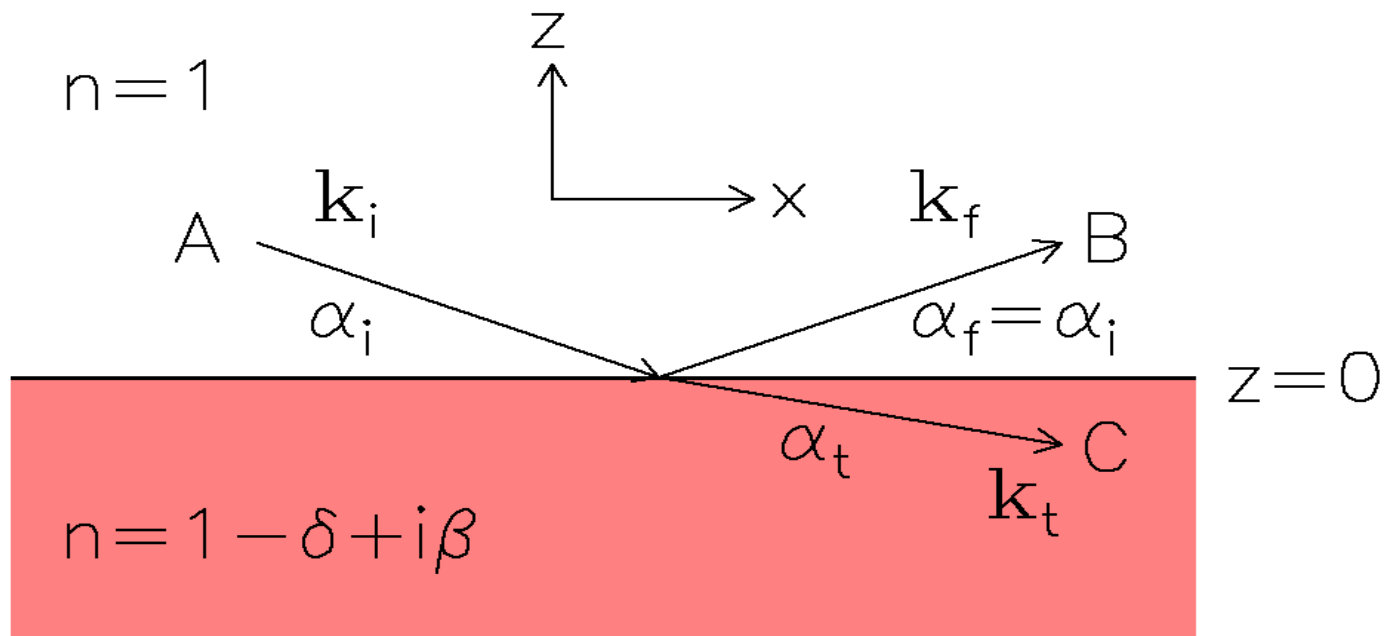
# Scattering Geometry & Notation



# Perfect & Imperfect „Mirrors“



# Basic Equation: X-Rays



Helmholtz-Equation & Boundary Conditions

$$\Delta E(\vec{r}) + k^2 n_x^2(\vec{r}) E(\vec{r}) = 0$$

# Refractive Index: X-Rays & Neutrons

$$n_x^2(\vec{r}) = 1 + N \frac{e^2}{m \varepsilon_0} \frac{f(\vec{r}, E)}{\omega_0^2 - \omega^2 - 2i \eta_0 \omega} + \text{magnetic part}$$

$$n_n^2(\vec{r}) = 1 - \frac{2m\lambda^2}{h^2} V(\vec{r}) + \text{magnetic part}$$

$$n(\vec{r}) = 1 - \delta(\vec{r}) + i \beta(\vec{r})$$

Minus!!

Dispersion

Absorption

# Refractive Index: X-Rays & Neutrons

$$n_x^2(\vec{r}) = 1 + N \frac{e^2}{m \varepsilon_0} \frac{f(\vec{r}, E)}{\omega_0^2 - \omega^2 - 2i \eta_0 \omega} + \text{magnetic part}$$

$$n_n^2(\vec{r}) = 1 - \frac{2m\lambda^2}{h^2} V(\vec{r}) + \text{magnetic part}$$

$$n(\vec{r}) = 1 - \delta(\vec{r}) + i \beta(\vec{r})$$

Minus!!

Dispersion

Absorption

# Refractive Index: X-Rays

$$n(z) = 1 - \frac{\lambda^2}{2\pi} r_e \varrho(z) + i \frac{\lambda}{4\pi} \mu(z)$$

	$r_e \varrho (10^{10} \text{cm}^{-2})$	$\delta (10^{-6})$	$\mu (\text{cm}^{-1})$	$\alpha_c (^{\circ})$
Vacuum	0	0	0	0
PS ( $\text{C}_8\text{H}_8$ ) <sub>n</sub>	9.5	3.5	4	0.153
PMMA ( $\text{C}_5\text{H}_8\text{O}_2$ ) <sub>n</sub>	10.6	4.0	7	0.162
PVC ( $\text{C}_2\text{H}_3\text{Cl}$ ) <sub>n</sub>	12.1	4.6	86	0.174
PBrS ( $\text{C}_8\text{H}_7\text{Br}$ ) <sub>n</sub>	13.2	5.0	97	0.181
Quartz ( $\text{SiO}_2$ )	18.0–19.7	6.8–7.4	85	0.21–0.22
Silicon (Si)	20.0	7.6	141	0.223
Nickel (Ni)	72.6	27.4	407	0.424
Gold (Au)	131.5	49.6	4170	0.570

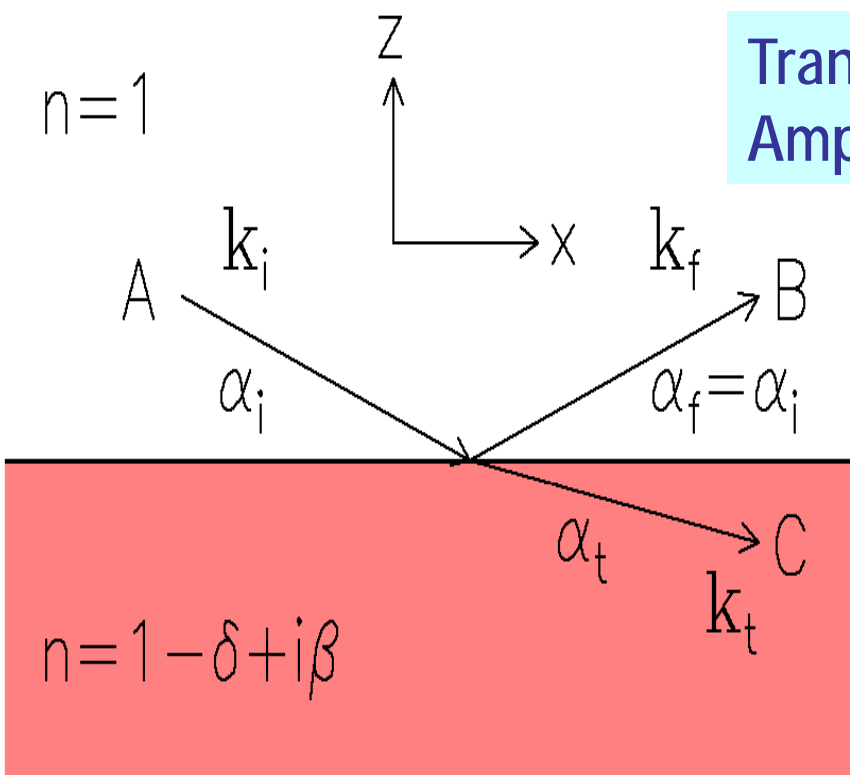
$$\varrho(z) = \langle \varrho(x, y, z) \rangle_{x,y}$$

Electron Density  
Profile !

$$E = 8 \text{ keV} \quad \lambda = 1.54 \text{ \AA}$$

# Single Interface: Vacuum/Matter

## Fresnel- Formulae



Reflected  
Amplitude

$$r = \frac{B}{A} = \frac{k_{i,z} - k_{t,z}}{k_{i,z} + k_{t,z}}$$

Transmitted  
Amplitude

$$t = \frac{C}{A} = \frac{2 k_{i,z}}{k_{i,z} + k_{t,z}}$$

Wave-  
Vectors

$$k_{i,z} = k \sin \alpha_i$$

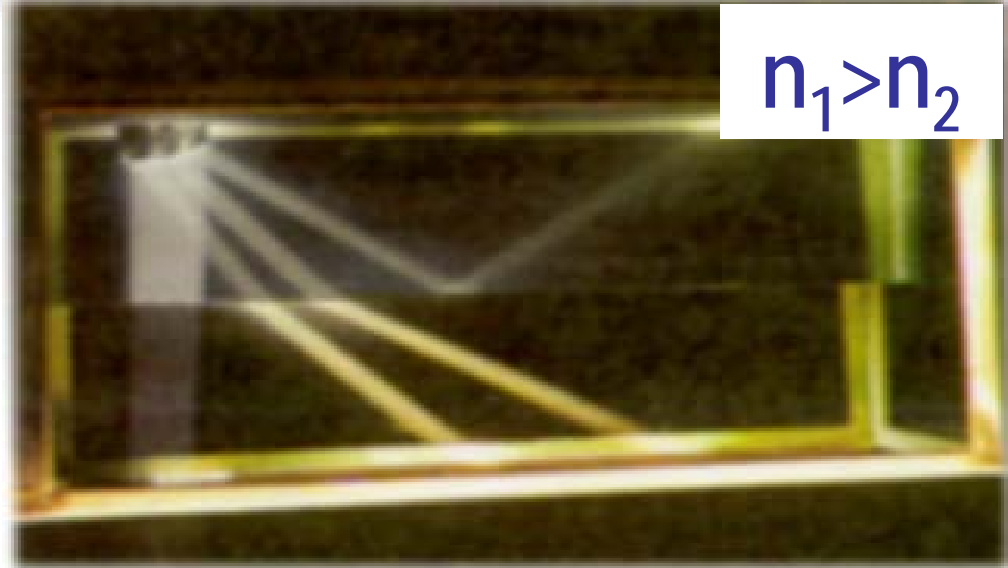
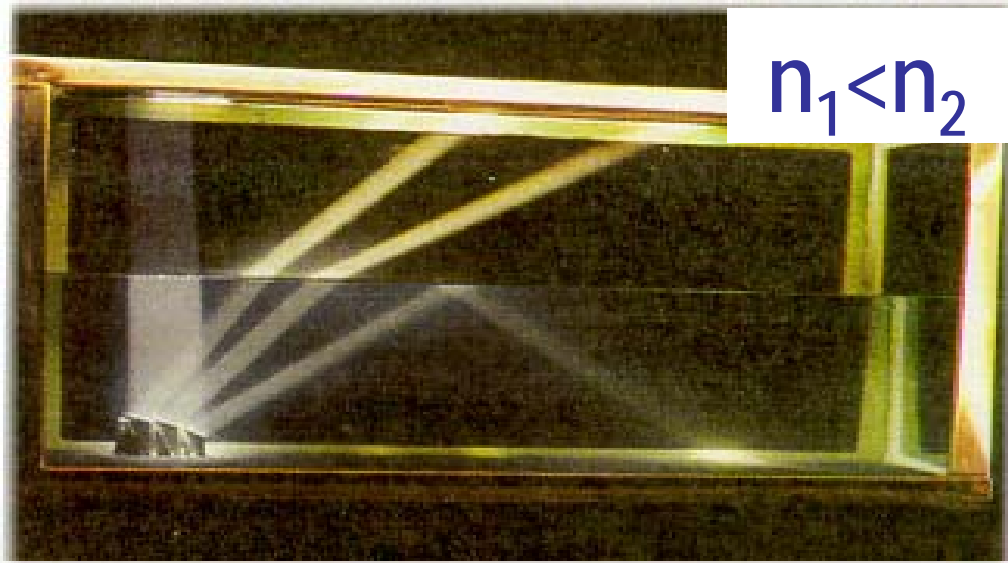
$$k_{t,z} = k(n^2 - \cos^2 \alpha_i)^{1/2}$$

# X-Ray Reflectivity: Principle

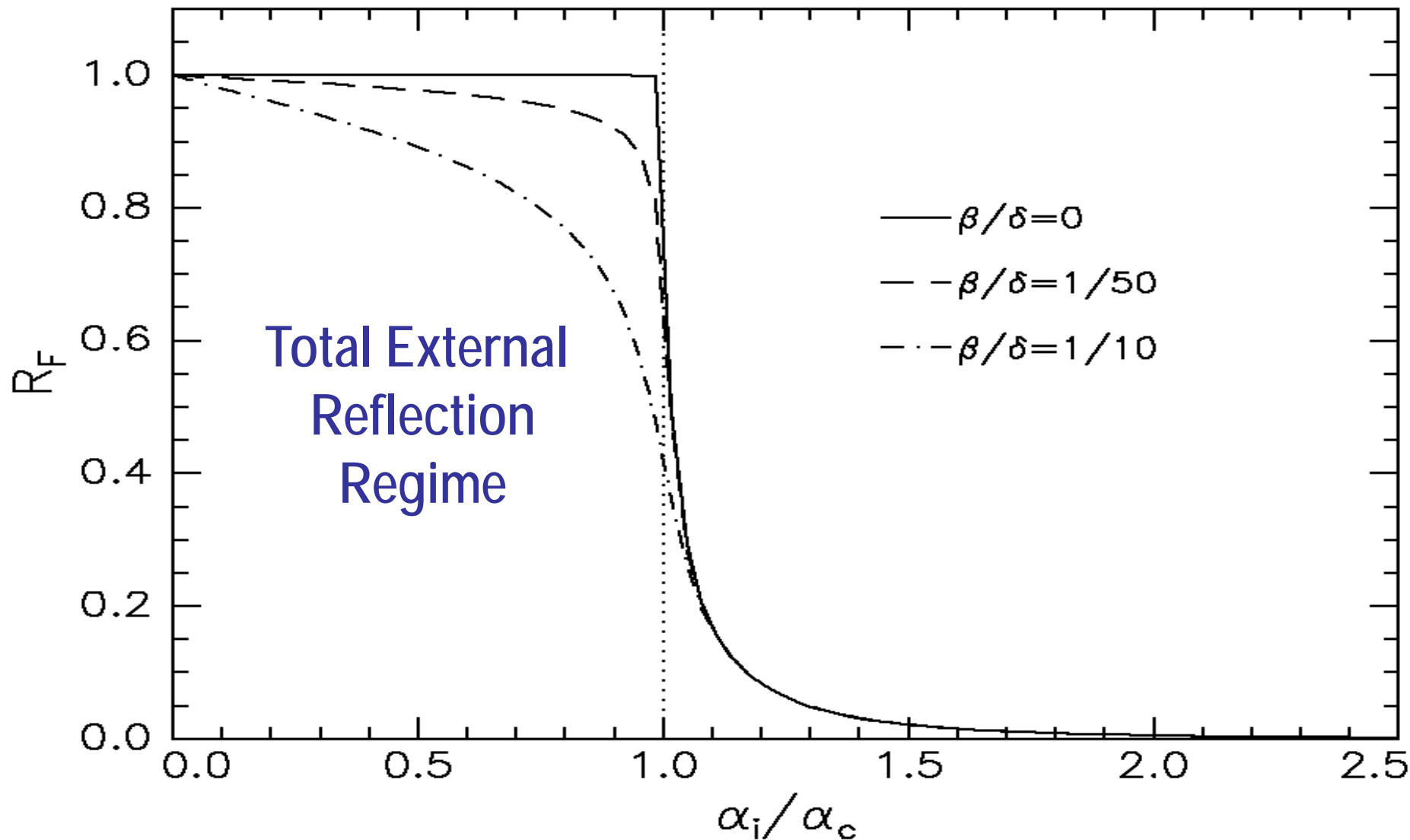
Visible Light  
Reflectivity:

$$\frac{n_1}{n_2} > 1$$

X-Ray  
Reflectivity:

$$\frac{n_1}{n_2} < 1$$


# Fresnel Reflectivity: $R_F(\alpha_i)$



# The „Master Formula“

## Reformulation for Interfaces

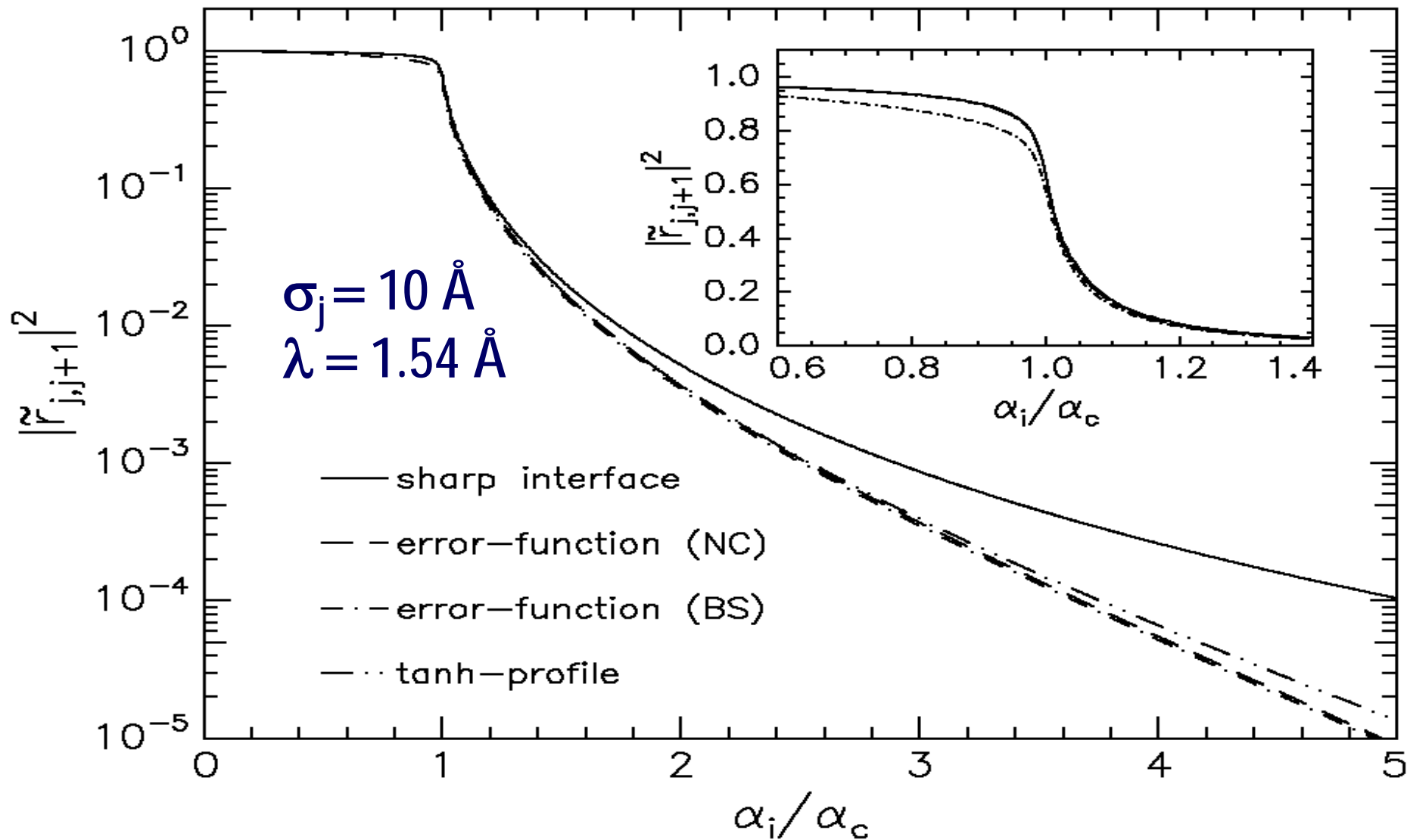
$$R(q_z) = R_F(q_z) \left| \frac{1}{\varrho_\infty} \int \frac{d\varrho(z)}{dz} \exp(i q_z z) dz \right|^2$$

Fresnel-Reflectivity  
of the Substrate

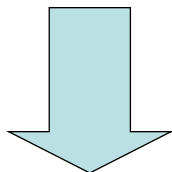
Electron Density Profile

$$R(q_z) = R_F \exp(-q_z^2 \sigma^2)$$

# Roughness Damps Reflectivity

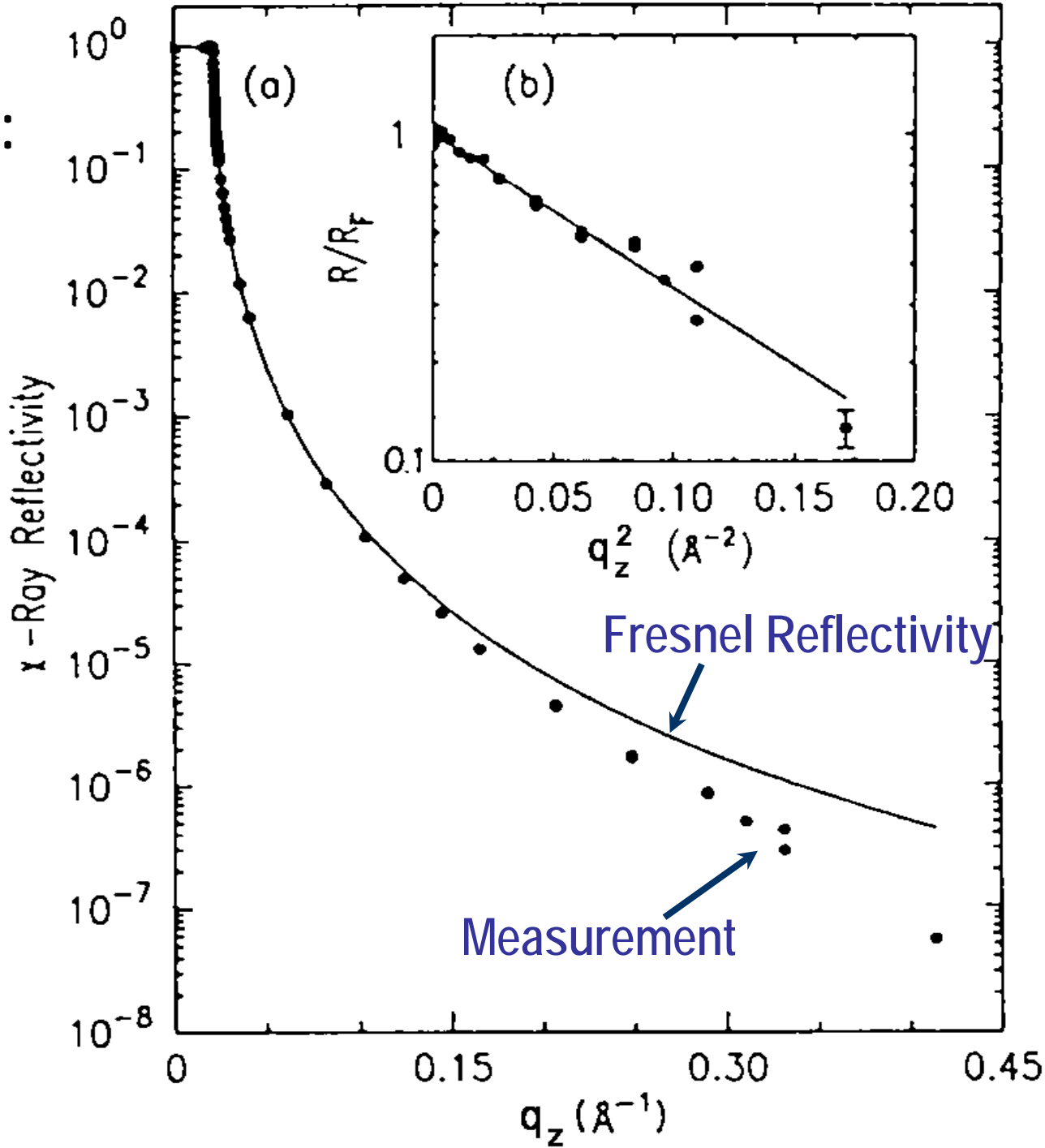


# X-Ray Reflectivity: Water Surface

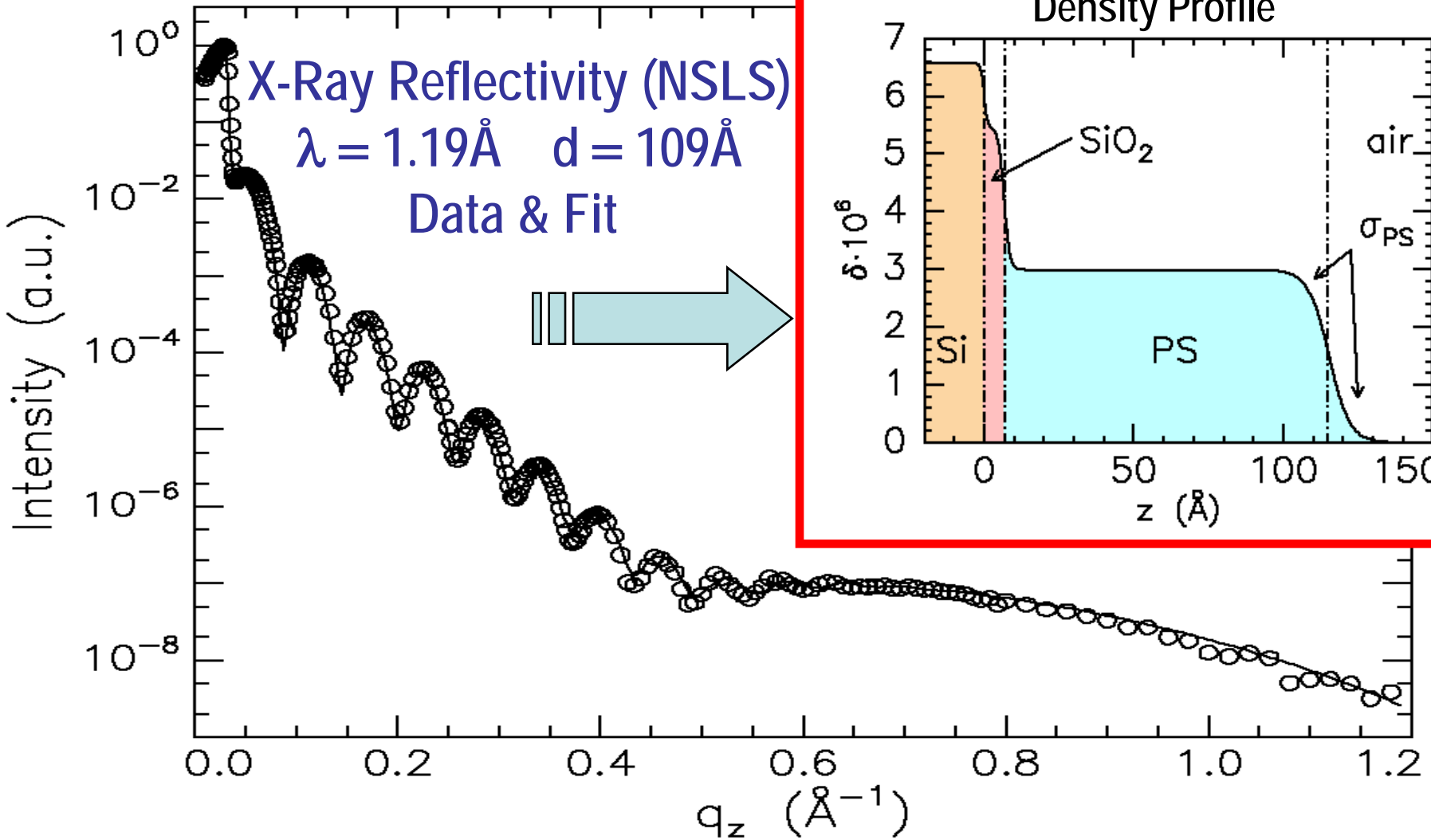


Difference  
Experiment-  
Theory:  
*Roughness !!*

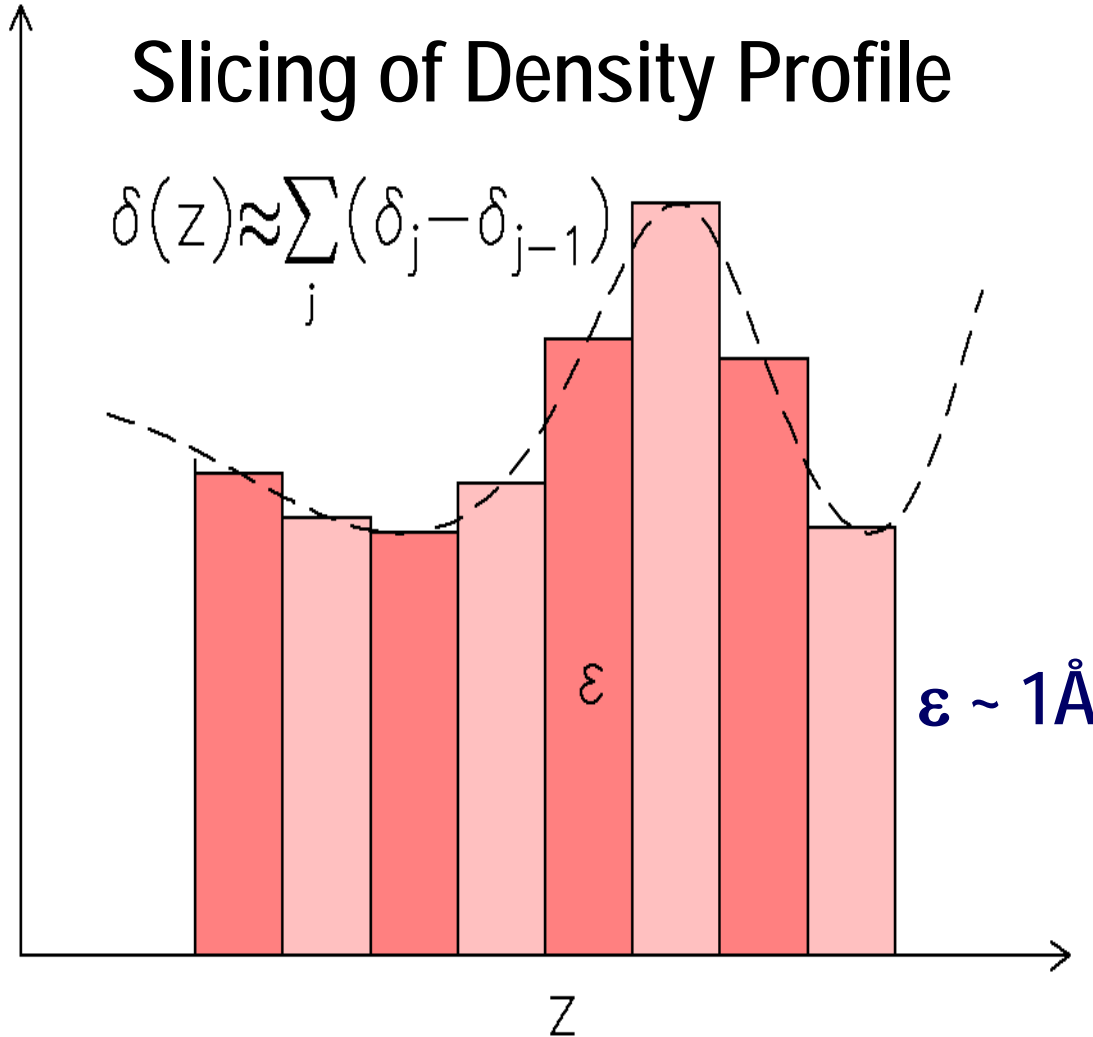
Braslau et al.  
PRL 54, 114 (1985)



# Example: PS Film on Si/SiO<sub>2</sub>



# Calculation of Reflectivity

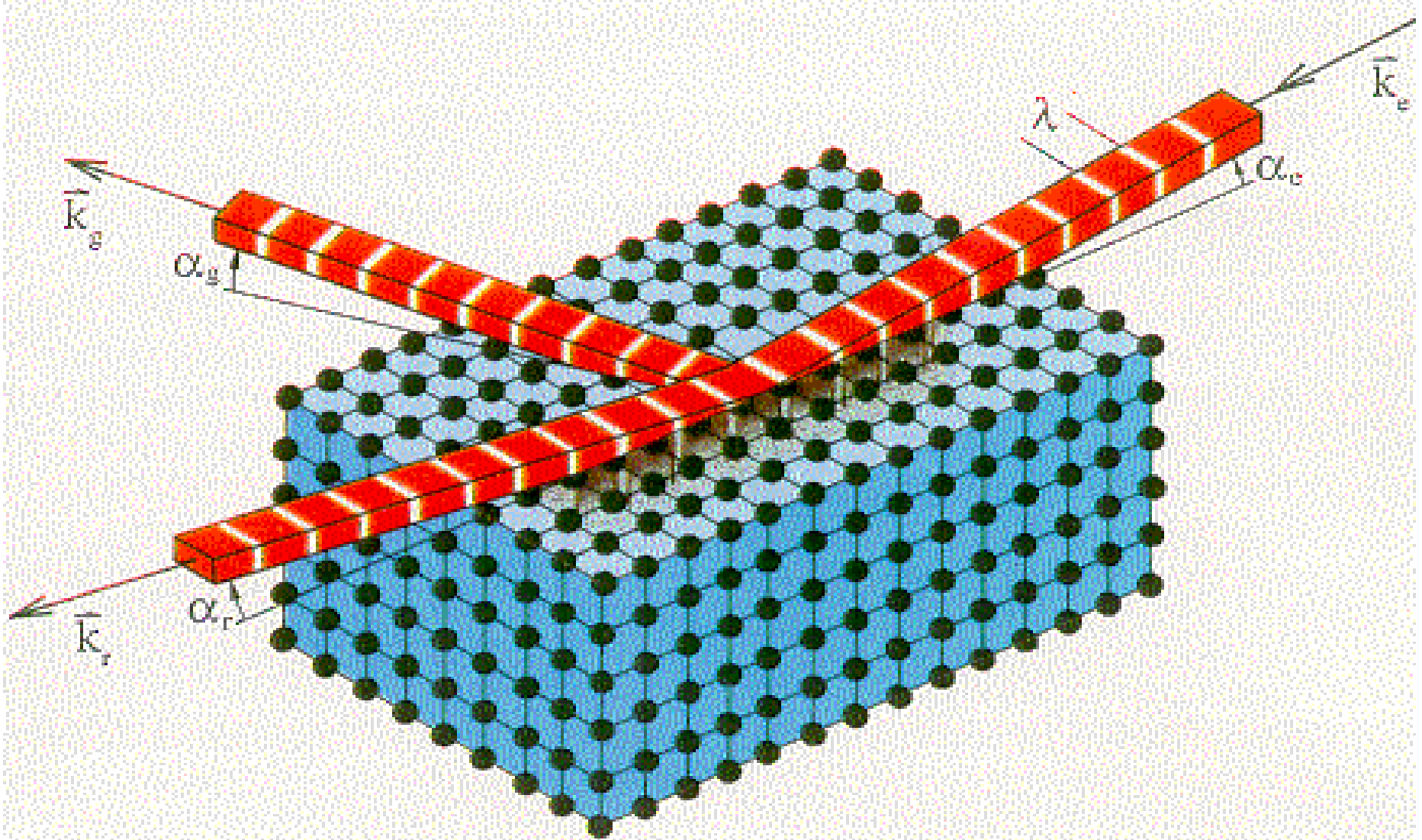


Slicing & Parratt-Iteration

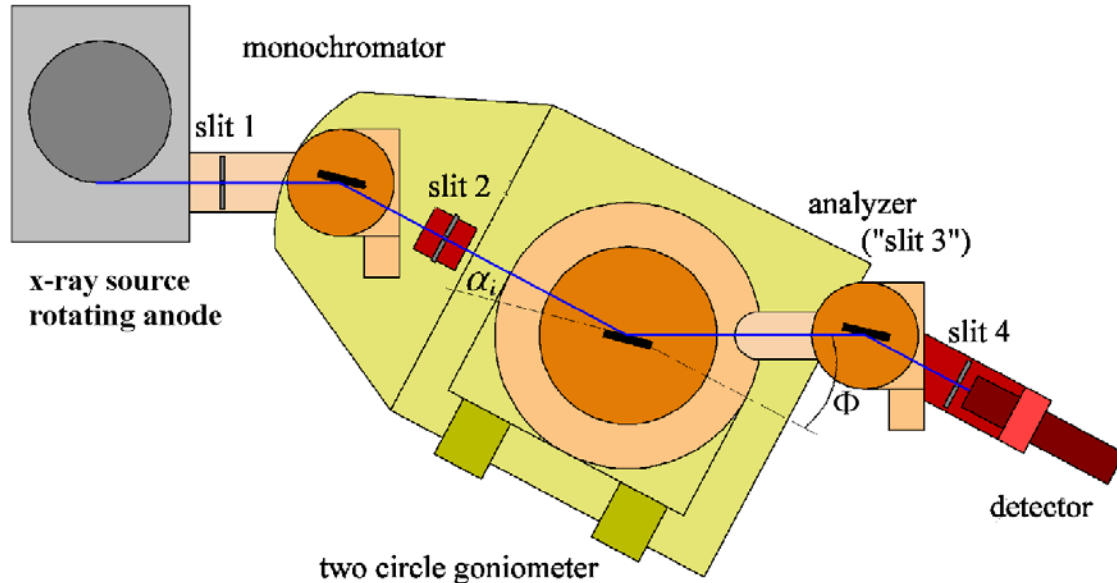
Reflectivity from Arbitrary Profiles !

- Drawback:  
Numerical Effort !

# Grazing-Incidence-Diffraction

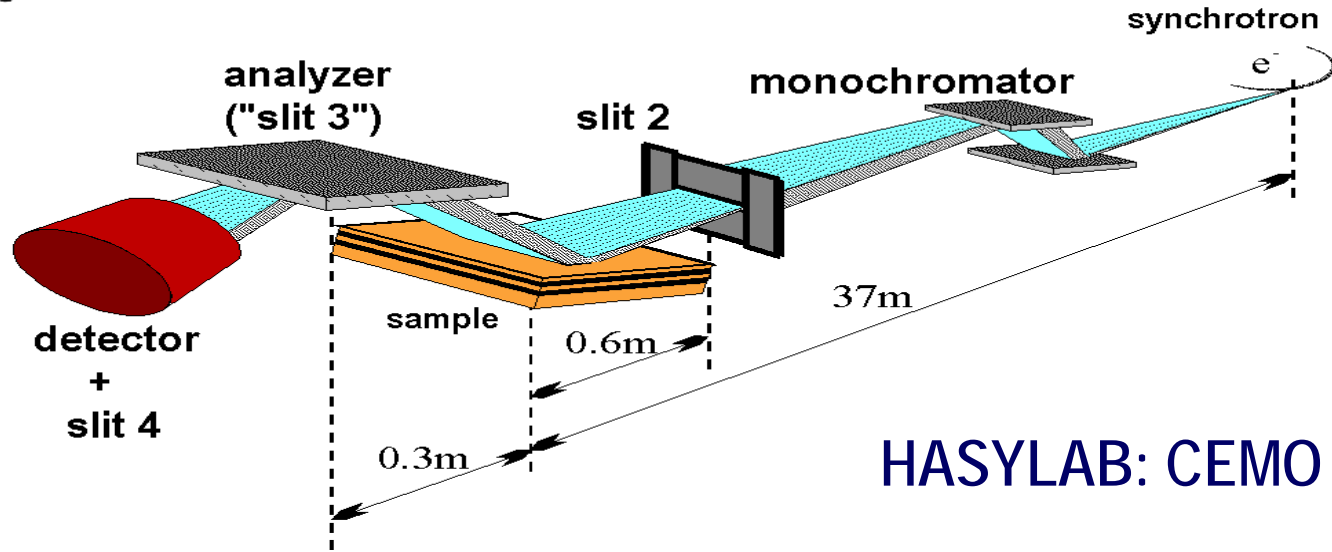


# X-Ray Reflectometers



*Laboratory  
Setup*

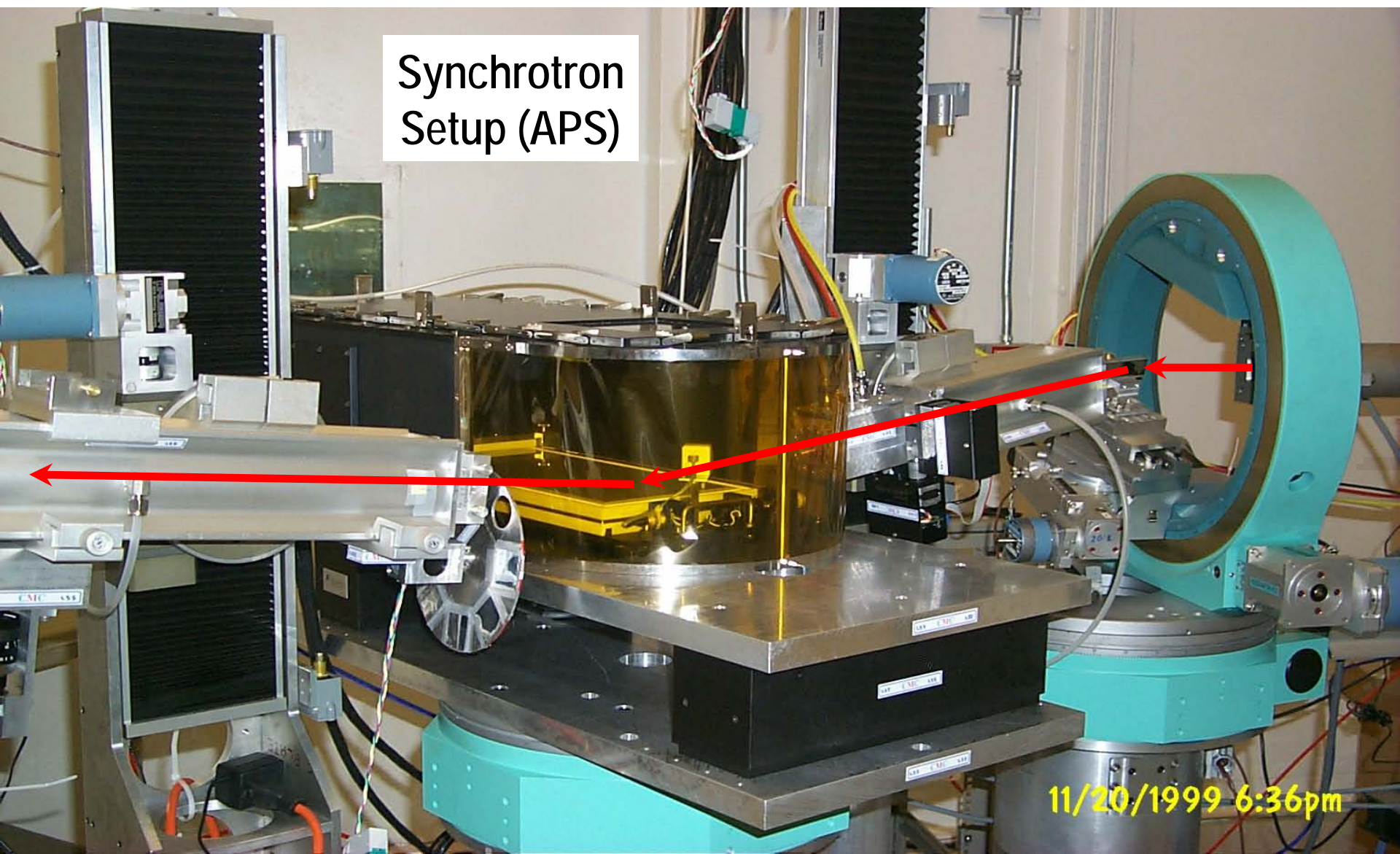
*Synchrotron  
Setup*



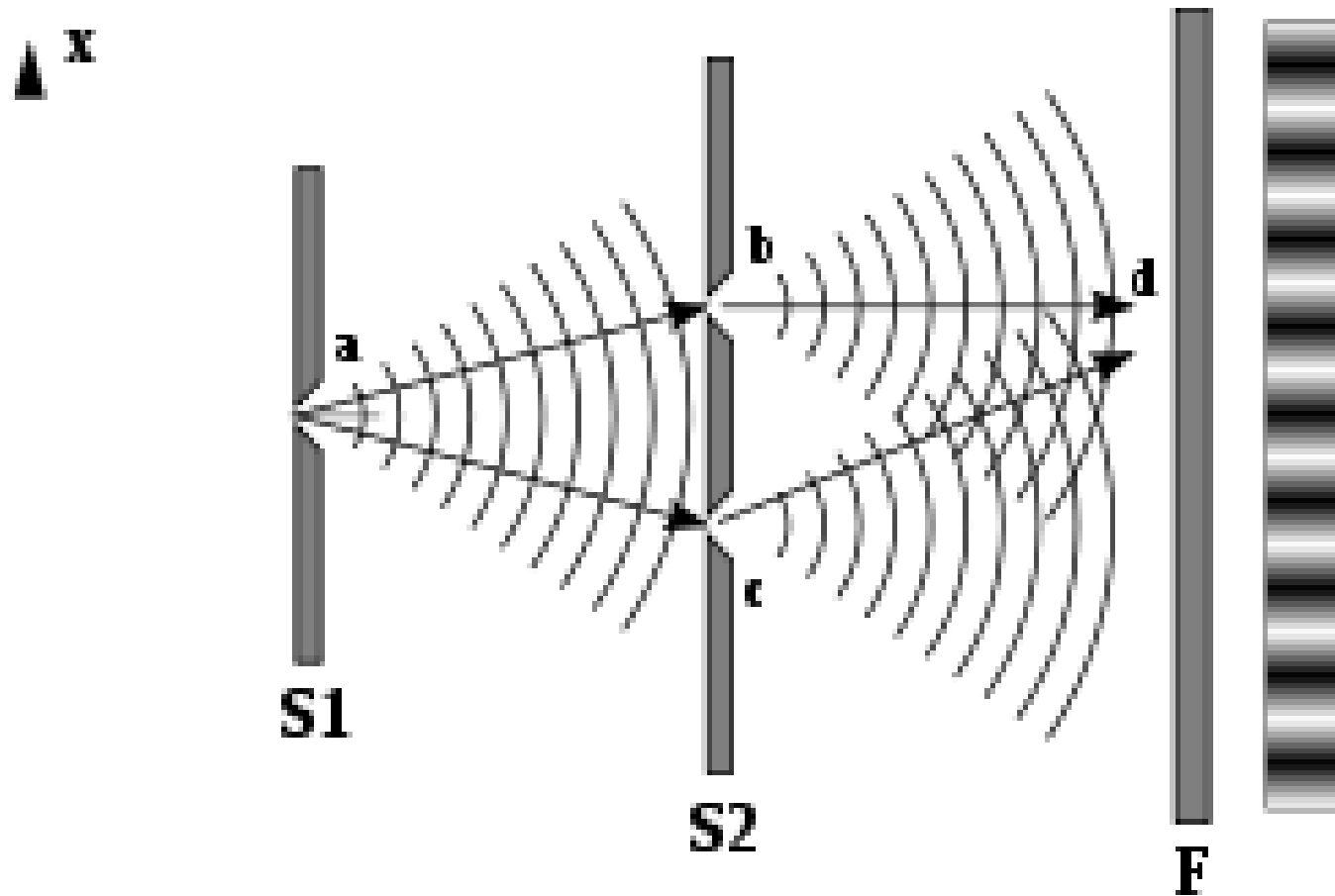
HASYLAB: CEMO

# Reflectivity from Liquids I

Synchrotron  
Setup (APS)



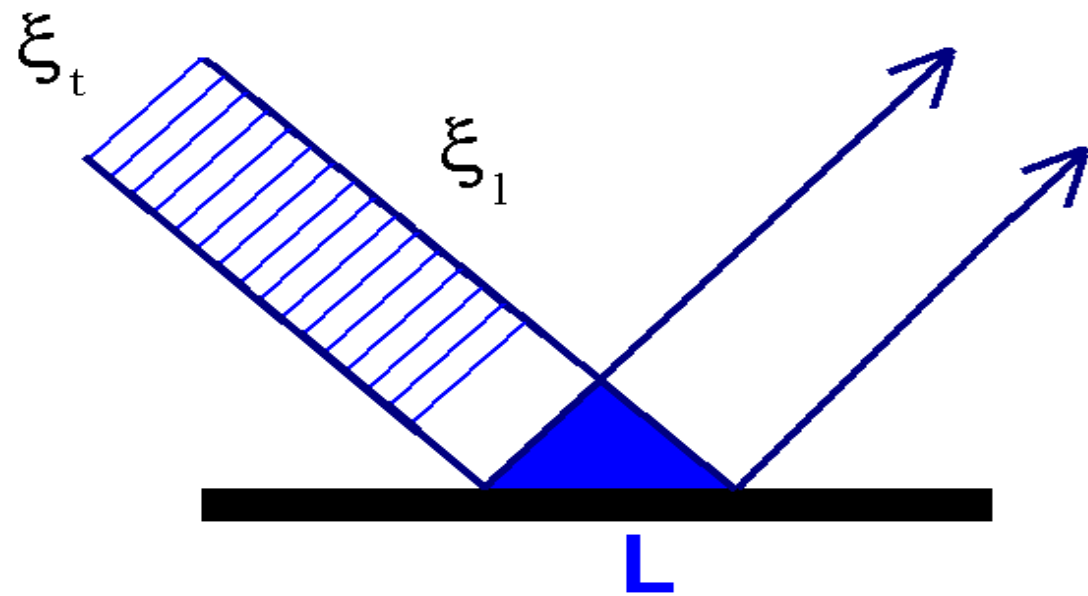
# Coherence of Light

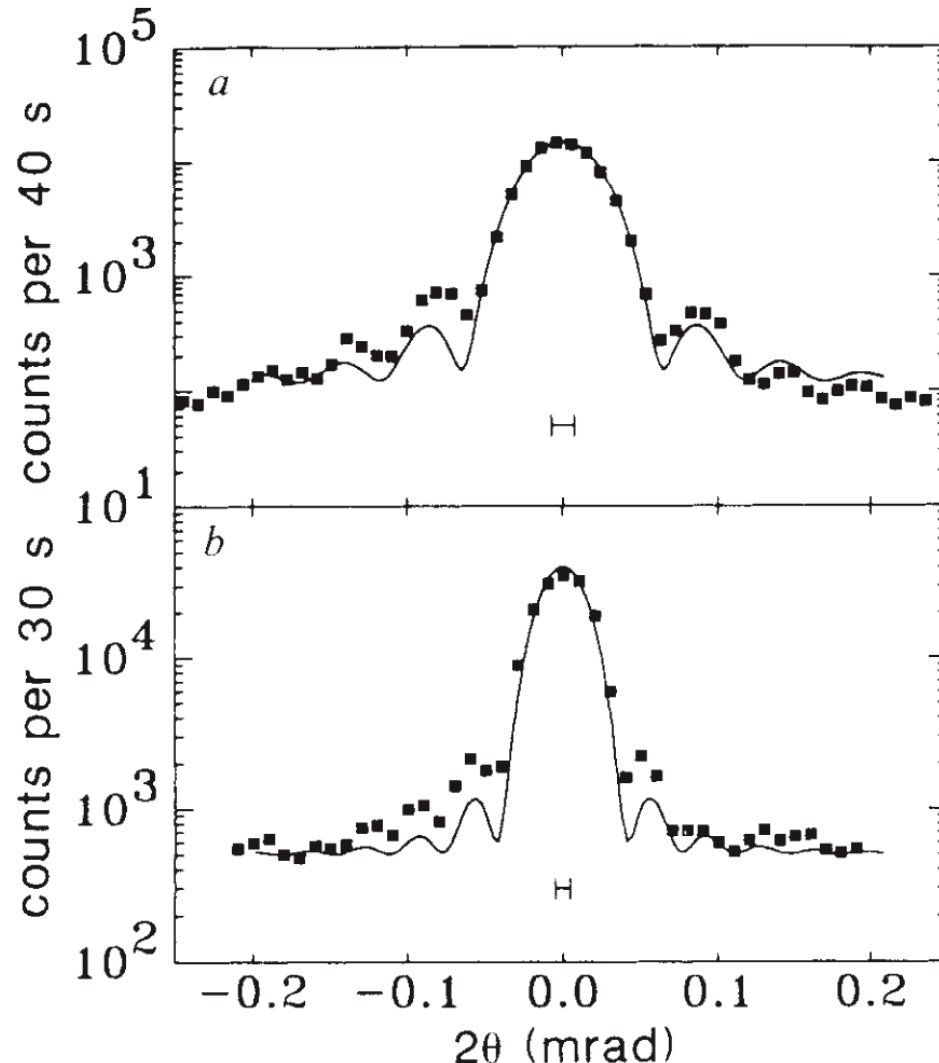


# Coherence Lengths

$$\xi_l = \lambda^2 / \Delta\lambda$$
$$= \lambda (\Delta\lambda / \lambda)^{-1}$$

$$\xi_t = \lambda R / s$$
$$(\xi_{\text{hor.}}, \xi_{\text{vert.}})$$





2 Fraunhofer diffraction from *a*, 2.5- $\mu\text{m}$  and *b*, 5- $\mu\text{m}$  nominal diameter holes. Error bars due to counting statistics are smaller than the symbol  $\square$ . The solid line represents the calculated diffraction pattern of a circular aperture convolved with the analyser resolution shown by the horizontal error bar. A constant background is included in the fit.

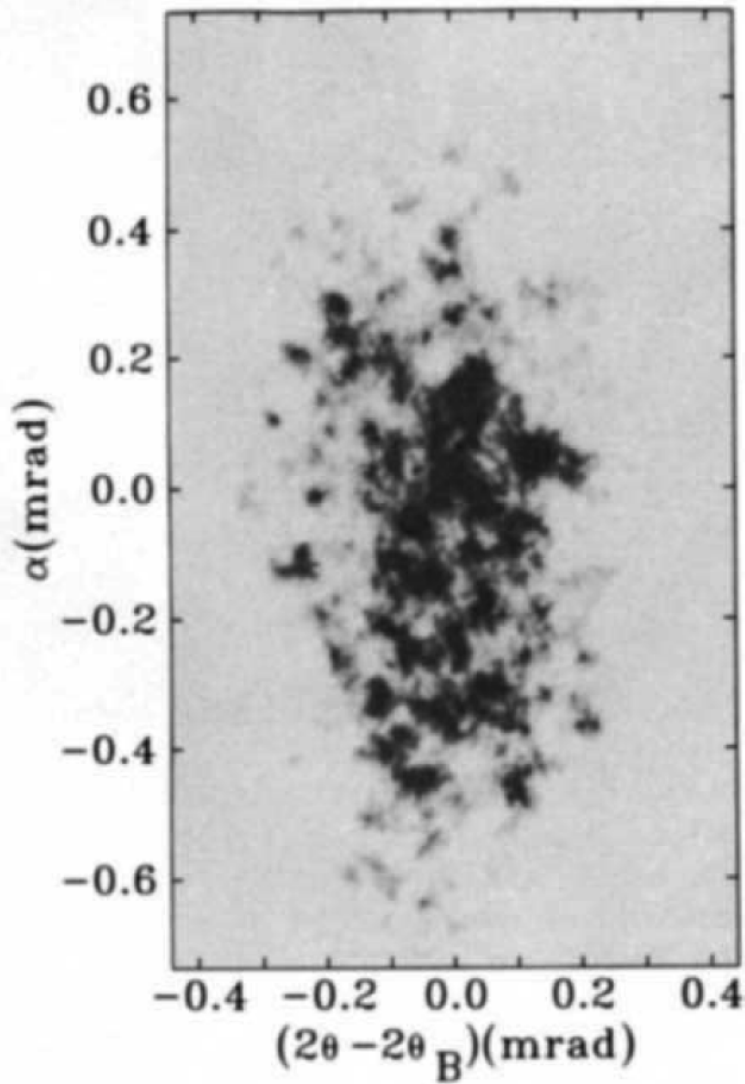


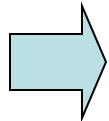
FIG. 3 Photograph of the speckle pattern in the diffuse (001) peak of  $\text{Cu}_3\text{B}$ , the collimating pinhole is  $2.5 \mu\text{m}$ .

NATURE · VOL 352 · 15 AUGUST 1991

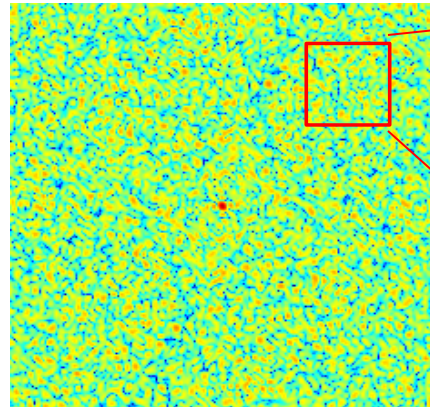
# Photon Correlation Spectroscopy

Brownian Motion of 100 particles

QuickTime™ and a Video decompressor are needed to see this picture.

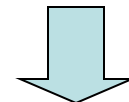


Diffraction Pattern

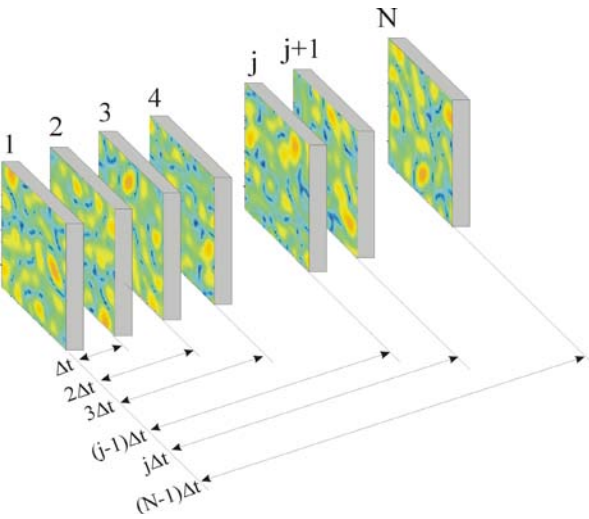
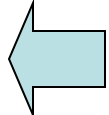
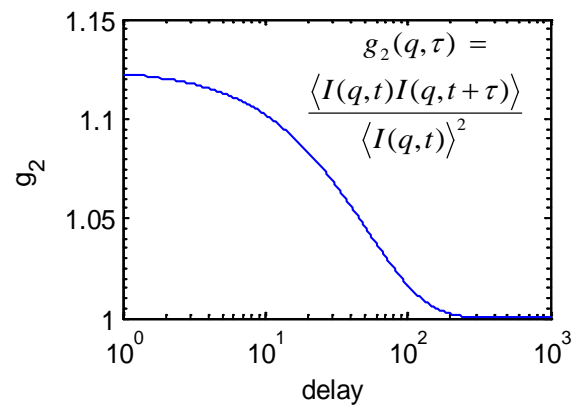


Speckles

QuickTime™ and a Video decompressor are needed to see this picture.

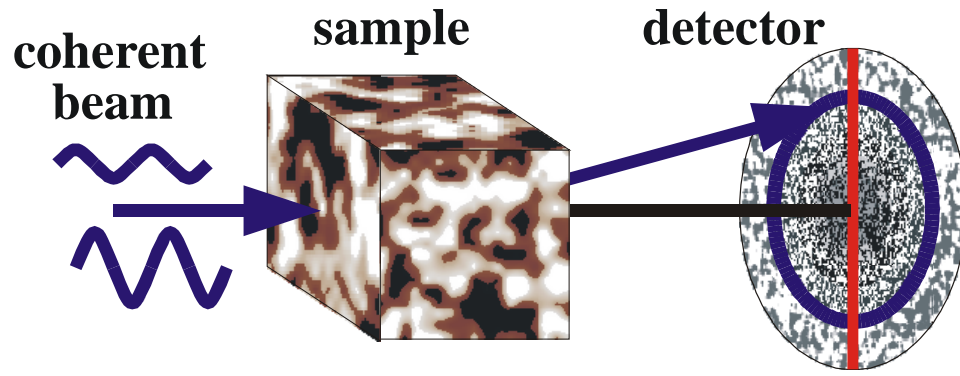


Intensity-intensity auto correlation

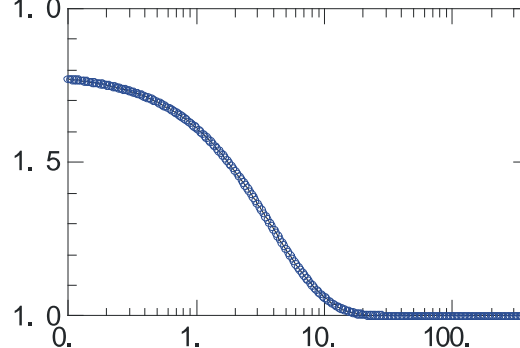
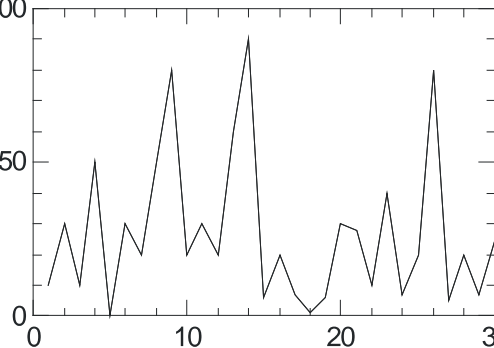
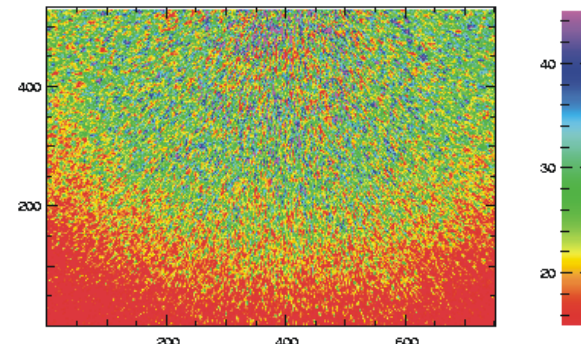


QuickTime™ and a Video decompressor are needed to see this picture.

# Photon Correlation Spectroscopy



X-ray speckle pattern from a static silica aerogel



Siegert Reln.  
$$g_2(\mathbf{q},t) = |g_1(\mathbf{q},t)|^2$$

$$g = \frac{\langle \dots \rangle}{\langle \dots \rangle}$$

$$g = \frac{\langle \dots \rangle - \langle \dots \rangle^2}{\langle \dots \rangle^2}$$

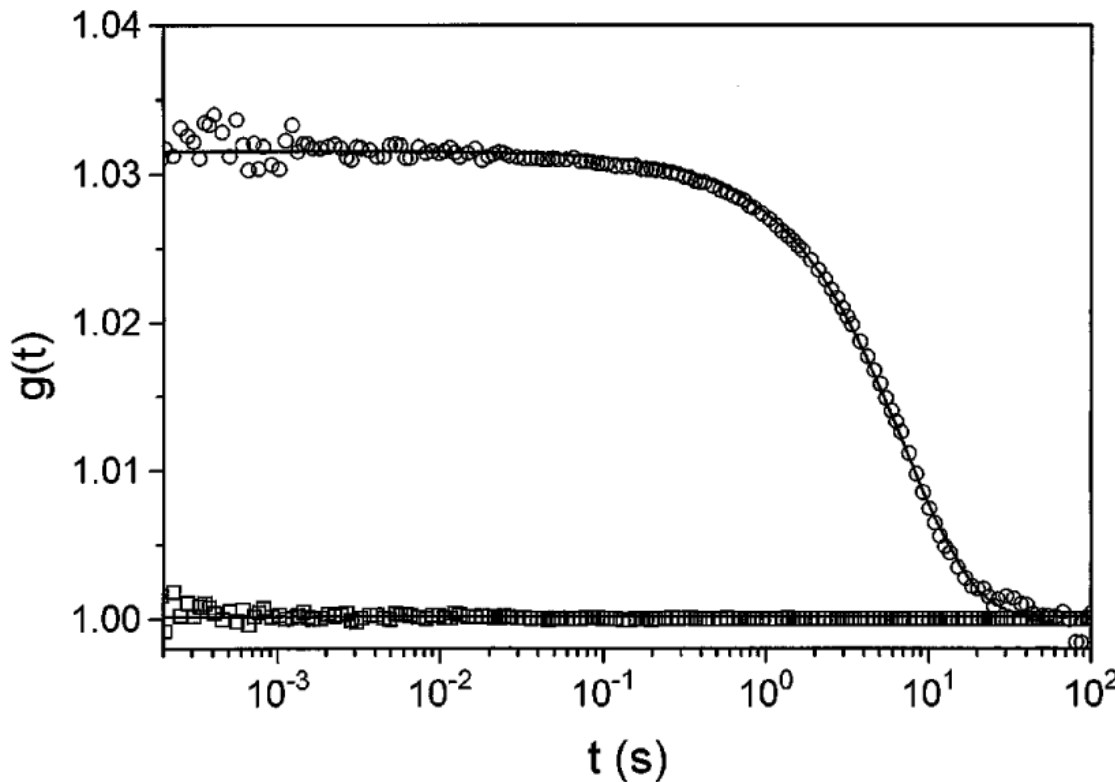


FIG. 3. Correlation function  $g(t)$  measured for palladium colloid in glycerol at  $q = 1.58 \times 10^{-3} \text{ \AA}^{-1}$  and  $T = 279 \text{ K}$ . The solid line corresponds to a fit with an exponential decay. For comparison a correlation function measured for the incident beam is shown.

T. Thurn-Albrecht et al., PRL 1996

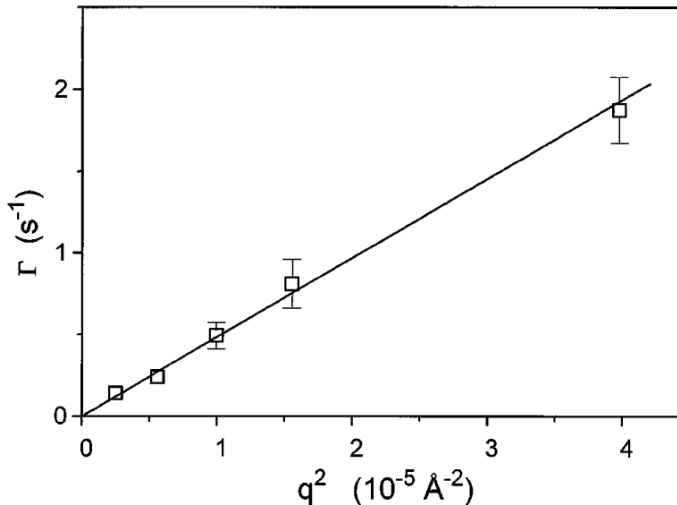


FIG. 4. Relaxation rates  $\Gamma$  determined from the correlation functions plotted vs  $q^2$ . The linear relationship confirms the diffusive nature of the process observed [Eq. (3)].

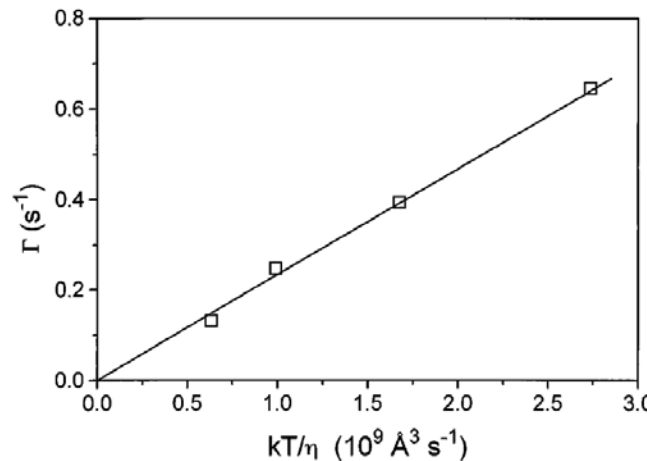
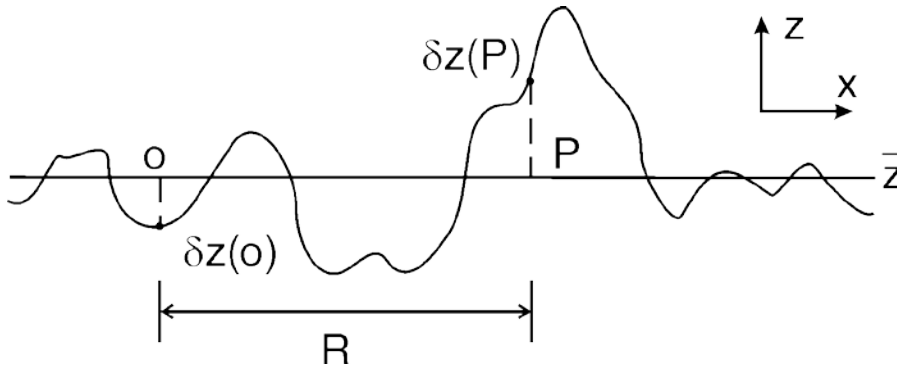


FIG. 5. Relaxation rates  $\Gamma$  determined from the correlation functions plotted vs  $kT/\eta$ . The linear dependence found in this representation is the expected behavior for a diffusion process [Eq. (4)].

# Statistical Description of Surfaces

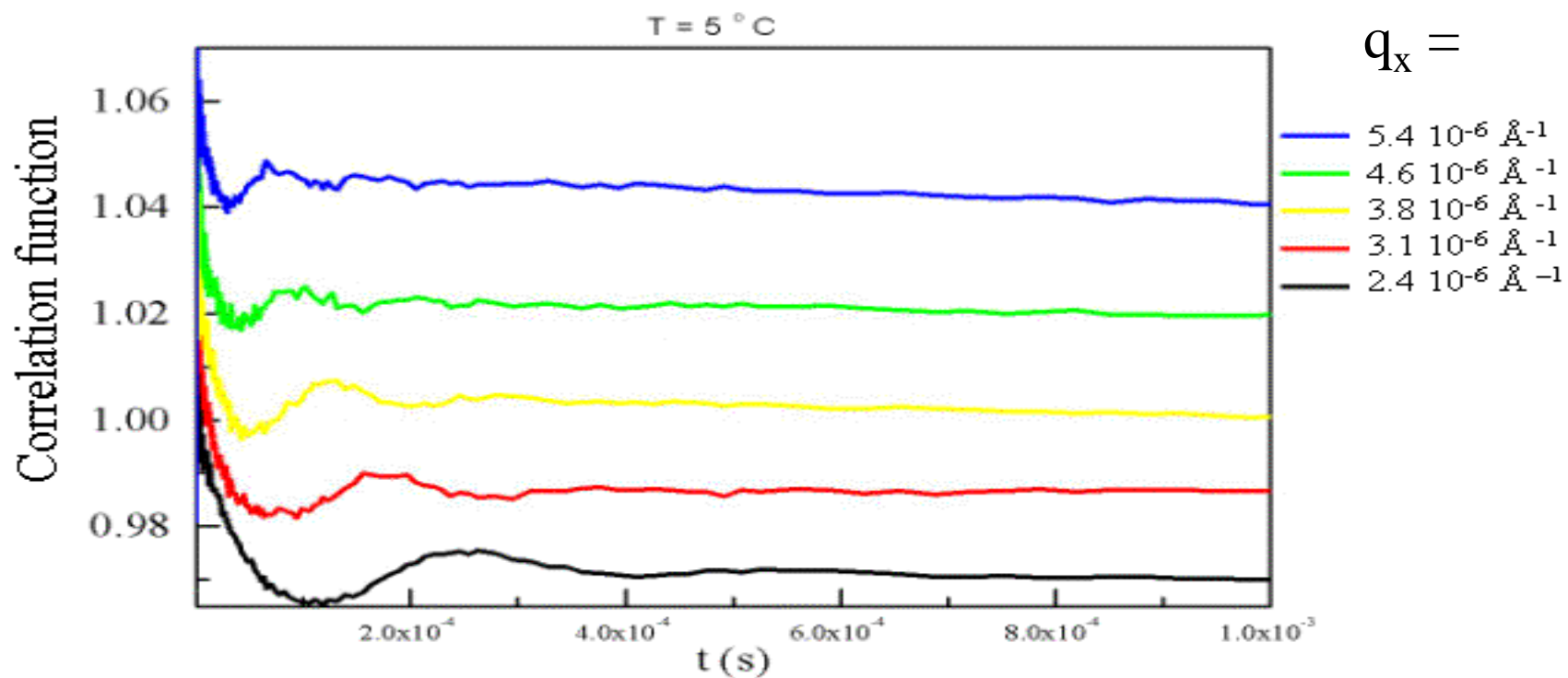


$$z(\vec{r}_{\parallel}) = \bar{z} + \delta z(\vec{r}_{\parallel})$$

$$C(R, \tau) = \langle \delta z(0) \delta z(R, \tau) \rangle$$

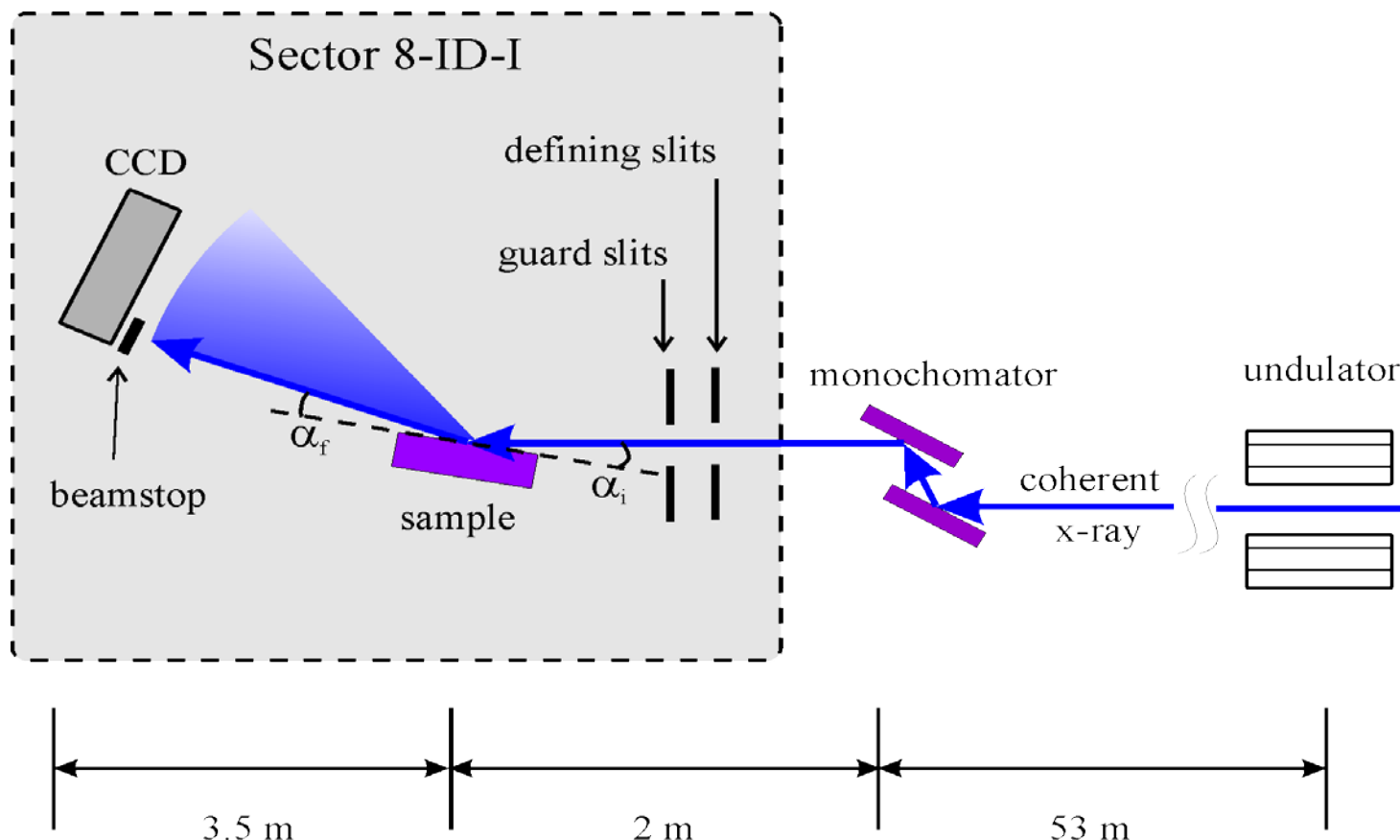
- Surface profile
- Height-height correlation function for a **homogeneous**, **isotropic** and **ergodic** surface
- $[C(R)]$  ( actually the Fourier Transform of a function related to  $C(R)$  ) is measured in a surface scattering experiment.

# Propagating Capillary Waves



Small contrast !

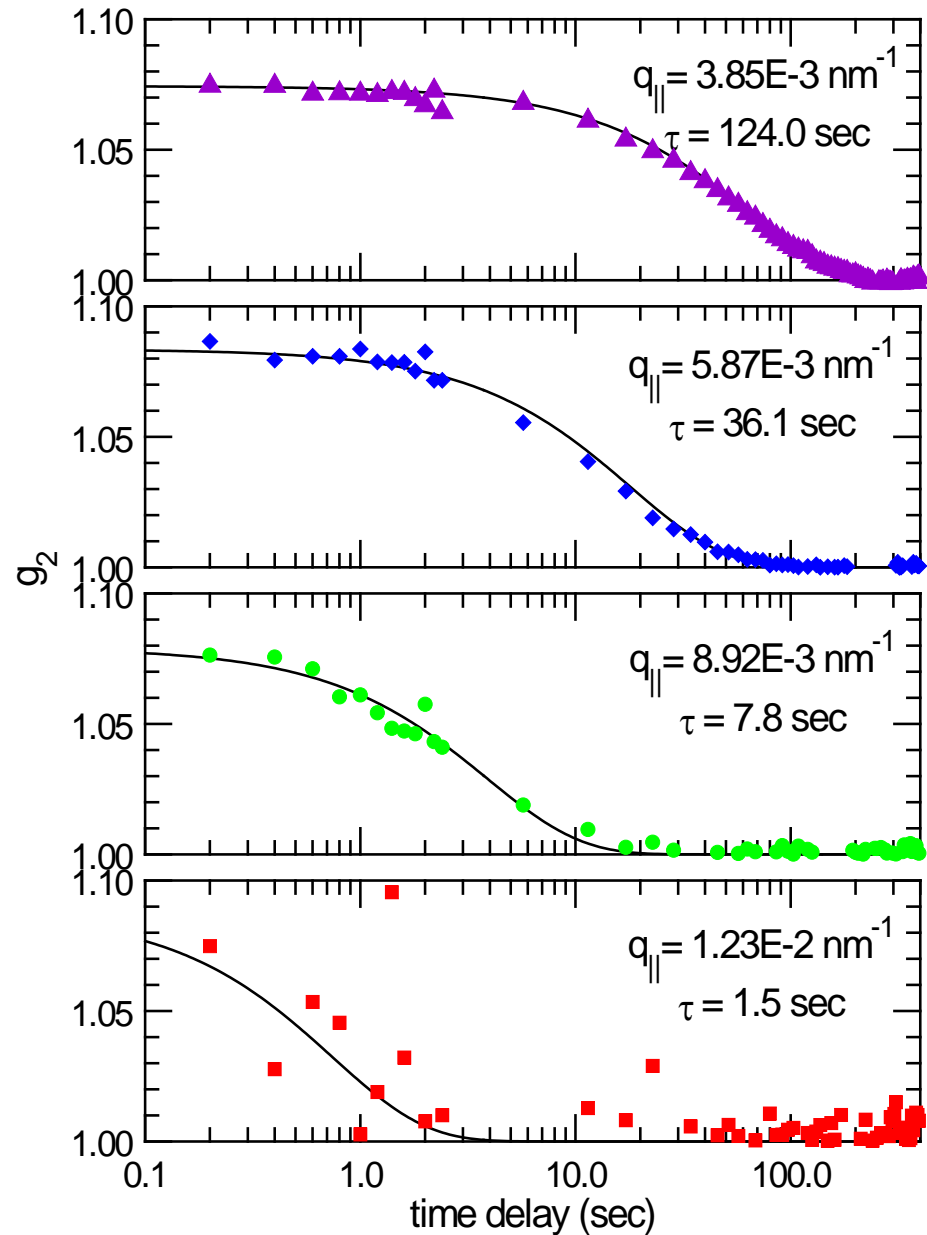
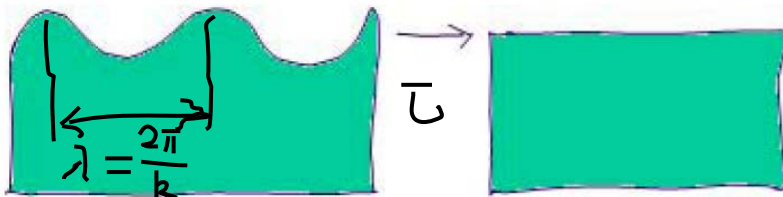
# Experiment Setup at Sector 8-ID-I, APS

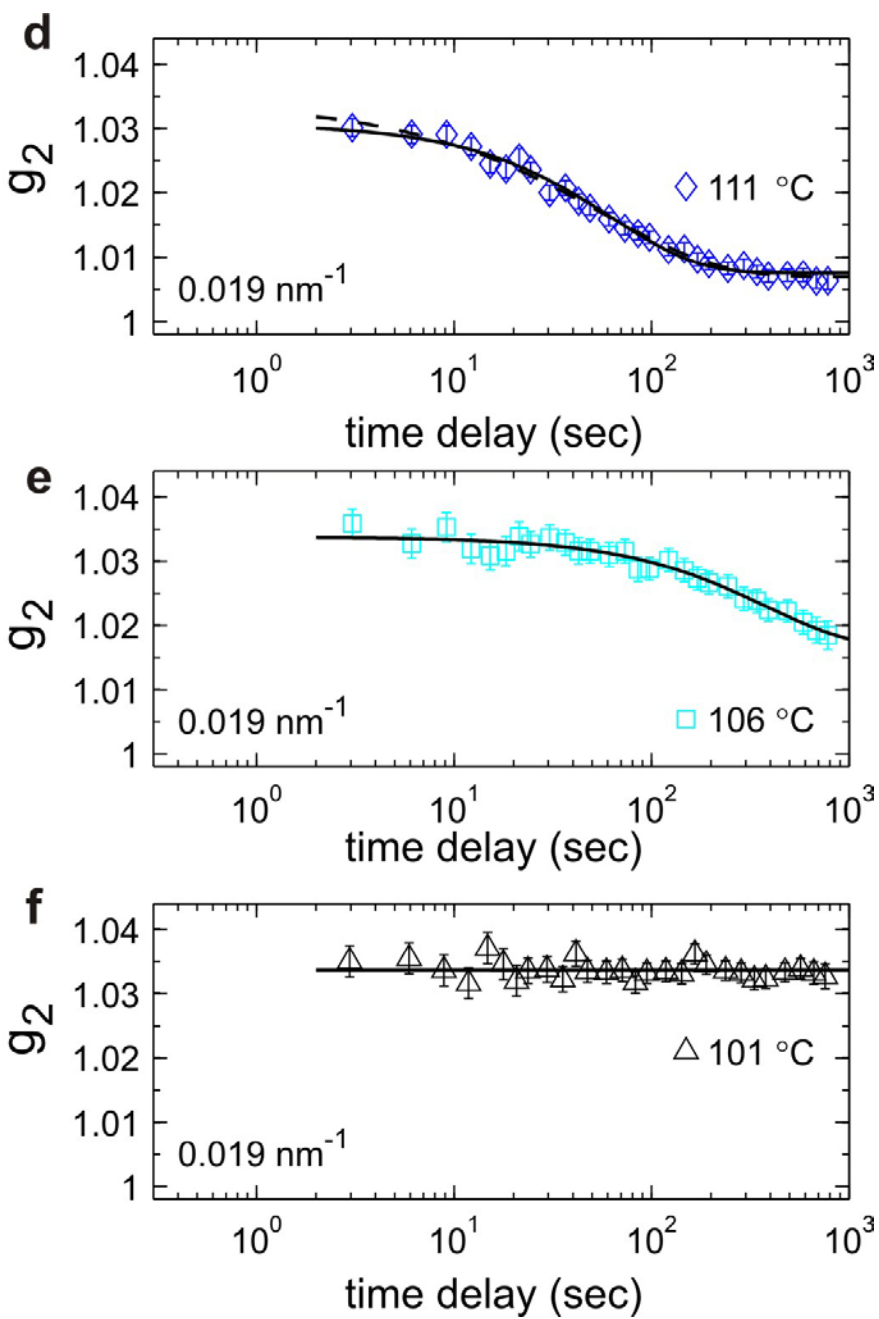
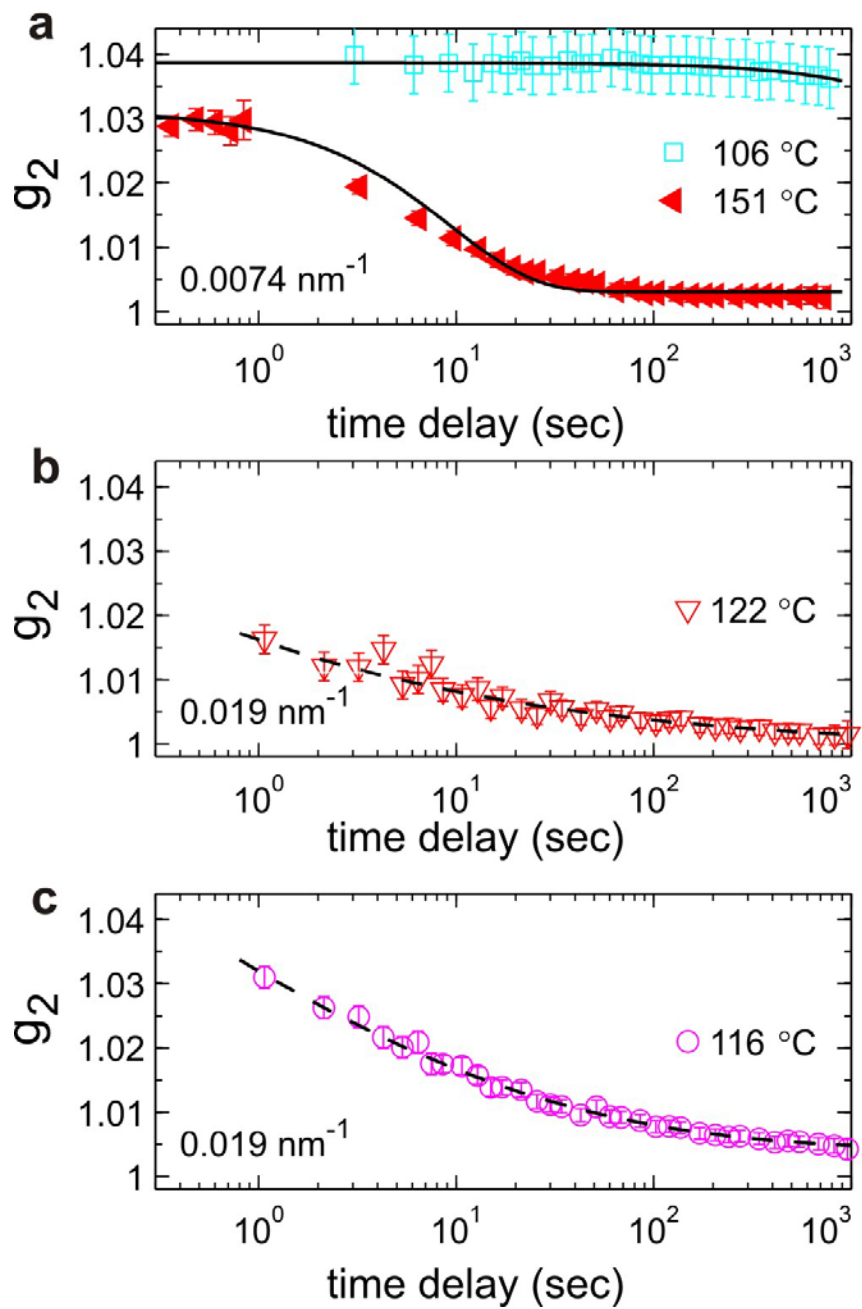


# Intensity Autocorrelation

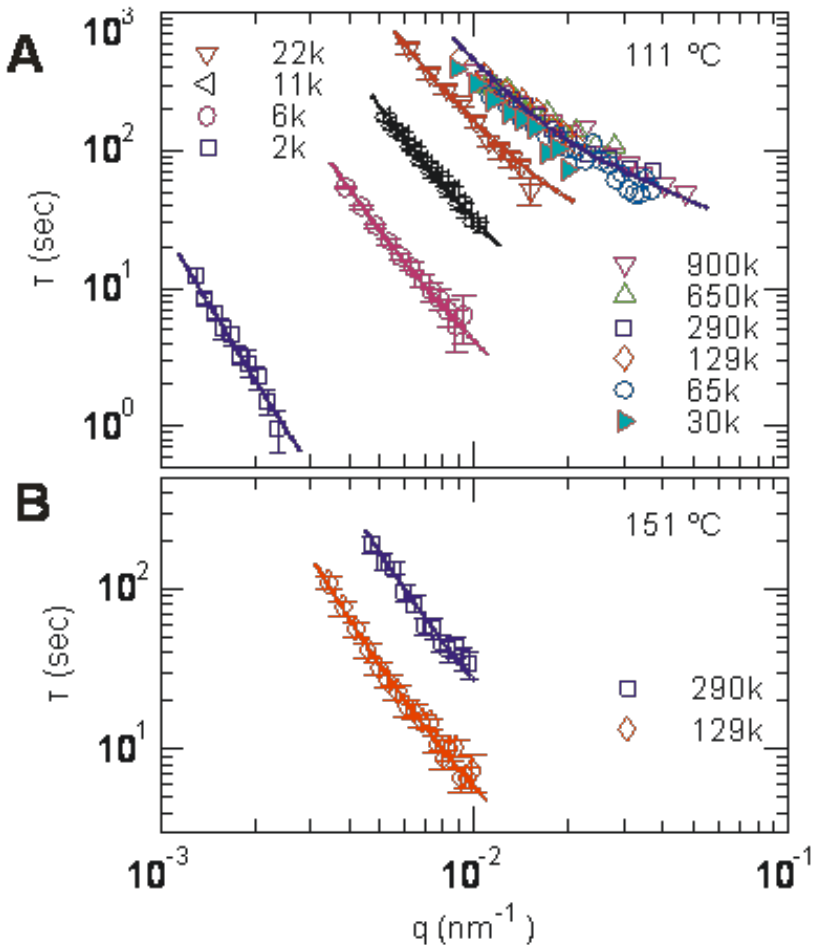
$$g_2(q, \tau) = \frac{\langle I(q, t)I(q, t + \tau) \rangle}{\langle I(q, t) \rangle^2}$$

$$g_2(q, \tau) = 1 + \beta e^{-2t/\tau}$$





# Over-damped Relaxation Time Constants



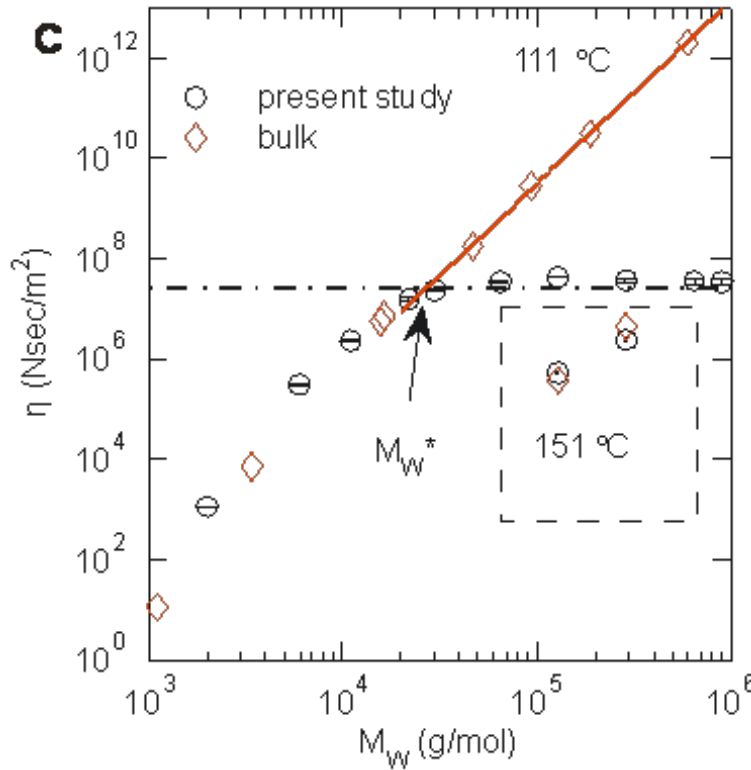
- **Identical thickness** for all films ( $h=160$  nm)
- When  $M_w > 30\text{k g/mol}$ , surface dynamics are
  - **dependent** on  $M_w$  at  $T \gg T_g$ ;
  - **independent** on  $M_w$  at near  $T_g$ .
- When  $M_w \leq 30\text{k g/mol}$ , surface dynamics are **dependent** on  $M_w$ , and **single exponential** for all  $T > T_g$ .
- Capillary wave relaxation:

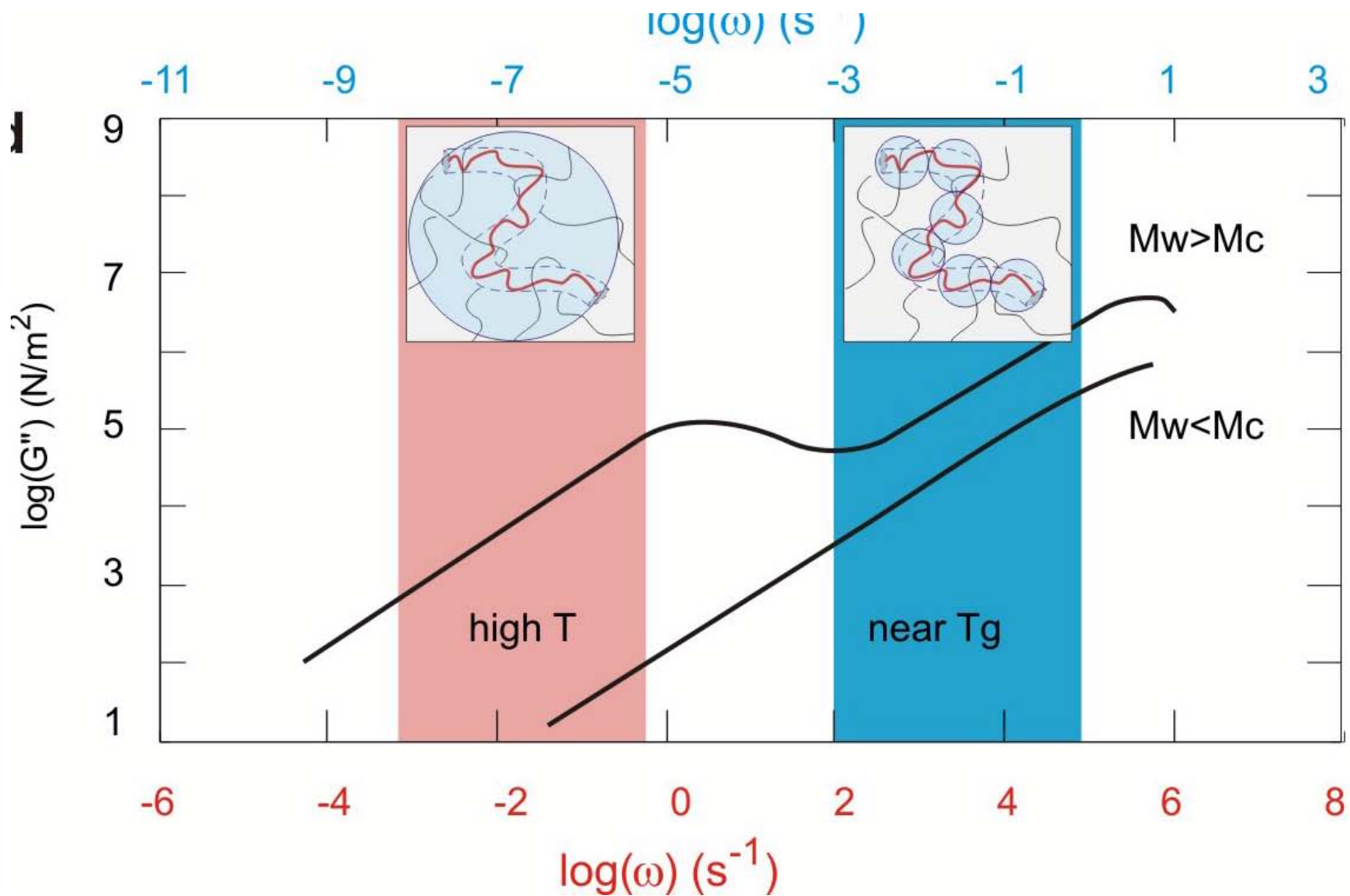
$$\tau(q_{||}) \cong \frac{2\eta}{\gamma q_{||}} \frac{[\cos(q_{||}h)^2 + (q_{||}h)^2]}{[\sinh(q_{||}h)\cosh(q_{||}h) - q_{||}h]}$$

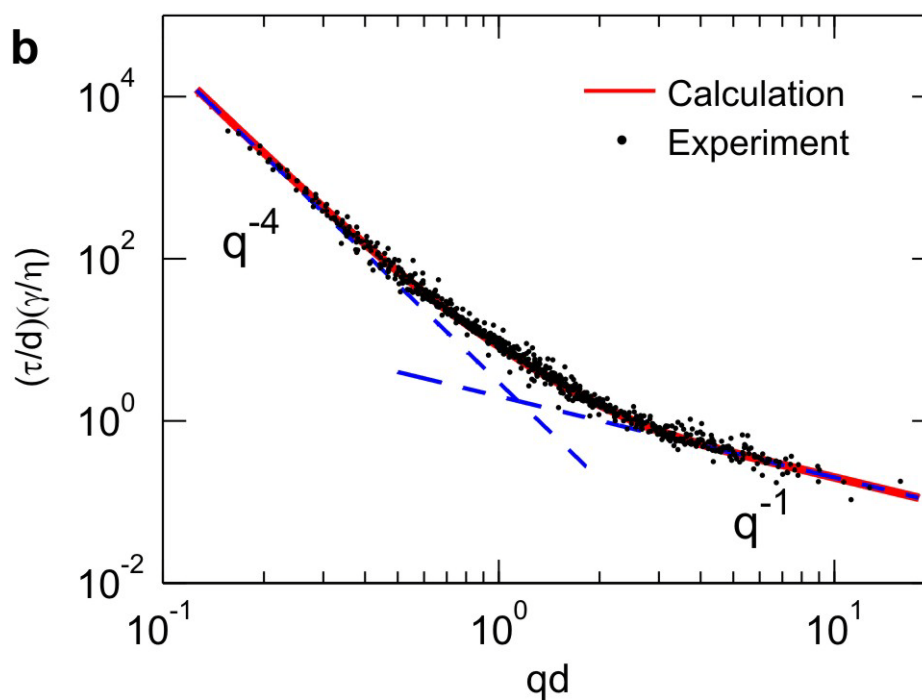
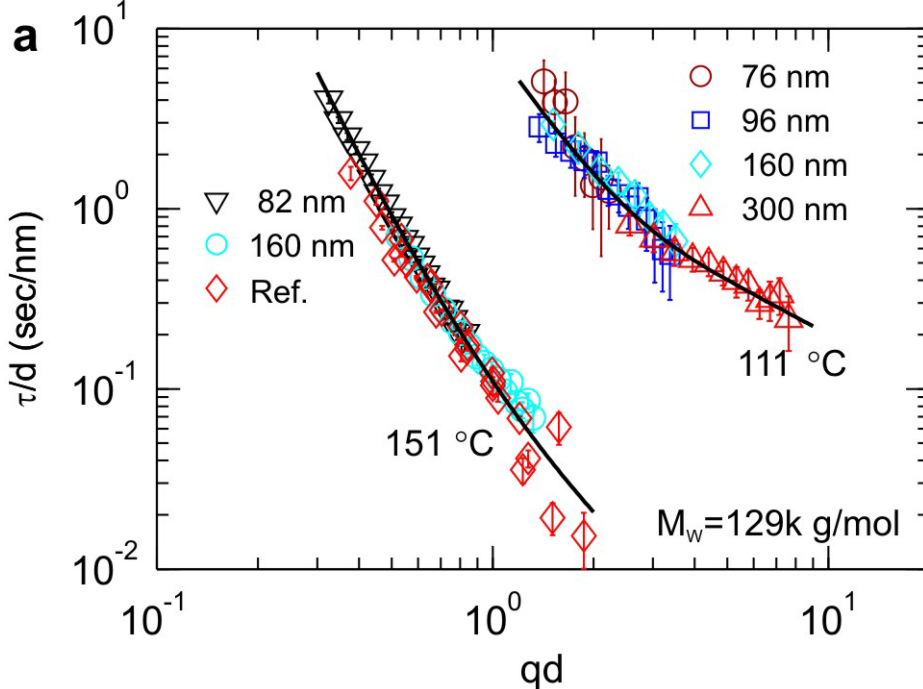
# “Apparent” Shear Viscosity

- Consistent with **bulk values** from rheological measurements at  $T >> T_g$ .
- Orders of magnitude less than bulk values and independent of  $M_w$  near  $T_g$ .
- Intersect with reptation theory ( $\eta \propto M_w^{3.4}$ ) at  $M_w^*$ 
  - $M_w^* = M_c$  ( $M_c = 31.2 \text{ k g/mol}$ : **critical molecular weight for entanglement**).
- Same  $M_w^*$  found at 106 °C, where surface dynamics are 7 times slower.

$$\eta = \lim_{\omega \rightarrow 0} \frac{G''(\omega)}{\omega}$$







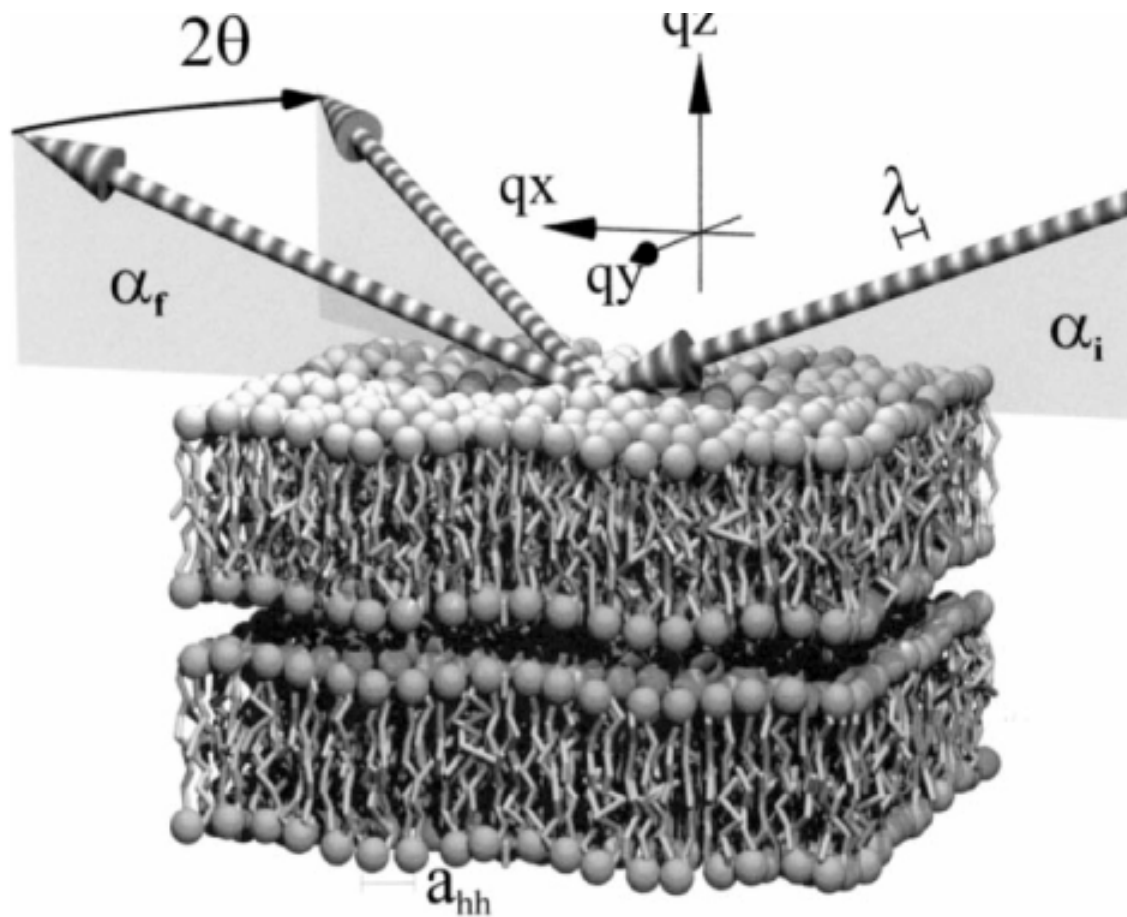
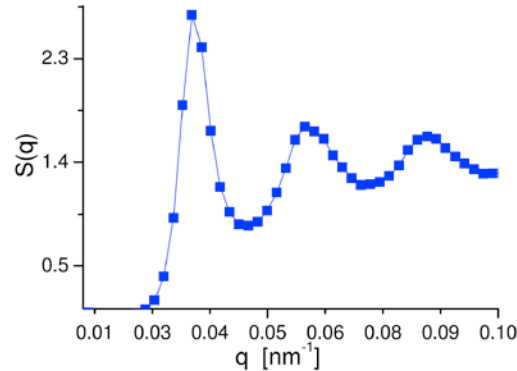
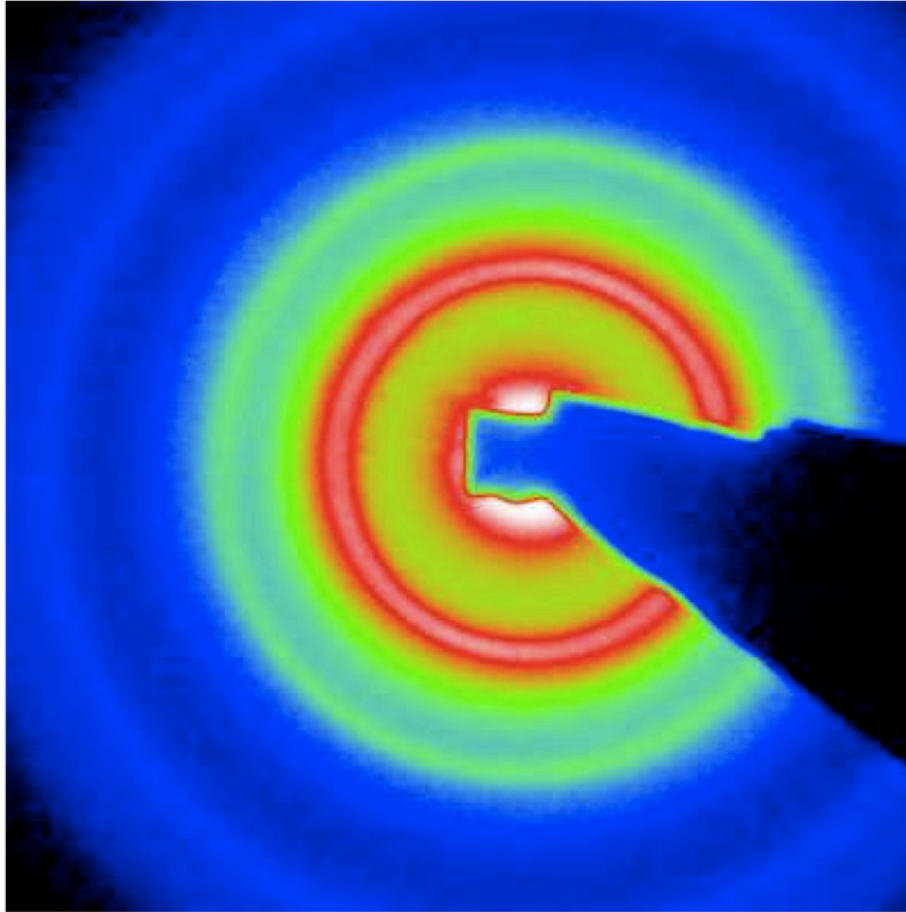


Fig. 1. Schematic of the scattering geometry with the incident, reflected and diffracted beams at grazing angles, from Münster et al. [13•].

# Incoherent SAXS



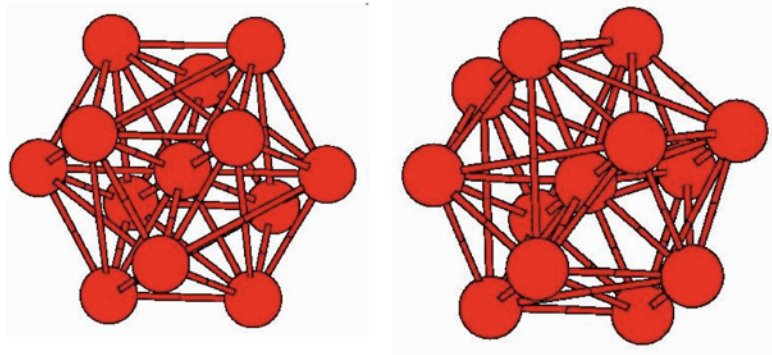
ensemble averaged structure factor

$$\langle S(Q) \rangle = 1 + n_0 \int (g(r) - 1) e^{iQr} dr$$

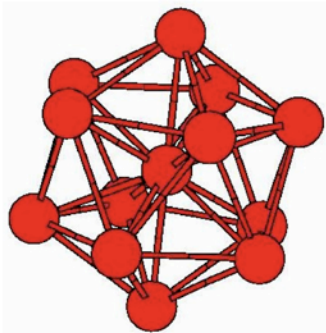
radial distribution function

$$g(r) = 4\pi r^2 n_0^{-2} \langle \rho(0) \rho(r) \rangle$$

information on local symmetries is lost



fcc and hcp structures can fill up space  
and form crystals



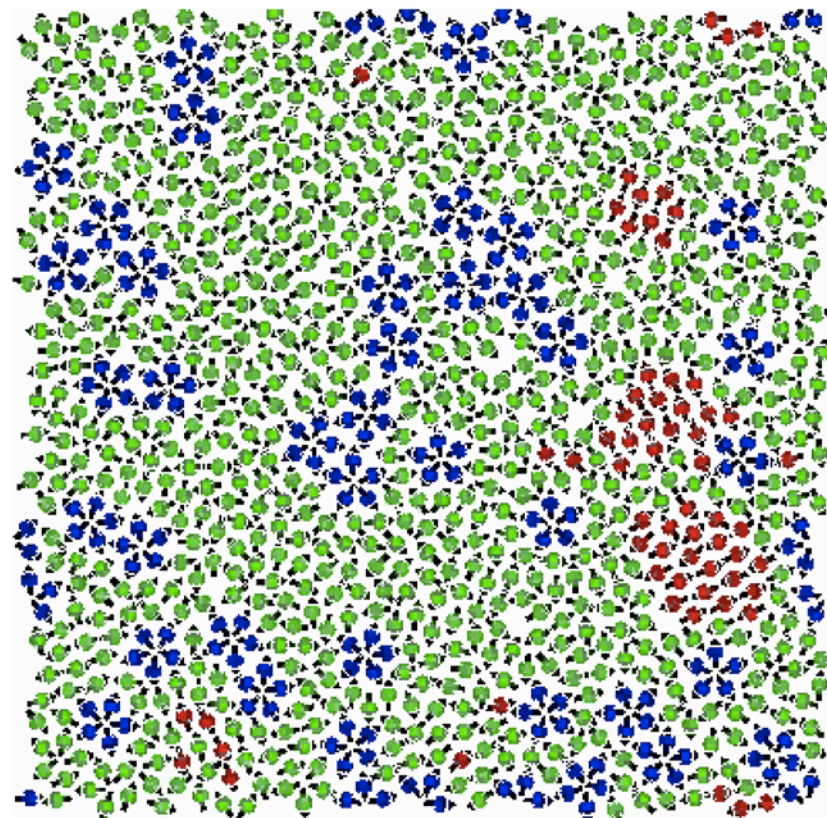
icosahedral structures can not fill space  
but may be energetically favored in liquids  
“locally favored structures (lsf)”

F. C. Frank, Proc. R. Soc. London A 215, 43 (1952).  
P. J. Steinhardt, D. R. Nelson, and M. Ronchetti, Phys.  
Rev. B 28, 784 (1983)

two popular glass forming scenarios

(a) general tendency towards icosahedral order,  
but locally favored structures cannot fill space

(b) general tendency towards crystalline order,  
frustration effect as locally favored structures  
prevent crystallization



Shintani and Tanaka, Nature Physics 2, 200 (2006)

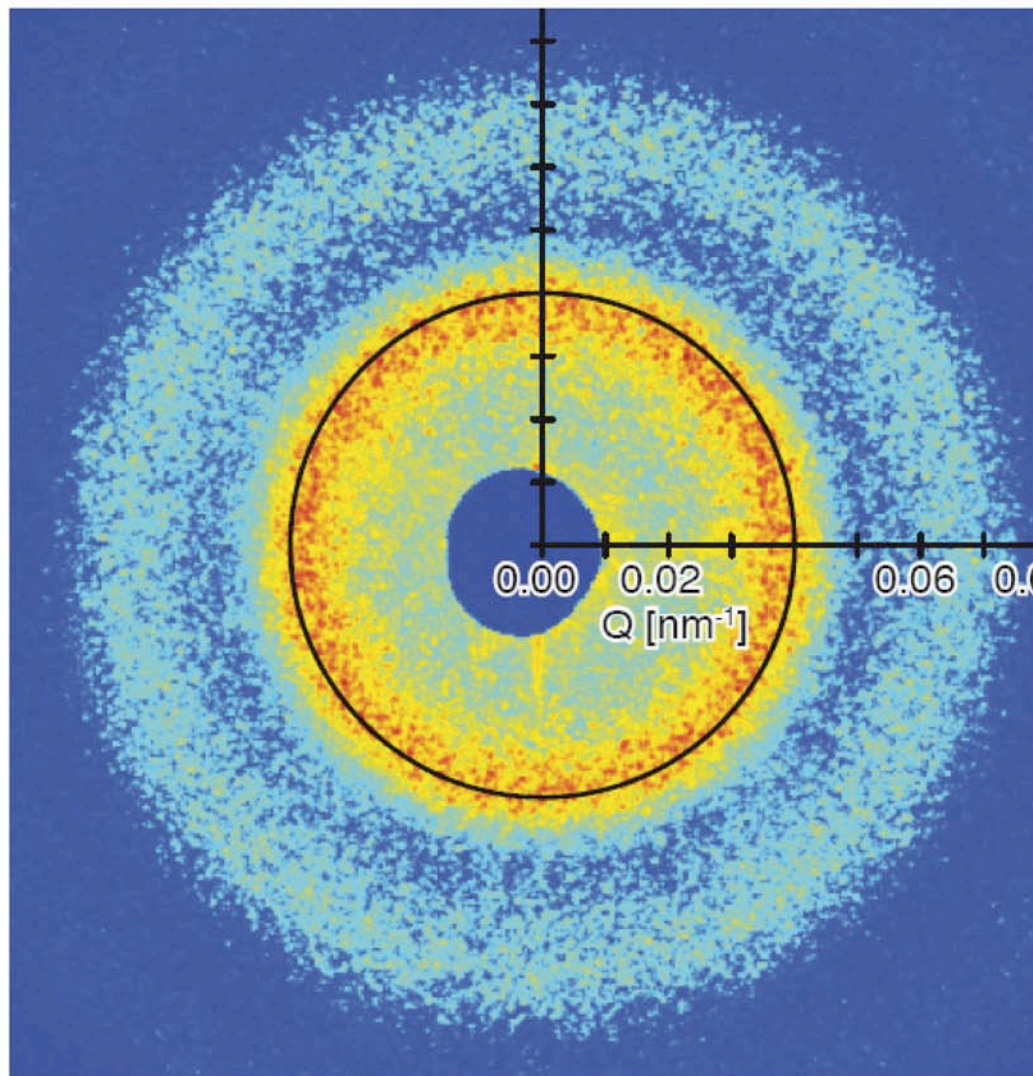
Christian Gutt | Hasylab tuesday meeting | 07.04.2009 | Seite 3

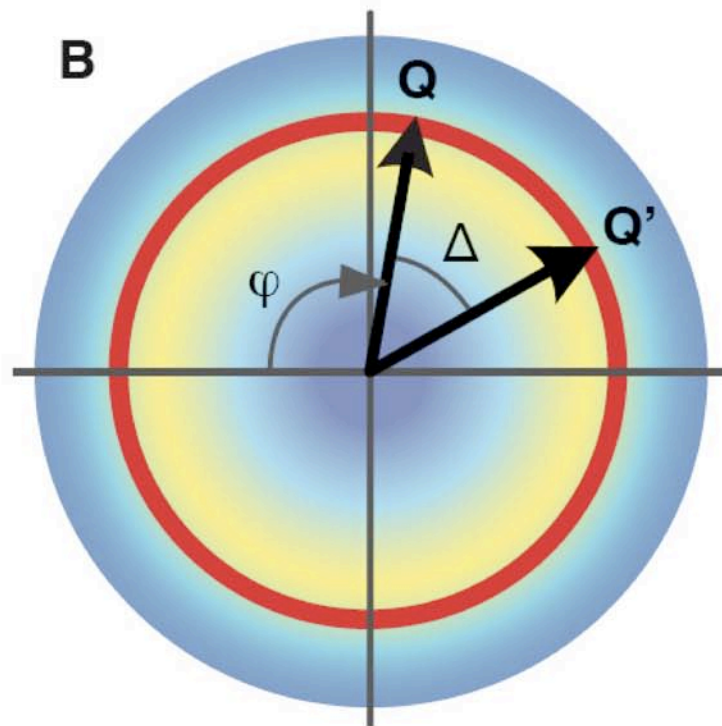
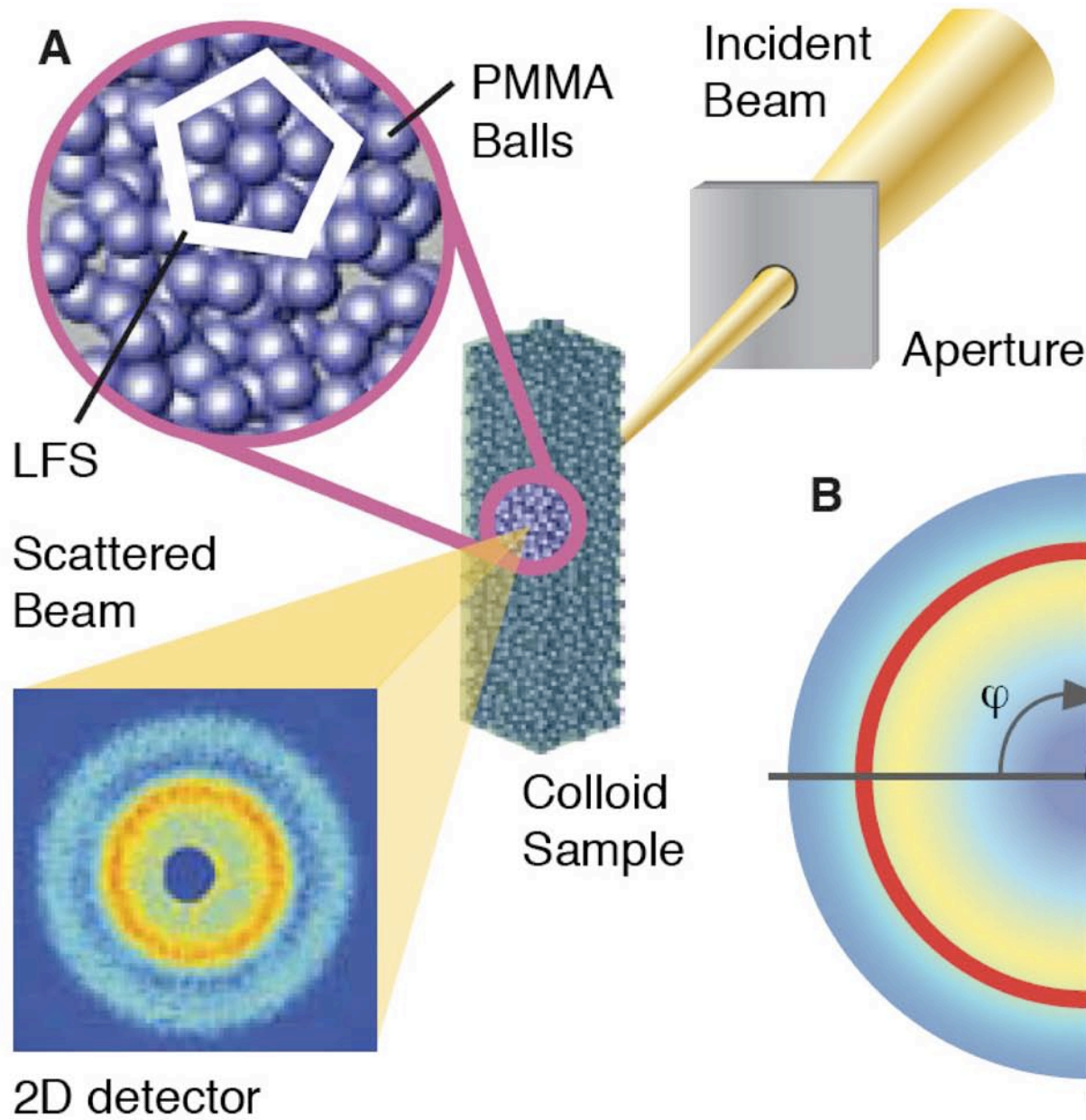


# Hard sphere systems – speckle pattern

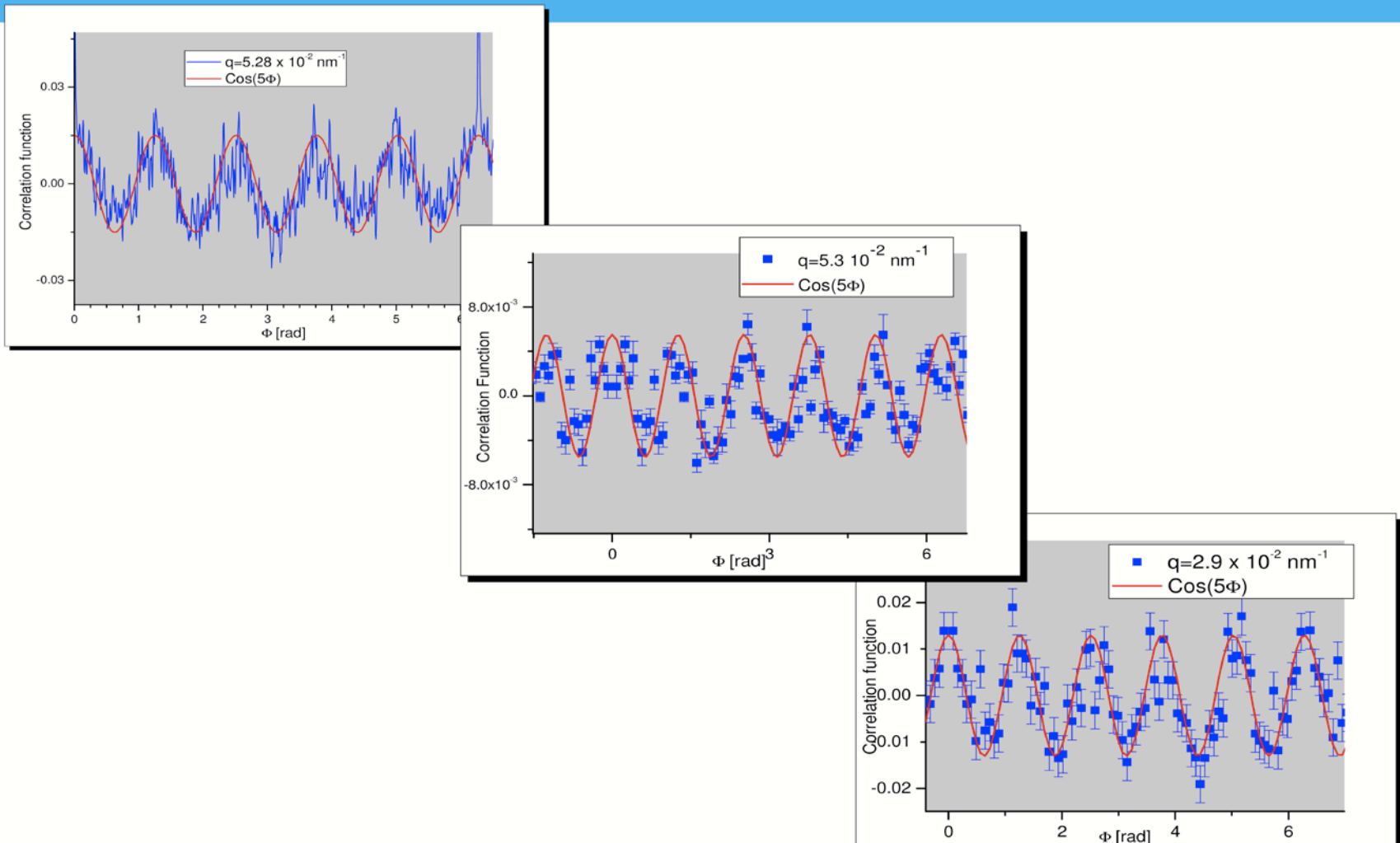
P.Wochner et al.

PNAS 2009





# 5-fold symmetry present in all hard sphere systems



# Why go lensless?

- A technique for 3D imaging of 0.5 – 20  $\mu\text{m}$  isolated objects
- Too thick for EM (0.5  $\mu\text{m}$  is practical upper limit)
- Too thick for tomographic X-ray microscopy (depth of focus < 1  $\mu\text{m}$  at 10 nm resolution for soft X-rays even if lenses become available)

## Goals

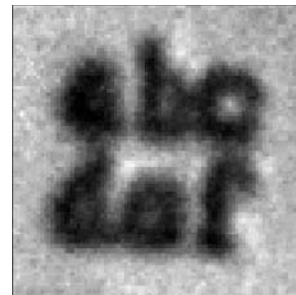
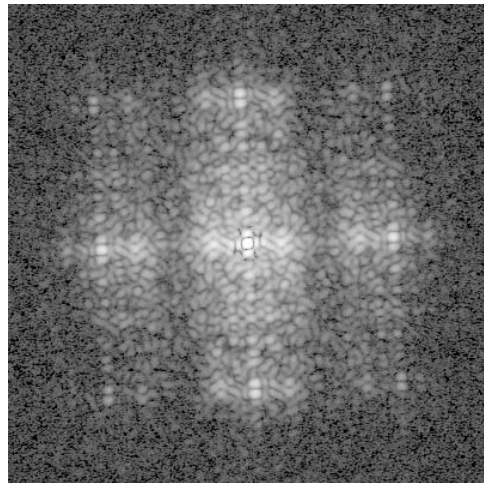
- <10 nm resolution (3D) in 1 - 10  $\mu\text{m}$  size biological specimens  
(small frozen hydrated cell, organelle; see macromolecular aggregates)  
Limitation: radiation damage!
- 2 nm resolution in less sensitive nanostructures  
(Inclusions, porosity, clusters, composite nanostructures, aerosols...)  
eg: molecular sieves, catalysts, crack propagation

# Image reconstruction from the diffraction pattern

- Lenses do it, mirrors do it
  - but they use the full complex amplitude!
- Recording the diffraction *intensity* leads to the "phase problem"!
- Holographers do it - but they mix in a reference wave, need very high resolution detector or similar precision apparatus
- Crystallographers do it - but they use MAD, isomorphous replacement, or other tricks (plus the amplification of many repeats)

Miao, Charalambous, Kirz, Sayre, *Nature* **400**, 342 (1999).

$\lambda=1.8$  nm  
soft x-ray  
diffraction  
pattern



Low angle data  
From optical  
micrograph

Scanning  
electron  
micrograph  
of object

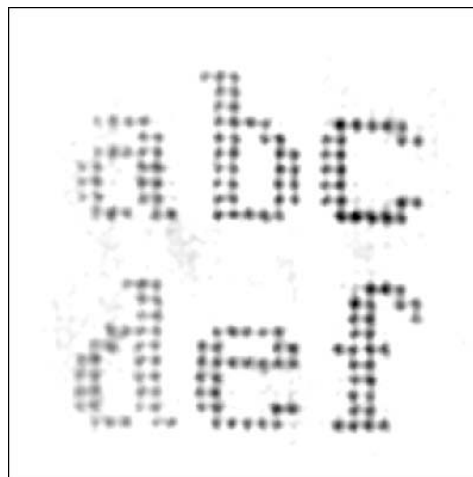
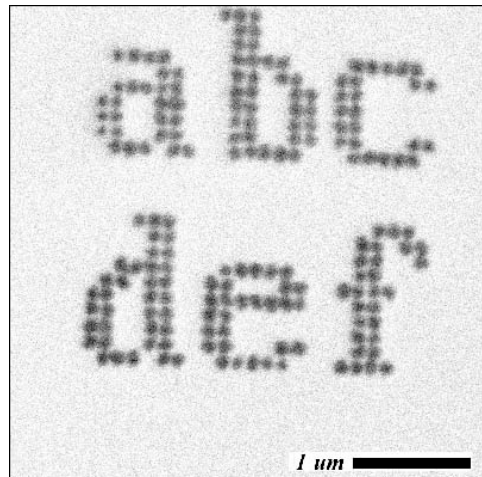


Image reconstructed  
from diffraction  
pattern ( $\theta_{\max}$   
corresponds to 80  
nm). Assumed  
positivity



# Basic principles

- Single object, plane wave incident,  
scattered amplitude is Fourier transform of (complex)  
electron density  $f(r)$

$$F(k) = \int f(r) e^{-2\pi i k \cdot r} dr$$

- Assume: Born Approximation
- Assume coherent illumination:  
for object size  $a$ , resolution  $d$ ,
  - spatial coherence  $\delta\theta < \lambda/4a$
  - temporal coherence  $\delta\lambda/\lambda < d/4a$

# Reconstruction

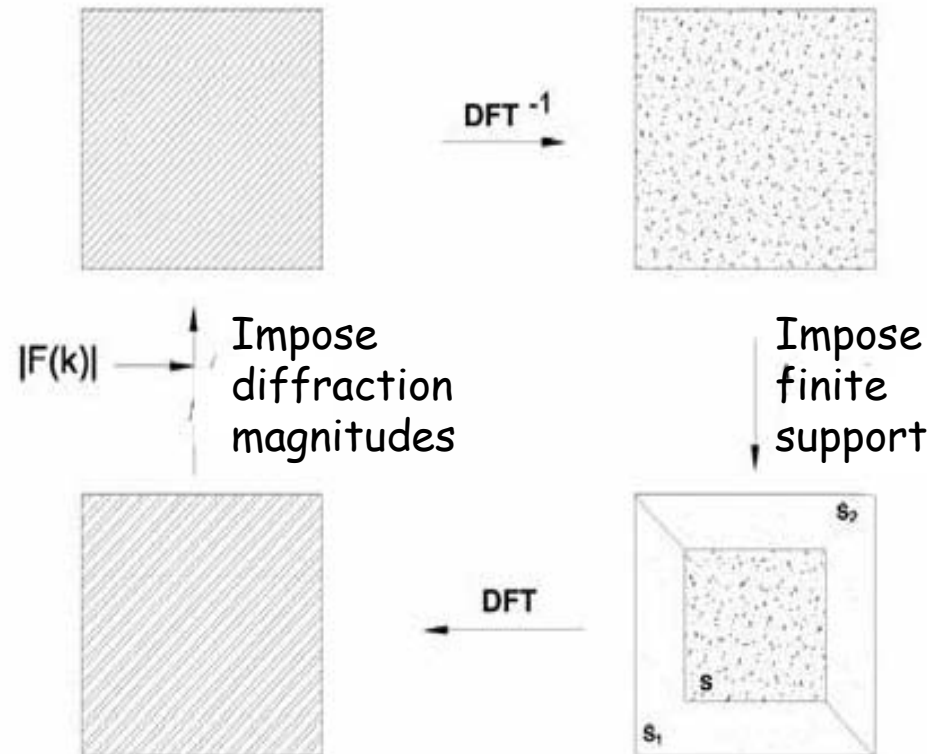
Equations can still not be solved analytically

Fienup iterative algorithm

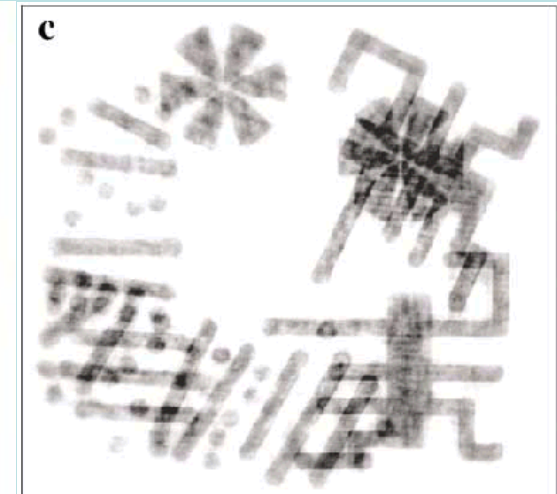
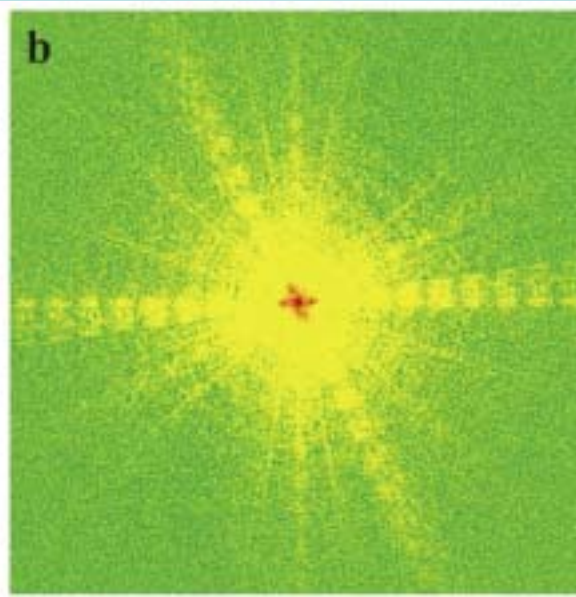
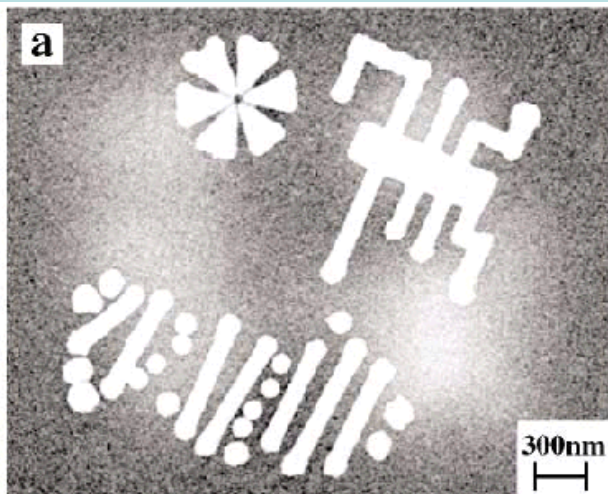
Reciprocal space

Real space

- Positivity of electron density helps!



# DIFFRACTION IMAGING BY J. MIAO ET AL



- From Miao, Ishikawa, Johnson, Anderson, Lai, Hodgson PRL Aug 2002
- SEM image of a 3-D Ni microfabricated object with two levels 1  $\mu\text{m}$  apart
- Only top level shows to useful extent

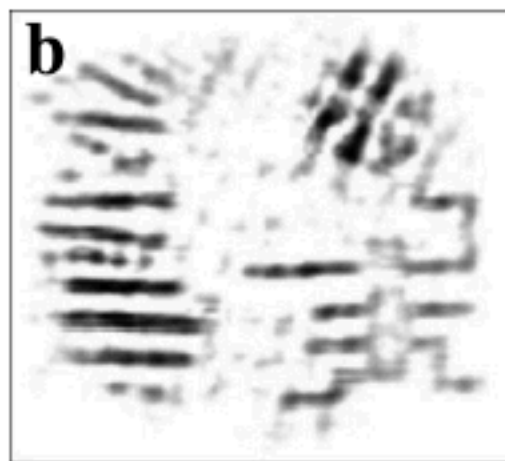
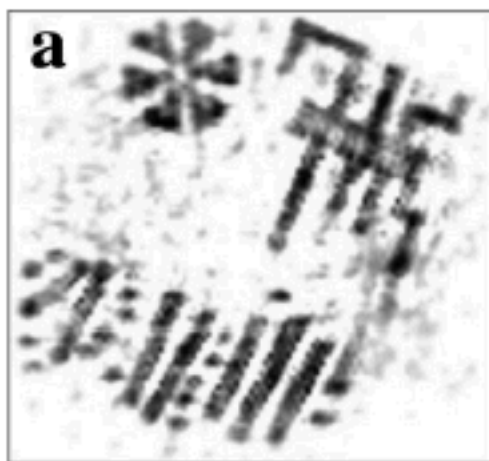
11/3/2009

- Diffraction pattern taken at 2  $\text{\AA}$  wavelength at SPring 8

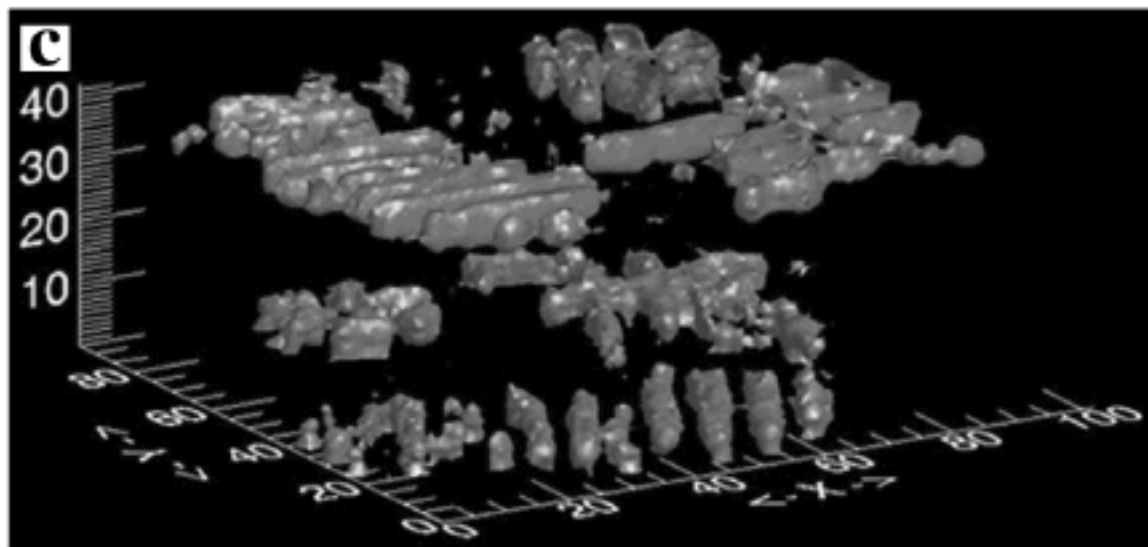
- 2-D reconstruction with Fienup-type algorithm
- Both levels show because the depth of focus is sufficient
- Resolution = 8 nm (new record)

from Howells

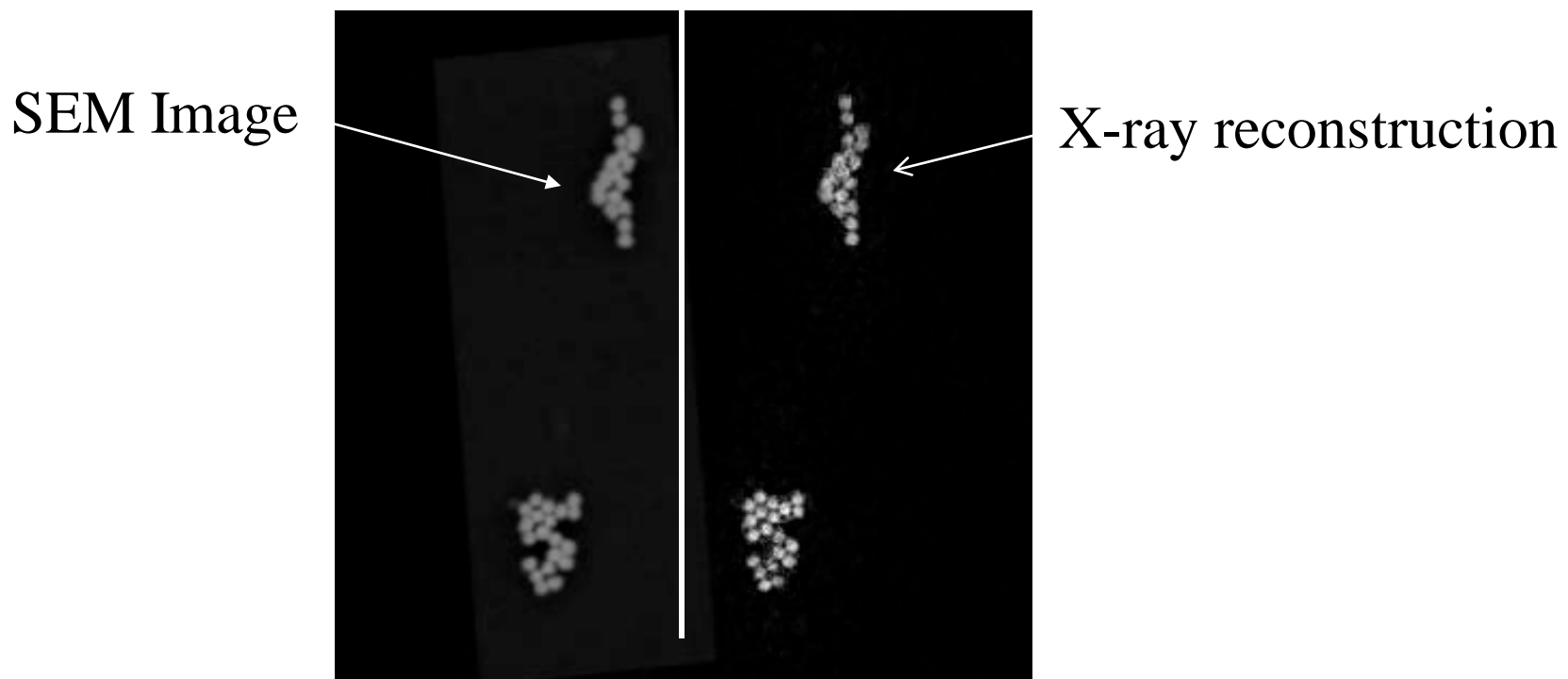
# MIAO ET AL 3-D RECONSTRUCTIONS



- Miao et al 3-D reconstruction of the same object pair
- a and b are sections through the *image*
- c is 3-D density
- Resolution = 55 nm



## Successful reconstruction of image from soft X-ray speckle alone.



50 nm diameter Gold Balls on transparent SiN membrane.

No “secondary image” was used

Approximate object boundary obtained from autocorrelation fn.

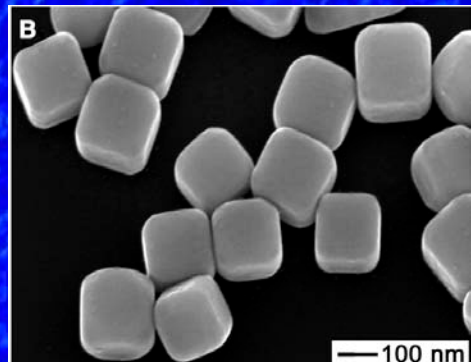
\*How to make an isolated object ? Use AFM to remove unwanted balls.

# *Imaging of individual nanoparticles at the APS*

Ross Harder, University of Illinois, Champaign

*Coherent diffraction pattern  
from 170 nm Ag particle*

*170 nm silver cubes*



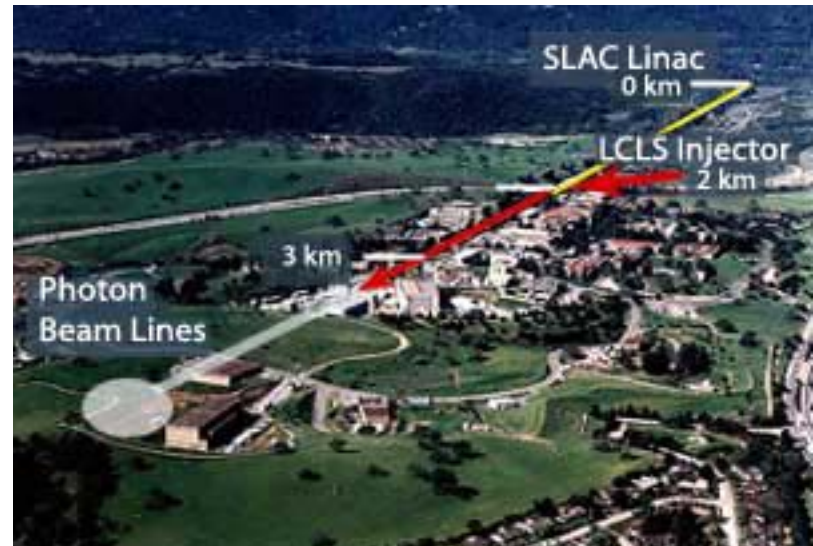
$5 \times 10^{-2} \text{ nm}^{-1}$

*inversion of  
diffraction pattern  
'lensless imaging'*

I.K. Robinson, et al., Science 298 2177 (2003)

# The Future?

- XPCS with completely coherent sources, eg. XFEL's or ERL's
- Large q
- Down to microseconds to nanosecs



# Single molecule imaging?

- Atomic resolution structures known for *few* mammalian membrane proteins!
- Collect many single molecule diffraction patterns from fast x-ray pulses, and reconstruct?
- Lysozyme explodes in ~50 fsec
- R. Neutze *et al.*, *Nature* **406**, 752 (2000)

